

UC San Diego

UC San Diego Electronic Theses and Dissertations

Title

Constraints on Quantum Entanglement in Symmetric Physical Systems

Permalink

<https://escholarship.org/uc/item/68n995zv>

Author

Meill, Alexander

Publication Date

2019

Peer reviewed|Thesis/dissertation

UNIVERSITY OF CALIFORNIA SAN DIEGO

Constraints on Quantum Entanglement in Symmetric Physical Systems

A dissertation submitted in partial satisfaction of the
requirements for the degree
Doctor of Philosophy

in

Physics

by

Alexander W. Meill

Committee in charge:

Professor David Meyer, Chair
Professor Daniel Arovas, Co-Chair
Professor Julio Barreiro
Professor John McGreevy
Professor Nolan Wallach

2019

Copyright
Alexander W. Meill, 2019
All rights reserved.

The dissertation of Alexander W. Meill is approved, and it is acceptable in quality and form for publication on microfilm and electronically:

Co-Chair

Chair

University of California San Diego

2019

TABLE OF CONTENTS

	Signature Page	iii
	Table of Contents	iv
	List of Figures	vi
	List of Tables	vii
	Acknowledgements	viii
	Vita	ix
	Abstract of the Dissertation	x
Chapter 1	Introduction - Entanglement	1
	1.1 Description and Applications	2
	1.2 Pure Bipartite State Entanglement	5
	1.3 Mixed Bipartite State Entanglement	9
	1.4 Multipartite Entanglement Measures	11
	1.5 Properties of Entanglement	13
Chapter 2	Fully Permutation Symmetric States	17
	2.1 Symmetric State Representations	20
	2.1.1 The Majorana Representation	21
	2.1.2 Superposition of Product States	24
	2.1.3 Canonical Forms	24
	2.2 Invariants of Three Qubit Symmetric States	28
	2.3 Local Unitary Equivalence of Symmetric States	32
Chapter 3	Translationally Invariant States	37
	3.1 Maximal Pairwise Concurrence	39
	3.2 Constraints on Shared Pairwise Concurrence	43

Chapter 4	Symmetric Matrix Product States	48
	4.1 Translationally Invariant MPS LU Canonical Form	50
	4.2 Fully Symmetric Representations and Entanglement	52
Chapter 5	Party-Site Symmetric States	58
	5.1 The Gross-Pitaevskii Equation	61
	5.2 Measuring Mean Field Approximation Validity	63
	5.2.1 Exact Fidelity Analysis	68
	5.2.2 Bounded Fidelity Analysis	73
Chapter 6	Conclusion and Future Directions	83
Appendix A	TIX State Achievable Pairwise Subconcurrence Boundaries	86
	A.1 4 Qubits	86
	A.2 5 Qubits	88
Appendix B	Proof of Theorem 4	92
Appendix C	Matrix Norms on PSS Bloch Vectors	97
	C.1 Bloch Vectors of PSS Reductions	97
	C.2 Hilbert-Schmidt Distance	112
	C.3 Super-Fidelity	114
Bibliography	118

LIST OF FIGURES

Figure 2.1:	Scatterplot from two points of view of invariants of randomly generated symmetric 3 qubit states.	30
Figure 2.2:	View of a slice of the boundaries of the volume of symmetric 3 qubit invariants superimposed over the points of Figure 2.1. The contour achieving equality in (2.46) is shown in green (the upper-left surface), (2.47) in blue (lower-left), and (2.48) in red (upper-right).	31
Figure 3.1:	Pairwise concurrences of 10^5 randomly generated 4 and 5 qubit TI states.	44
Figure 3.2:	Pairwise subconcurrences of 10^5 randomly generated 4 and 5 qubit TI states.	46
Figure 3.3:	Pairwise subconcurrences of 10^5 randomly generated 4 and 5 qubit TI and TIX (darker blue) states.	47
Figure A.1:	The 4 qubit TIX state subconcurrence boundaries.	88
Figure A.2:	The 5 qubit TIX state subconcurrence boundaries.	89
Figure A.3:	The bounding conditions on the $(s\mathcal{C}_{1,\nu}^{(5)}, s\mathcal{C}_{2,\nu}^{(5)})$ pairs (darker blue) with the overall boundary.	90
Figure A.4:	The bounding conditions on the $(s\mathcal{C}_{1,\mu}^{(5)}, s\mathcal{C}_{2,\nu}^{(5)})$ pairs (darker blue) with the overall boundary.	91

LIST OF TABLES

Table 3.1:	Maximum concurrences of 4 and 5 qubit CSX states. The analytic results for $n = 5$ are the roots of complicated polynomials, so their rounded numerical values are reported instead.	43
Table 3.2:	Threshold concurrences of 4 and 5 qubit TIX states. The analytic result for $n = 5$ are the roots of complicated polynomials, so the rounded numerical value is reported instead.	47

ACKNOWLEDGEMENTS

I would like to thank my undergraduate mentors at Dartmouth college, Professors Chandrasekhar Ramanathan and Lorenza Viola, for instilling in me an excitement for physics research and specifically for quantum information science. Then to my graduate adviser at UC San Diego, Professor David Meyer, for giving me the direction and guidance to contribute meaningfully to the research community. And finally, to my family for their polite smiles and nods.

Chapter 2 is, in part, a reprint of material from published work done in collaboration with David Meyer, as it appears in Physical Review A, as well as on the arXiv. Alexander Meill and David A. Meyer, “Symmetric 3 Qubit Invariants,” Phys. Rev. A **96**, 062310 (2017), arXiv:1702.07295. The dissertation author was the primary investigator and author of this material.

Chapter 3 is, in part, a reprint of material from published work done in collaboration with David Meyer, as it appears on the arXiv. Alexander Meill and David A. Meyer, “Pairwise Concurrence in Cyclically Symmetric Quantum States,” arXiv:1802.06877. The dissertation author was the primary investigator and author of this material.

The work in this thesis was supported, in part, by NSF grant PHY-1620846.

VITA

2013 B. S. in Physics, Dartmouth College
2015 M. S. in Physics, University of California San Diego
2019 Ph. D. in Physics, University of California San Diego

PUBLICATIONS

Alexander Meill and David A. Meyer, “Symmetric 3 Qubit Invariants,” *Phys. Rev. A* **96**, 062310 (2017), arXiv:1702.07295.

Alexander Meill and David A. Meyer, “Pairwise Concurrence in Cyclically Symmetric Quantum States,” arXiv:1802.06877.

ABSTRACT OF THE DISSERTATION

Constraints on Quantum Entanglement in Symmetric Physical Systems

by

Alexander W. Meill

Doctor of Philosophy in Physics

University of California San Diego, 2019

Professor David Meyer, Chair
Professor Daniel Arovas, Co-Chair

Quantum entanglement rapidly becomes unwieldy to calculate as the number of particles and the dimension of the spaces associated to those particles increase. One meaningful approach which simplifies that analysis is the restriction to subsets of states which obey some physically relevant symmetry. In this dissertation, entanglement properties of totally permutation-symmetric, translationally invariant, and party-site symmetric states are examined, as well as those of small bond-dimensional matrix product states.

Chapter 1

Introduction - Entanglement

The advent of quantum mechanics as a physical model resolved many outstanding questions in early 1900's physics. It triumphantly provided a consistent description of the Hydrogen atom, photoelectric effect, and black-body radiation. While quantum mechanics was celebrated for its agreement with the experiments of the time, some theorists were concerned by new implications of such a model, in particular with the new concept of 'Entanglement' [1]. Entanglement, which will be formally defined in this chapter, extends the rules of quantum mechanics to multi-particle state descriptions and challenged the previously held classical notions of locality and correlation. Einstein famously referred to entanglement as "spooky action at a distance", noting the surprising nature of the phenomenon. Since those early doubts and thought experiments, entanglement has been replicated in numerous physical implementations, and is now a hallmark of modern quantum research. Entanglement has enabled fruitful new fields such as quantum computing and communication, while providing interesting new context to both condensed matter and fundamental physics theories. In this chapter I will define entanglement, describe the properties and measures of entanglement, and briefly elaborate on its applications.

1.1 Description and Applications

This thesis will exclusively examine quantum states of particles which live in finite-dimensional Hilbert spaces, whose dimension can be labeled as d . A pure state for such a single particle could then be expressed, in some basis, as

$$|\psi\rangle = \sum_{i=1}^d a_i |i\rangle, \quad (1.1)$$

for $a_i \in \mathbb{C}$ normalized to $\sum |a_i|^2 = 1$. Such a state is physically motivated by a quantum particle of spin, $(d-1)/2$, where a natural choice of basis associates each of the $|i\rangle$ with the eigenstates of the z -axis spin operator, S_z , for that particle. States of multiple particles, say n particles, where particle j has dimension d_j , can then be constructed through the tensor product as

$$|\psi\rangle = \sum_{i_1=1}^{d_1} \dots \sum_{i_n=1}^{d_n} a_{i_1 \dots i_n} |i_1 \dots i_n\rangle, \quad (1.2)$$

where

$$|i_1 \dots i_n\rangle = \bigotimes_{j=1}^n |i_j\rangle. \quad (1.3)$$

In all but Chapter 5, I will be solely examining spin 1/2 particles ($d=2$), which are canonically referred to as ‘qubits’ for their role in quantum information. In accordance with that quantum information interpretation, the indexing for qubit basis elements is shifted to $|0\rangle$ and $|1\rangle$. This basis will heretofore be referred to as the “computational” basis.

Consider the following particular two-qubit state,

$$|\psi\rangle = \frac{1}{2} \left(|00\rangle + |01\rangle + |10\rangle + |11\rangle \right). \quad (1.4)$$

For such a state, one could ask what the possible measurement outcomes are for either particle in the computational basis. For both particles, 0 and 1 are present with equal amplitudes, so 0 and 1 are equally likely. More formally, those measurement statistics for the first particle could have

been determined from that particle's reduced density matrix, obtained through the partial trace,

$$\rho_1 = \text{Tr}_2(|\psi\rangle\langle\psi|) \quad (1.5)$$

$$\rho_1 = \begin{pmatrix} \frac{1}{2} & \frac{1}{2} \\ \frac{1}{2} & \frac{1}{2} \end{pmatrix}. \quad (1.6)$$

The measurement probabilities are then

$$\text{Prob}(0) = \text{Tr}(|0\rangle\langle 0|\rho_1) = \frac{1}{2}, \quad (1.7)$$

and likewise it can be found that $\text{Prob}(1) = 1/2$, confirming the initial intuition that both outcomes are equally likely. The same analysis on the second particle yields the same result.

Now consider actually performing a computational basis measurement on the second particle. With probability $1/2$, the outcome of that measurement will be 0, and the overall state will collapse to

$$|\psi^{(0)}\rangle = \frac{1}{\sqrt{2}}(|00\rangle + |10\rangle), \quad (1.8)$$

or, with the same probability, the outcome of 1 will collapse the overall state to

$$|\psi^{(1)}\rangle = \frac{1}{\sqrt{2}}(|01\rangle + |11\rangle). \quad (1.9)$$

In either case, if we now ask what the measurement outcomes are for the first particle, we find that both 0 and 1 are *still* equally likely. This can be seen directly from the first particle's reduced density matrix, which remains (1.6) for either outcome.

Now consider performing the same analysis for the following state,

$$|\phi\rangle = \frac{1}{\sqrt{2}}(|00\rangle + |11\rangle). \quad (1.10)$$

We find that both particles initially have 0 and 1 present with the same amplitude, or more formally, that

$$\rho_1 = \rho_2 = \begin{pmatrix} \frac{1}{2} & 0 \\ 0 & \frac{1}{2} \end{pmatrix}, \quad (1.11)$$

which implies that $\text{Prob}(0) = \text{Prob}(1) = 1/2$ for both particles. But now, performing the measurement on the second particle will, with equal probability, collapse the overall state to

$$|\phi^{(0)}\rangle = |00\rangle, \quad (1.12)$$

if the outcome is 0, or to

$$|\phi^{(1)}\rangle = |11\rangle, \quad (1.13)$$

if the outcome is 1. In the case of an outcome of 0, if we now ask what the measurement statistics are for the first particle, we find that only 0 is possible now. Assuming the outcome of the second particle's measurement is known to the first particle (more on this shortly), we can see the change in the first particle's measurement statistics in the change of its density matrix, which has now become

$$\rho_1^{(0)} = \begin{pmatrix} 1 & 0 \\ 0 & 0 \end{pmatrix}. \quad (1.14)$$

Likewise if the outcome had been 1, the first particle's density matrix would have changed to

$$\rho_1^{(1)} = \begin{pmatrix} 0 & 0 \\ 0 & 1 \end{pmatrix}. \quad (1.15)$$

In either case, we can see that the measurement statistics of the first particle now depend on the outcome of the second particle's measurement. This example gives us the first initial interpretation of entanglement - that $|\phi\rangle$ is 'entangled' where $|\psi\rangle$ is not because measuring either particle in $|\phi\rangle$ changes the measurement statistics for the other particle, unlike for those in $|\psi\rangle$. Mathematically, this resembles the notion of classical correlations between probability distributions, but it has been extensively proven that the statistics for entanglement are uniquely quantum [2].

This was a surprising phenomenon for physicists of the time to encounter when exploring the rules of quantum mechanics, particularly because we established that the basis elements for these states are associated to spin, and thus have no dependence on location. So, in principle, this experiment could be implemented on particles separated an arbitrary distance. This is particularly concerning given the notion of locality in physics, as it may seem that this process could be used to transfer information faster than the speed of light. Upon closer inspection, however, we find that this is not the case. If the particles in $|\phi\rangle$ were in separate, distant laboratories, the physicists in the first particle's laboratory would not know the outcome of the second particle's measurement

until its physicists communicated that result classically. Until that time, all the physicists in the first particle's lab know of their particle is that if a measurement were made on the second particle, the first particle would be in $\rho_1^{(0)}$ with 50 percent probability, and in $\rho_1^{(1)}$ with 50 percent probability. But this means that the overall density matrix for that particle is then

$$\rho_1 = \frac{1}{2}\rho_1^{(0)} + \frac{1}{2}\rho_1^{(1)} = \begin{pmatrix} \frac{1}{2} & 0 \\ 0 & \frac{1}{2} \end{pmatrix}, \quad (1.16)$$

which is the original, pre-measurement density matrix for that particle.

While entanglement does not break fundamental principles of physics, it does enable tasks which are impossible or impractical by purely classical means. The previous example demonstrated that information cannot be transferred along the entangled pair alone. With more entangled particles and the aid of classical communication, however, information can be securely transferred between distant labs with no risk of a third party intercepting that information [3] [4]. Entanglement is also largely responsible for the speed ups provided by quantum computers [5]. Various tasks such as search [6] and factorization [7] support algorithms which, acting on quantum particles rather than classical bits, perform those tasks faster than the associated classical algorithms. Beyond being a crucial resource to quantum information processing, entanglement has also found a home in other fields of theoretical physics. In condensed matter theory, preserving entanglement was shown to be a key feature of the density matrix renormalization group in quantum phase transitions [8]. Entanglement has even drawn interest in string theory for its role in anti-de Sitter/conformal field theory correspondence [9].

1.2 Pure Bipartite State Entanglement

Given the expansive research attention being shown to entanglement, knowledge of its properties is in high demand. The most obvious question at the outset of examining entanglement is: How do we determine whether a quantum state is entangled or not? Looking back to the

states from the previous section, we established that $|\phi\rangle$ is entangled because measuring one particle changes the measurement statistics of the other, unlike for $|\psi\rangle$, which is not entangled. Another way to interpret the entanglement, or lack thereof, of these states comes from the idea of ‘separability’. Namely that $|\psi\rangle$ is unentangled, or ‘separable’, because it can be expressed as the tensor product of pure states for each particle,

$$|\psi\rangle = \left(\frac{1}{\sqrt{2}} |0\rangle + \frac{1}{\sqrt{2}} |1\rangle \right) \otimes \left(\frac{1}{\sqrt{2}} |0\rangle + \frac{1}{\sqrt{2}} |1\rangle \right), \quad (1.17)$$

where $|\phi\rangle$ cannot. This notion allows us to finally give a formal definition to entanglement for bipartite quantum states.

Definition 1. *A pure bipartite quantum state, $|\chi\rangle$, is **separable** if it can be expressed as a tensor product of pure states for either party,*

$$|\chi\rangle = |\chi_1\rangle \otimes |\chi_2\rangle. \quad (1.18)$$

*If $|\chi\rangle$ admits no such factoring, it is **entangled**.*

Separability provides a valuable conceptual interpretation of entanglement in that we can fully describe the individual particle states in a separable bipartite state, where we cannot for an entangled state. This context additionally motivates the continuous nature of entanglement because the precision with which we can describe a state is continuous, and therefore so too is entanglement. This notion will be formalized shortly in the definition of the Entanglement of Formation.

After recognizing that entanglement is continuous, the natural question raised then is how do we quantify entanglement in pure quantum states? It turns out that there are multiple methods for doing so. Each method for measuring entanglement satisfies the properties which are described at the end of this chapter, and certain measures are more relevant than others to different applications. In the following, I will describe a short, non-exhaustive sampling of the entanglement measures which are most relevant to this thesis. A more extensive review of entanglement measures can be found in [10].

The following are measures of entanglement of an arbitrary bipartite pure quantum state,

$$|\psi\rangle = \sum_{i_1=1}^{d_1} \sum_{i_2=1}^{d_2} a_{i_1 i_2} |i_1 i_2\rangle. \quad (1.19)$$

- *The Schmidt Rank:* While not a continuous measure, the Schmidt Rank is a particularly simple starting point for determining entanglement. According to the Schmidt decomposition [11], $|\psi\rangle$ can be decomposed as

$$|\psi\rangle = \sum_{i=1}^r \sqrt{\lambda_i} |\psi_i^{(1)}\rangle \otimes |\psi_i^{(2)}\rangle, \quad (1.20)$$

where λ_i are positive real numbers and $|\psi_i^{(j)}\rangle$ are orthonormal basis vectors for either particle's Hilbert space. The Schmidt Rank, r , can then be defined as a measure of entanglement, which ranges from $r = 1$ for separable states, to states of increasing entanglement from $r = 2$ to $r = \min\{d_1, d_2\}$.

The Schmidt Rank partially informs the conceptual motivation for entanglement in regard to our ability to describe the single particle states. One can determine that the single party reduced density matrices of $|\psi\rangle$ are

$$\rho_j = \sum_{i=1}^r \lambda_i |\psi_i^{(j)}\rangle \langle \psi_i^{(j)}|. \quad (1.21)$$

It is then clear that, for separable states ($r = 1$), the single party density matrix is pure and therefore we have full information on the single particle state. For entangled states, on the other hand, the single party reduced density matrices are mixed.

- *The Entanglement of Formation:* Formally, the amount of information contained in a mixed quantum state, ρ , is determined through the Von Neumann entropy,

$$S(\rho) = -\text{Tr}(\rho \log \rho). \quad (1.22)$$

The Entanglement of Formation [12], E_F , then formalizes the inverse relationship between information of the single party reduced states and entanglement of the overall state as

$$E_F(|\psi\rangle) = S(\rho_1). \quad (1.23)$$

Note that the Schmidt decomposition of $|\psi\rangle$ implies that $S(\rho_1) = S(\rho_2)$, which makes E_F symmetric in the choice of party.

- *Negativity*: A density matrix, ρ , can only be associated to a quantum state if ρ obeys the following three properties,

$$\text{Normalization : } \text{Tr}(\rho) = 1, \quad (1.24)$$

$$\text{Hermiticity : } \rho^\dagger = \rho, \quad (1.25)$$

$$\text{Positivity : } \rho \geq 0. \quad (1.26)$$

Intuitively, if ρ is a quantum state, then so too is its transpose, ρ^T . Consider, then, transposing only the elements of the first party in $\rho = |\psi\rangle\langle\psi|$, known as performing the partial transpose of ρ ,

$$\rho^{T_1} = \sum_{i_1, i_2} \sum_{j_1, j_2} a_{i_1, i_2} a_{j_1, j_2}^* |j_1 i_2\rangle\langle i_1 j_2|. \quad (1.27)$$

It follows that if $|\psi\rangle$ is separable, then $\rho = \rho_1 \otimes \rho_2$, so $\rho^{T_1} = \rho_1^T \otimes \rho_2$, which is still a quantum state. If $|\psi\rangle$ is entangled, however, then $\rho \neq \rho_1 \otimes \rho_2$, so there is no reason to expect that ρ^{T_1} would likewise be a quantum state because (1.26) may no longer be true. Conceptually, the Negativity [13], $\mathcal{N}(\rho)$, determines entanglement by measuring the extent to which ρ^{T_1} violates (1.26). More formally,

$$\mathcal{N}(\rho) = \frac{1}{2} (\|\rho^{T_1}\| - 1), \quad (1.28)$$

where $\|A\| = \text{Tr}\sqrt{A^\dagger A}$.

- *The Geometric Measure of Entanglement*: A particularly intuitive way to determine the entanglement of $|\psi\rangle$ is to find a separable state with maximal overlap with $|\psi\rangle$, then let the complement of that overlap measure entanglement. The Geometric Measure of Entanglement [14], E_G , accomplishes this exactly and is defined as

$$E_G(|\psi\rangle) = 1 - \max_{|\phi_1\rangle \otimes |\phi_2\rangle} \left| \left(\langle \phi_1 | \otimes \langle \phi_2 | \right) |\psi\rangle \right|^2. \quad (1.29)$$

While a conceptually simple measure of entanglement, the maximization over separable states makes E_G challenging to determine in general.

The final bipartite measure of entanglement which I will define is the most relevant to the

work of this thesis, but is only defined for states of two qubits,

$$|\psi\rangle = \sum_{i_1=0}^1 \sum_{i_2=0}^1 a_{i_1 i_2} |i_1 i_2\rangle. \quad (1.30)$$

- *The Concurrence*: Consider the coefficients of $|\psi\rangle$ arranged in a 2×2 matrix as below,

$$\psi = \begin{pmatrix} a_{00} & a_{01} \\ a_{10} & a_{11} \end{pmatrix}. \quad (1.31)$$

The Schmidt decomposition implies that ψ can be diagonalized, in some basis, to

$$\psi = \begin{pmatrix} \sqrt{\lambda_1} & 0 \\ 0 & \sqrt{\lambda_2} \end{pmatrix}. \quad (1.32)$$

Then, given that the Schmidt Rank measures entanglement, it is plausible that so too would the determinant of ψ , as separable states ($\lambda_2 = 0$) would measure to 0 entanglement, while entangled states ($\lambda_2 > 0$), would have non-zero entanglement. This concept is formalized by the Concurrence [15], \mathcal{C} , which is defined as

$$\mathcal{C}(|\psi\rangle) = 2 |\det(\psi)| = 2 |a_{00}a_{11} - a_{01}a_{10}|. \quad (1.33)$$

The Concurrence is often expressed alternatively as an inner product,

$$\mathcal{C}(|\psi\rangle) = \langle \psi | \tilde{\psi} \rangle, \quad (1.34)$$

where

$$|\tilde{\psi}\rangle = \sigma_y \otimes \sigma_y |\psi\rangle^*, \quad (1.35)$$

where σ_y is the Pauli-y matrix.

1.3 Mixed Bipartite State Entanglement

While the analysis of pure state entanglement is of great theoretical value, the need often arises to consider the entanglement of mixed quantum states. As will be detailed in the next section, the reduced states of subsets of particles in an overall ensemble are potentially mixed. And in experimental settings, interaction with the environment tends to decohere the state of the physical system, leaving it mixed. How then do we extend the definition of pure state

entanglement to that of mixed states? Consider an arbitrary bipartite mixed quantum state,

$$\rho = \sum_{i=1} p_i |\psi_i\rangle\langle\psi_i|, \quad (1.36)$$

where $|\psi_i\rangle$ are pure bipartite states of the form (1.19). One might reasonably expect that ρ could be defined as separable if each of the $|\psi_i\rangle$ are separable, and that each of the measures of pure bipartite entanglement listed in the previous section could extend to mixed states as a convex sum,

$$E(\rho) = \sum_i p_i E(|\psi_i\rangle). \quad (1.37)$$

The concern with this approach, however, is that the decomposition of ρ into convex sums of pure states, $(p_i, |\psi_i\rangle)$, is not necessarily unique. The resolution to this ambiguity, known as the ‘Convex Roof Extension’ [16], is to consider the entire set of decompositions of ρ ,

$$\{(p_i, |\psi_i\rangle)\} = \left\{ \{p_i\} \in [0, 1], \{|\psi_i\rangle\} \in \mathcal{H}_{d_1} \otimes \mathcal{H}_{d_2} \mid \sum_i p_i |\psi_i\rangle\langle\psi_i| = \rho \right\}, \quad (1.38)$$

and minimize the average pure state entanglement over that set. This informs a new definition for mixed state entanglement.

Definition 2. A mixed bipartite quantum state, ρ , is **separable** if it can be decomposed into a convex sum of separable pure states,

$$\rho = \sum_i p_i \left(\left| \psi_i^{(1)} \right\rangle \otimes \left| \psi_i^{(2)} \right\rangle \right) \left(\left\langle \psi_i^{(1)} \right| \otimes \left\langle \psi_i^{(2)} \right| \right). \quad (1.39)$$

If ρ admits no such decomposition, it is **entangled**.

For any pure state entanglement measure, E , the convex roof extension constructs a mixed state measure,

$$E(\rho) = \min_{\{(p_i, |\psi_i\rangle)\}} \sum_i p_i E(|\psi_i\rangle). \quad (1.40)$$

which, as will be detailed at the end of the chapter, satisfies important properties we expect from an entanglement measure. Unfortunately, this minimization is, in most cases, quite difficult to perform, leaving the convex roof extension as a mostly theoretical tool. A notable exception to this is that the minimization can be performed analytically in the case of the Concurrence.

- *Mixed State Concurrence:* For mixed states of two qubits, ρ , the convex roof extension of

the Concurrence was solved in [15]. Begin by defining

$$\tilde{\rho} = \sigma_y \otimes \sigma_y \rho^* \sigma_y \otimes \sigma_y, \quad (1.41)$$

then determine, $\{\lambda_i\}$, the square roots of the eigenvalues of $\rho \tilde{\rho}$, labeled so that $\lambda_1 \geq \lambda_2 \geq \lambda_3 \geq \lambda_4$. The concurrence of ρ can then be found to be

$$\mathcal{C}(\rho) = \max\{0, \lambda_1 - \lambda_2 - \lambda_3 - \lambda_4\}. \quad (1.42)$$

While most entanglement measures require the convex roof extension to measure entanglement in mixed states, the Negativity is a remarkable exemption. In fact, the Negativity, as defined in (1.28), was shown to be a proper entanglement measure for mixed states as well as pure [13]. It is still possible to apply the convex roof extension to the Negativity, yielding a new entanglement measure altogether, known as the ‘Convex Roof Extended Negativity’ [17]. The fact that the Negativity works seamlessly in both pure and mixed states makes it a common choice in condensed matter theoretic research.

1.4 Multipartite Entanglement Measures

In states of more than two particles, there are multiple partitions and subsets of parties among which entanglement could be considered. This gives rise to multiple definitions for, and approaches to, determining multipartite entanglement.

The simplest approach to examining entanglement in multipartite states is to group the parties of the overall state into two sets, A and B , and measure the entanglement between those sets of parties, $E_{A|B}$. The advantage to such an approach is that the spaces for the parties in either set can be clumped into a single particle state with appropriately large dimension. For the purpose of computing $E_{A|B}$, then, the overall state is effectively a pure bipartite state, enabling the use of many of the measures described previously. This method is commonly used in condensed matter theory in the study of spin chains and tensor networks, which will be discussed in Chapter 4.

Another simple extension of bipartite entanglement methods to multipartite states is to

examine ‘pairwise entanglement’ within the state; the entanglement between only a pair of parties from the overall ensemble. Consider a multipartite state, $|\psi\rangle$, of the form (1.2), with the aim of determining the entanglement between parties k and l , labeled $E_{k,l}$. We can find the reduced state, $\rho_{k,l}$, for parties k and l by tracing out the remaining $n - 2$ parties,

$$\rho_{k,l} = \text{Tr}_{\overline{k,l}}(|\psi\rangle\langle\psi|), \quad (1.43)$$

and find the entanglement of this, potentially mixed, reduced state through some bipartite mixed state measure. This method, with the Concurrence as the entanglement measure of choice, will be the most relevant to the work of this thesis.

An alternate approach to pairwise entanglement, referred to as the ‘Entanglement of Assistance’ [18], relies on the influence of an outside party to maximize the entanglement between the particles of interest. If that outside party were to perform an incomplete measurement on the remaining $n - 2$ particles in some basis, \mathcal{M} , particles k and l would collapse one of the possible pure states, $|\phi_i^{(\mathcal{M})}\rangle$, associated to that measurement basis, with probability $p_i^{(\mathcal{M})}$. The entanglement of those resultant states can then be determined by the pure bipartite measure of choice, E , and weighted by the associated probabilities,

$$E^{(\mathcal{M})}(|\psi\rangle) = \sum_i p_i^{(\mathcal{M})} E\left(|\phi_i^{(\mathcal{M})}\rangle\right). \quad (1.44)$$

The Entanglement of Assistance, labeled $E_{k,l}^\#$, maximizes this averaged entanglement over the possible measurement bases, $\{\mathcal{M}\}$,

$$E_{k,l}^\#(|\psi\rangle) = \max_{\{\mathcal{M}\}} \sum_i p_i^{(\mathcal{M})} E\left(|\phi_i^{(\mathcal{M})}\rangle\right). \quad (1.45)$$

Beyond bipartite measures applied to multipartite states, there are interesting examples of genuine multipartite entanglement. The most simple example of this arises when one studies entanglement in three qubit states,

$$|\psi\rangle = \sum_{i_1=0}^1 \sum_{i_2=0}^1 \sum_{i_3=0}^1 a_{i_1 i_2 i_3} |i_1 i_2 i_3\rangle. \quad (1.46)$$

- *The Three-Tangle:* Consider the concurrence between party 1 and the set of parties 2 and 3, $\mathcal{C}_{1|2,3}$. One might expect the entanglement that particle 1 shares with the other particles is

a function of the entanglement that it shares individually with those particles, expressed by $\mathcal{C}_{1,2}$ and $\mathcal{C}_{1,3}$. Surprisingly, however, it was found in [19] that

$$\mathcal{C}_{1|2,3}^2 \geq \mathcal{C}_{1,2}^2 + \mathcal{C}_{1,3}^2, \quad (1.47)$$

suggesting that there is some amount of entanglement in $\mathcal{C}_{1|2,3}$ which is unaccounted for by entanglement simply between the pairs. This implies that there is some entanglement unique to the parties as a trio. This led to the definition of the Three-Tangle, τ , often referred to as the ‘Residual Entanglement’, which measures that unaccounted for entanglement,

$$\tau = \mathcal{C}_{1|2,3}^2 - \mathcal{C}_{1,2}^2 + \mathcal{C}_{1,3}^2. \quad (1.48)$$

The Three-Tangle can alternately be expressed mathematically as a determinant much like the Concurrence could in the 2 qubit case. In three qubits we can arrange the coefficients of $|\psi\rangle$ now in a $2 \times 2 \times 2$ tensor and compute the hyperdeterminant of that tensor to determine the Three-Tangle,

$$\tau(|\psi\rangle) = 4|d_1 - 2d_2 + 4d_3|, \quad (1.49)$$

where

$$d_1 = a_{000}^2 a_{111}^2 + a_{001}^2 a_{110}^2 + a_{010}^2 a_{101}^2 + a_{011}^2 a_{100}^2 \quad (1.50)$$

$$d_2 = a_{000} a_{001} a_{110} a_{111} + a_{000} a_{010} a_{101} a_{111} + a_{000} a_{011} a_{100} a_{111} \quad (1.51)$$

$$+ a_{001} a_{010} a_{101} a_{110} + a_{001} a_{011} a_{100} a_{110} + a_{010} a_{011} a_{100} a_{101}$$

$$d_3 = a_{000} a_{110} a_{101} a_{011} + a_{100} a_{010} a_{001} a_{111}. \quad (1.52)$$

1.5 Properties of Entanglement

Each of the entanglement measures which I have described to this point has an intuitive interpretation and correctly identifies separable quantum states, but I have yet to formally define what constitutes a measure of entanglement. The following properties which a function, E , must have to be considered an entanglement measure are, in some sense, the most general properties of

entanglement itself.

The first requirement is that E identifies separable states, be them pure or mixed, as having zero entanglement. Formally, if ρ is separable, then

$$E(\rho) = 0. \quad (1.53)$$

Notably this condition is not sufficient in determining separability, meaning that there may be an entangled state, ρ , for which $E(\rho) = 0$. This condition also mandates that the Schmidt Rank be subtracted by 1 to be considered a proper entanglement measure.

The next requirement on E is motivated by physical restrictions on entanglement. Entanglement is fundamentally a non-local phenomenon, meaning that it cannot be created by purely local means. The simplest exhibition of this principle is that the entanglement of a quantum state is invariant under local unitary (LU) evolution. More precisely, for any local unitary operator,

$$U = \bigotimes_{i=1}^n U_i, \quad (1.54)$$

where $U_i \in U(d_i)$, then

$$E(\rho) = E(U\rho U^\dagger). \quad (1.55)$$

Going beyond unitary evolution, if one expands the possible local action to ‘Stochastic Local Operations and Classical Communication’ (SLOCC) [20], then we now enforce that entanglement does not increase on average. More precisely, if, under the action of some SLOCC operation, ρ evolves to ρ'_i with probability p_i , then

$$E(\rho) \leq \sum_i p_i E(\rho'_i). \quad (1.56)$$

The final formal requirement on E is convexity. Intuitively, if one has access to two quantum states, ρ_A and ρ_B , then mixing the two states should not increase the average entanglement. Formally, for $p_A + p_B = 1$, then

$$E(p_A \rho_A + p_B \rho_B) \leq p_A E(\rho_A) + p_B E(\rho_B). \quad (1.57)$$

Conveniently, the convex roof extension guarantees that any pure state measure extends to mixed states while satisfying convexity.

Together, (1.53-1.57) formally define the set of conditions which an entanglement measure, E , must satisfy. While not an explicit in the definition of entanglement, several interesting features appear when comparing different measures of entanglement against each other. The first is that they recognize very different classes of states as entangled. Consider the following pair of three qubit states,

$$|W\rangle = \frac{1}{\sqrt{3}} \left(|001\rangle + |010\rangle + |100\rangle \right) \quad (1.58)$$

$$|GHZ\rangle = \frac{1}{\sqrt{2}} \left(|000\rangle + |111\rangle \right). \quad (1.59)$$

Each state is considered maximally entangled in three qubits by some measure. By the work of this thesis in conjunction with [21], it can be shown that $|W\rangle$ maximizes the pairwise concurrence among three qubit states for which $\mathcal{C}_{1,2} = \mathcal{C}_{2,3} = \mathcal{C}_{3,1}$, while $|GHZ\rangle$ has maximal three-tangle. Interestingly, however, $|W\rangle$ has 0 three-tangle, while $|GHZ\rangle$ has 0 pairwise concurrence. This example clearly demonstrates the distinct forms which entanglement can take, which is particularly relevant to protocols which rely on specific types of entanglement as a resource. This motivates some of the prevalent questions which this thesis seeks to answer. Namely, what types of states exhibit which types of entanglement, and which states maximize certain entanglement measures? In Chapter 3 I examine maximal pairwise concurrence in translationally invariant rings, while in Chapter 4 I show that even the simplest of fully symmetric matrix product states can achieve maximal pairwise concurrence. And in Chapter 5 I examine how pairwise entanglement evolves in highly symmetric quantum random walks.

The other notably property of entanglement is the constraining of shared entanglement in multipartite states. This phenomenon was first observed in [19] as a consequence of (1.47). If its left hand side is maximized, (1.47) takes the form

$$1 \geq \mathcal{C}_{1,2}^2 + \mathcal{C}_{1,3}^2. \quad (1.60)$$

This implies that if parties 1 and 2 are maximally entangled ($\mathcal{C}_{1,2} = 1$), then neither party can share any entanglement with any other ($\mathcal{C}_{1,3} = \mathcal{C}_{2,3} = 0$). This behavior is commonly referred

to as the ‘monogamy’ of entanglement, reflecting that the amount of entanglement that can be shared among multiple parties is highly constrained. In three qubits, the full achievable space of pairwise entanglements, $\mathcal{C}_{i,j}$, was found in [22] to be the convex hull of the Roman-Steiner surface [23]. This was later expanded in [24] to also constrain the Three-Tangle,

$$t^2 (1 - x^2 - y^2 - z^2 - t^2) - (x^2y^2 + x^2z^2 + y^2z^2 - 2xyz) \geq 0, \quad (1.61)$$

where $(x, y, z, t) = (\mathcal{C}_{1,2}, \mathcal{C}_{2,3}, \mathcal{C}_{3,1}, \tau)$. In Chapter 2 I add the final polynomial LU invariant and find the full achievable space when restricted to permutation symmetric states. In Chapter 3 I return to the constraints on just shared pairwise concurrences, only looking at 4 and 5 qubit translationally invariant states.

Chapter 2

Fully Permutation Symmetric States

Quantifying entanglement and its properties, while of great value for both experimental and theoretical applications, is a challenging task for multiple reasons. As the number of particles grows, so too do the number of ways to define, measure, and share entanglement. The dimension of the overall state space also grows quickly in the number of particles, as well with the dimensions of those individual particles. Entanglement calculations become quite difficult with so many degrees of freedom. For a single state with given numerical coefficients, calculating entanglement is merely a question of computational power. But, when trying to determine maximal entanglements and constraints on shared entanglement, the entire state space must be considered, making each degree of freedom a variable in the calculations. Even for the smallest particle dimension ($d = 2$), determining pairwise concurrence in states of multiple qubits amounts to finding the eigenvalues of a 4×4 matrix, which is challenging enough for an arbitrary matrix let alone for one whose entries are potentially complex functions of the many state coefficients. These factors make the study of entanglement difficult in the most general cases. Even in three qubits, our knowledge of entanglement constraints is incomplete [24].

A common approach to managing the complexity of entanglement calculations is to consider only the most relevant portions of the overall Hilbert space. Consider, for example, the

translationally invariant 1-D ferromagnetic Ising model [25] with no external field,

$$\mathcal{H} = -J \sum_i \vec{\sigma}_i \cdot \vec{\sigma}_{i+1}, \quad (2.1)$$

where $\vec{\sigma}$ is the vector of Pauli matrices and $J > 0$. The energy associated to a given state in this physical system is a function of the inner product between adjacent spins. The ground state for this system, then, is the family of states in which each spin is pointed in the same direction. Likewise, states of high energy are ones where many adjacent spins are pointed in opposite directions. Such states are of less physical interest in this system, and therefore so too are their entanglement properties. One might then restrict entanglement calculations to states where the spins are more aligned. In four qubits in the σ_z basis, say, one could reasonably eliminate $|0101\rangle$ and $|1010\rangle$ from the state space, reducing the number of degrees of freedom and simplifying the calculations, while still finding meaningful results on the remaining states.

This procedure of restricting to a subset of particularly relevant subset of states is a commonly used approach to entanglement theoretic work and is a central theme to the work of this thesis. Rather than individually selecting the states which are most favorable to any given Hamiltonian, however, I will be choosing to exploit the symmetries which are common in widely studied physical systems. The first such symmetry I will examine, and the topic of this chapter, is total permutation invariance. A state, $|\psi\rangle$, is totally permutation symmetric if it is unchanged when any two of its particles exchange party labels. Given that the full permutation group is generated by such arbitrary swaps, $|\psi\rangle$ is then invariant under *any* permutation of the party labels. We can formalize this concept in a definition of full permutation invariance on states of n qubits, which will be the sole focus of this chapter.

Definition 3. An n qubit state, $|\psi\rangle$, is *fully permutation symmetric* if

$$U_\pi |\psi\rangle = |\psi\rangle \quad \forall \quad \pi \in S_n, \quad (2.2)$$

where U_π is the unitary representation of π on n qubits.

Henceforth, such states will simply be referred to as ‘symmetric’ states, while states obeying

other symmetries will be labeled by the full description of that symmetry.

Beyond shrinking the size of the state space to analyze over, the restriction to the symmetric subspace also reduces the number of entanglements to determine. For instance, consider two disjoint subsets of parties, A and B , from the overall state, as well as some bipartite measure of entanglement on those sets, $E_{A,B}(|\psi\rangle)$. The symmetry of $|\psi\rangle$ then implies that, for any $\pi \in S_n$,

$$E_{A,B}(|\psi\rangle) = E_{A,B}(U_\pi |\psi\rangle) = E_{A',B'}(|\psi\rangle), \quad (2.3)$$

where $A' = \pi^{-1}A$ and $B' = \pi^{-1}B$. This reduces the possible $E_{A,B}(|\psi\rangle)$ to a single $E_{a,b}$ where $a = |A|$ and $b = |B|$. Since the labels of the parties themselves are irrelevant, we can see that the entanglement now only depends on how many parties are being considered.

Symmetric states clearly offer a great simplification to the analysis of entanglement, but importantly they do so while maintaining substantial physical relevance. Symmetric states are key to the state preparation required to perform measurement-based quantum computing [26]. The ground states of various translationally invariant Hamiltonians are symmetric [27], such as that of (2.1). Symmetric states also appear in the context of quantum computing algorithms, such as Grover's search algorithm, the initial state for which is symmetric [28]. The analytical simplicity and physical value of symmetric states have made them the focus for a great deal of research into entanglement properties. A complete picture of the geometric entanglement in symmetric states was given in [29]. The maximal pairwise concurrence for symmetric states was found in [21]. Symmetric states with maximally mixed single party reductions were found and analyzed in [30], while their two-party reductions were studied in [31].

The attention of this chapter is paid to the entanglement properties of symmetric states in three qubits, as well as to their representations under local unitary action. In Chapters 4 and 5 we will return to symmetric states with additional constraints.

2.1 Symmetric State Representations

Before examining the various entanglement properties of symmetric states, we should first discuss their representations. Consider, for instance, a symmetric state, $|\psi\rangle$, of four qubits. Say that, in the computational basis, the element, $|0011\rangle$, in $|\psi\rangle$ has coefficient a . Given that $|\psi\rangle$ is invariant under permutations of the party labels, we should examine the permutations of $|0011\rangle$, which are

$$|0101\rangle, |1001\rangle, |0110\rangle, |1010\rangle, |1100\rangle. \quad (2.4)$$

To keep $|\psi\rangle$ invariant under permutations, each of the above elements in $|\psi\rangle$ should have the same coefficient, a . Turning to the other basis elements, it is then clear that each basis element should share the same coefficient with other elements of the same ‘Hamming Weight’, or number of 1’s in the string associated to that element. This leads to the grouping of basis elements by Hamming weight, i , into what is known as the Dicke basis [32],

$$|S_i^{(n)}\rangle = \binom{n}{i}^{-\frac{1}{2}} \sum_{\pi \in \mathcal{S}_n} U_\pi |\underbrace{00\dots 0}_{n-i} \underbrace{11\dots 1}_i\rangle. \quad (2.5)$$

The Dicke basis elements being normalized allows the overall state to be expressed as

$$|\psi\rangle = \sum_{i=0}^n a_i |S_i^{(n)}\rangle, \quad (2.6)$$

where $\sum |a_i|^2 = 1$. In this form we can already see the simplification offered by symmetric states in regards to the reduced degrees of freedom. The 2^n complex degrees of freedom in an unconstrained n qubit state are reduced to the $n + 1$ complex coefficients, a_i , in a symmetric state. Normalization and the factoring out of a global phase from the overall state leaves only n complex, or $2n$ real, degrees of freedom for a symmetric state of n qubits.

The Dicke basis is a natural starting point for the representation of symmetric multi-qubit states. Symmetric states of higher dimensional particles admit analogous bases, where computational basis elements are now grouped by the number of each possible entry, $1 - d$. Likewise, bases for other symmetries can be constructed by adjusting the sum over π to only the permutations associated to that symmetry. For both of these modifications, the normalization

coefficient would need adjusting as well.

2.1.1 The Majorana Representation

Other representations for symmetric states do exist, and offer intuitive and analytical advantages over the Dicke basis. An alternate representation was developed in [33] and is known as the ‘Majorana Representation’. The Majorana representation offers a powerful and intuitive geometric interpretation for symmetric states, their evolution under local unitary and SLOCC operations, and their geometric entanglement properties [29]. It states that to any n qubit symmetric state, $|\psi\rangle$, is associated a set of n pure, single qubit states, $\{|\phi_j\rangle\}$, each expressed as

$$|\phi_j\rangle = \cos \frac{\theta_j}{2} |0\rangle + \sin \frac{\theta_j}{2} e^{i\phi_j} |1\rangle. \quad (2.7)$$

The original state can remarkably be uniquely constructed by the sum over all permutations of product states in ϕ_j ,

$$|\psi\rangle = \frac{1}{\sqrt{A}} \sum_{\pi \in \mathcal{S}_n} U_\pi \bigotimes_{j=1}^n |\phi_j\rangle, \quad (2.8)$$

where the normalization coefficient, A , evaluates to

$$A = n! \sum_{\pi \in \mathcal{S}_n} \prod_{j=1}^n \langle \phi_j | \phi_{\pi(j)} \rangle. \quad (2.9)$$

At first glance, this representation is obviously symmetric and has the correct number of degrees of freedom; the $2n$ real angles $\{\theta_j\}$ and $\{\phi_j\}$. Note that the angles $\{\theta_j, \phi_j\}$ can be associated to points, $\{z_j\} \in \mathbb{R}_3$, on the Bloch sphere where

$$z_j = \{\sin \theta_j \cos \phi_j, \sin \theta_j \sin \phi_j, \cos \theta_j\}. \quad (2.10)$$

These points are referred to as the ‘Majorana Points’ and allow for a convenient visualization of a symmetric state by its set of n points on the Bloch sphere. Given that the Majorana representation is unique, the full space of symmetric states can be visualized as sets of points on the Bloch sphere.

I will now prove that any symmetric state can be uniquely described with the Majorana representation and show how to find the set of $\{|\phi_j\rangle\}$ from the Dicke basis coefficients, $\{a_i\}$.

Proof. Start by defining

$$|\Gamma\rangle = |\gamma\rangle^{\otimes n}, \quad (2.11)$$

which is n copies of the same pure single qubit state, $|\gamma\rangle = \cos \frac{\alpha}{2} |0\rangle + \sin \frac{\alpha}{2} e^{-i\beta} |1\rangle$. It will be useful to divide each of the $|\gamma\rangle$ by $\cos \frac{\alpha}{2}$ to observe that

$$|\gamma\rangle \propto |0\rangle + \gamma^* |1\rangle, \quad (2.12)$$

where $\gamma^* = \tan \frac{\alpha}{2} e^{-i\beta}$. Using this unnormalized version of $|\gamma\rangle$, the combined state can then be expressed as,

$$|\Gamma\rangle \propto \sum_{i=0}^n \sqrt{\binom{n}{i}} \gamma^{*i} |S_i^{(n)}\rangle. \quad (2.13)$$

This state allows us to pick out the $\{|\phi_i\rangle\}$ states that make up the Majorana representation of $|\psi\rangle$.

Consider the projection of $|\psi\rangle$ onto $|\Gamma\rangle$,

$$\langle \Gamma | \psi \rangle \propto \sum_{\pi \in S_n} \prod_{j=1}^n \langle \gamma | \phi_{\pi(j)} \rangle \quad (2.14)$$

$$\propto \prod_{j=1}^n \langle \gamma | \phi_j \rangle \quad (2.15)$$

This makes it clear that $|\psi\rangle$ and $|\Gamma\rangle$ are orthogonal if and only if $|\gamma\rangle$ is orthogonal to one or more of the $|\phi_i\rangle$. So constructing the Majorana representation becomes a matter of finding the $|\gamma\rangle$ which make $\langle \Gamma | \psi \rangle = 0$ and setting the $|\phi_j\rangle$'s to be the states orthogonal to the $|\gamma\rangle$'s. It is entirely possible, however, that some of the $|\phi_j\rangle$'s will be the same, which introduces degeneracy. We can see this by expanding the inner product,

$$\langle \Gamma | \psi \rangle \propto \sum_{i=0}^n a_i \gamma^i. \quad (2.16)$$

The polynomial in γ on the right-hand side of the above expression is known as the ‘Majorana Polynomial’. Its roots, $\{\gamma_j\}$, known as the ‘Majorana Roots’, are unique according first fundamental theorem of algebra. The Majorana roots also identify the $|\Gamma\rangle$ which are orthogonal to $|\psi\rangle$, so one can map the root γ_j to $|\phi_j\rangle = \sin \frac{\alpha_j}{2} |0\rangle - \cos \frac{\alpha_j}{2} e^{-i\beta_j} |1\rangle$. The degree of the root also then specifies how many copies of that state there are in the Majorana representation. By this method of finding the roots of the Majorana polynomial and converting them into the states, $|\phi_j\rangle$, the state $|\psi\rangle$ can be uniquely converted from the Dicke basis to the Majorana representation. \square

There is an important caveat to this procedure, however, which should be addressed. In order for one of the $|\phi_j\rangle$ to be a $|0\rangle$, the corresponding root, γ_j , would have to be infinite. This corresponds to the Majorana polynomial having degree less than n . When the degree of the Majorana polynomial, D , is less than n , there are exactly $n - D$ roots that approach infinity, and therefore $n - D$ of the $|\phi_j\rangle$ are $|0\rangle$.

The Majorana representation additionally allows for convenient visualization of symmetric LU operations on symmetric states. Consider the action of a symmetric local unitary operator, $U = U_1^{\otimes n}$, on $|\psi\rangle$,

$$U|\psi\rangle = \frac{1}{\sqrt{A}} \sum_{\pi \in S_n} U_\pi \bigotimes_{j=1}^n U_1 |\phi_j\rangle. \quad (2.17)$$

It is then clear that the Majorana representation for $U|\psi\rangle$ is constructed by the set of $\{U_1|\phi_j\rangle\}$. The new associated Majorana points are then the collective rotation of the original points by $U_1 \in O(3)$. The action of symmetric SLOCC operators also admits a geometric interpretation [34]. The conversion from γ_j to z_j is done in two steps; a stereographic projection of γ_j onto the Bloch sphere, followed by an inversion through the origin to find z_j . An SLOCC operator acting on $|\phi\rangle$ translates the Bloch sphere through \mathbb{R}_3 before performing the stereographic projection.

One might wonder if the Majorana representation extends to symmetric states of higher dimensional particles. This can be easily demonstrated to be impossible by counting the necessary degrees of freedom for such a representation. For instance, a symmetric state of two qutrits ($d = 3$) has 6 basis elements, and therefore has 10 real degrees of freedom after normalization and the elimination of a global phase. This does not agree with a pair of single qutrit states, which have 4 real degrees of freedom each, for a total of only 8.

2.1.2 Superposition of Product States

It was shown in [35] that a symmetric state of n qubits can be represented as a superposition of $D \leq n + 1$ symmetric product states,

$$|\psi\rangle = \sum_{j=1}^D x_j |\phi_j\rangle^{\otimes n}, \quad (2.18)$$

for some $x_j \in \mathbb{C}$ and $|\phi_j\rangle$ defined as in (2.7). This representation can be improved upon by an approximation, as discussed below, and will be revisited in Chapter 4 as a means to construct a matrix product state representation for symmetric states.

2.1.3 Canonical Forms

A powerful tool in the study of entanglement theory is the usage of canonical forms for quantum states. Local unitary operators can be used to simplify the state space and reduce the number of degrees of freedom, all while not changing the entanglement properties of those states. This fact has motivated the search for canonical forms which parametrize particular sets of states after the action of local unitaries. This has been successfully done for arbitrary multi-qubit states [36] as well as for symmetric states under the action of symmetric local unitaries to preserve the state symmetry. What follows is a compilation of canonical forms for symmetric states, the last of which is of my own creation. Each one eliminates 3 real degrees of freedom from the state space.

- *Rotated Majorana Representation:* The convenient visualization of local unitary rotations of symmetric states in the Majorana representation makes for an equally intuitive canonical form. The n states, $\{|\phi_j\rangle\}$, can be collectively rotated so that $|\phi'_1\rangle = |0\rangle$, preceding a final z -axis rotation to eliminate the phase of $|\phi'_2\rangle$, leaving

$$U|\psi\rangle = \frac{1}{\sqrt{A}} \sum_{\pi \in S_n} U_\pi |0\rangle \bigotimes_{j=2}^n U_1 |\phi'_j\rangle, \quad (2.19)$$

where $|\phi'_2\rangle = \cos \theta'_2 |0\rangle + \sin \theta'_2 |1\rangle$. This canonical form was presented in [37] and used to parametrize the SLOCC and LU invariants of symmetric 3 qubit states.

- *Mandilara Canonical Form:* The following form was originally developed in [38]. I slightly altered this form on three qubits in [39]. I showed and will now prove that most 3 qubit states,

$$|\psi\rangle = \sum_{i=0}^3 a_i |S_i^{(3)}\rangle, \quad (2.20)$$

can be transformed by symmetric local unitaries to

$$|\psi'\rangle = A \left(|000\rangle + ye^{i\phi} |\theta\rangle^{\otimes 3} \right), \quad (2.21)$$

where $y \in [0, 1)$, $\theta \in [0, \pi]$, $\phi \in [0, 2\pi)$, and $|\theta\rangle = \cos(\theta/2)|0\rangle + \sin(\theta/2)|1\rangle$ is a single qubit state with purely real coefficients, and A is a normalization constant.

Proof. Start by computing the Majorana polynomial, (2.16), of $|\psi\rangle$,

$$\langle \Gamma | \psi \rangle = a_0 + \sqrt{3}a_1\gamma + \sqrt{3}a_2\gamma^2 + a_3\gamma^3, \quad (2.22)$$

and the associated Majorana roots, $\{\gamma_j\}$. We can then alternately express $|\psi\rangle$ as

$$|\psi\rangle = A \left(|\phi_1\rangle^{\otimes 3} + c |\phi_2\rangle^{\otimes 3} \right), \quad (2.23)$$

where $|\phi_j\rangle$ are defined as in (2.7), $c \in \mathbb{C}$, and A is a normalization coefficient, by confirming that this state has the same Majorana roots for some choice of c , $\{\theta_j\}$, and $\{\phi_j\}$. The Majorana polynomial of (2.23) can be expressed as

$$\langle \Gamma | \psi \rangle = \left(\cos \theta_1 + \gamma \sin \theta_1 e^{i\phi_1} \right)^3 + c \left(\cos \theta_2 + \gamma \sin \theta_2 e^{i\phi_2} \right)^3. \quad (2.24)$$

Note that the normalization factor, A , has been dropped since this polynomial need only be specified up to a scaling factor. We can further simplify by dividing by $\cos \theta_1$, which leaves,

$$\langle \Gamma | \psi \rangle = (1 + \gamma\beta_1)^3 + c' (1 + \gamma\beta_2)^3, \quad (2.25)$$

where $\beta_j = \tan \theta_j e^{i\phi_j}$ and $c' = c(\cos \theta_2)/(\cos \theta_1)$. Enforcing that (2.22) and (2.25) have the same roots establishes the following constraints on $\{\beta_j\}$ and c' ,

$$0 = (1 + \gamma_1\beta_1)^3 + c' (1 + \gamma_1\beta_2)^3 \quad (2.26)$$

$$0 = (1 + \gamma_2\beta_1)^3 + c' (1 + \gamma_2\beta_2)^3. \quad (2.27)$$

Additionally, we can require that the projection of (2.23) onto $|\Gamma\rangle$ be the same as that of

(2.20) when evaluated at $\gamma = 0$, which provides the third constraint,

$$a_0 = c_1 (\cos \theta_1)^3 + c_2 (\cos \theta_2)^3. \quad (2.28)$$

Equations (2.26-2.28) provide sufficient constraints on $\{\beta_j\}$ and c' to equate the two representations of $|\psi\rangle$, so long as no Majorana root, γ_j , is degenerate with degree 2. We can then act on (2.23) by a local unitary, U , which rotates $|\phi_1\rangle$ to $|0\rangle$, resulting in

$$U|\psi\rangle = A(|000\rangle + c|\chi\rangle), \quad (2.29)$$

where $|\chi\rangle = U|\Phi_1\rangle = (\cos \theta/2|0\rangle + \sin \theta/2e^{i\chi}|1\rangle)^{\otimes 3}$. A final local unitary can then be applied to eliminate the relative phase in $|\chi\rangle$. \square

This method can be generalized to symmetric states of n qubits by expressing $|\psi\rangle$ as

$$|\psi\rangle = A \begin{cases} |\phi_1\rangle^{\otimes n} + \sum_{j=2}^{(n+1)/2} c_j |\phi_j\rangle^{\otimes n} & n \text{ odd} \\ |\phi_1\rangle^{\otimes n} + c_2 |\phi_1^\perp\rangle^{\otimes n} + \sum_{j=3}^{n/2} c_j |\phi_j\rangle^{\otimes n} & n \text{ even} \end{cases}, \quad (2.30)$$

where $\langle \phi_1^\perp | \phi_1 \rangle = 0$, so long as $|\psi\rangle$ has no Majorana roots degenerate with degree $2 \leq \mathcal{D} \leq n-1$. Local unitaries can then simplify the state to

$$|\psi'\rangle = A \begin{cases} |0\rangle^{\otimes n} + c_2 |\theta\rangle^{\otimes n} + \sum_{j=3}^{(n+1)/2} c_j |\phi'_j\rangle^{\otimes n} & n \text{ odd} \\ |0\rangle^{\otimes n} + |c_2| |1\rangle^{\otimes n} + \sum_{j=3}^{n/2} c_j |\phi'_j\rangle^{\otimes n} & n \text{ even} \end{cases}. \quad (2.31)$$

- *Rotated Dicke Basis:* The previous two canonical forms offer powerful simplifications to the state space, but are difficult to express in the computational basis, unlike the following form which is of my own development. I will show that an n qubit symmetric state can be rotated by symmetric local unitaries to

$$|\psi'\rangle = a'_0 S_0^{(n)} + a'_2 S_2^{(n)} + \sum_{i=3}^n a'_i |S_i^{(n)}\rangle, \quad (2.32)$$

where $a'_0, a'_2 \in \mathbb{R}$ and $a'_j \in \mathbb{C}$ for $j \geq 3$. Before doing so, however, it will be important to examine the proof of the following Lemma, which was originally presented in [40].

Lemma 1. *For any n qubit state,*

$$|\psi\rangle = \sum_{i_1, \dots, i_n=0}^1 a_{i_1 \dots i_n} |i_1 \dots i_n\rangle \quad (2.33)$$

there is a choice of bases for the tensor factors, rotated to by a local unitary, U , for which

$$U|\psi\rangle = \sum_{i_1, \dots, i_n=0}^1 a'_{i_1 \dots i_n} |i_1 \dots i_n\rangle \quad (2.34)$$

where $a_{i_1 \dots i_n} = 0$ if the Hamming weight of $|i_1 \dots i_n\rangle$ is 1.

Proof. Let $|\Phi\rangle = \bigotimes_{j=1}^n |\phi_j\rangle$ be an n qubit product state which maximizes the overlap with $|\psi\rangle$ over product states. Consider, then, acting upon $|\psi\rangle$ by the local unitary, U , for which $U|\Phi\rangle = |0\rangle^{\otimes n}$,

$$U|\psi\rangle = \sum_{i_1, \dots, i_n=0}^1 a'_{i_1 \dots i_n} |i_1 \dots i_n\rangle \quad (2.35)$$

We can show that in this basis, $a'_{i_1 \dots i_n} = 0$ if the Hamming weight of $|i_1 \dots i_n\rangle$ is 1, by contradiction. After the action of U , the inner product, $|\langle\Phi|\psi\rangle|^2$, evaluates to $|\langle 0|^{\otimes n} U|\psi\rangle|^2 = |a'_{0 \dots 0}|^2$. Consider the case where $a'_{10 \dots 0} \neq 0$. One could then act on $U|\psi\rangle$ by the local unitary,

$$V = \frac{1}{\sqrt{|a'_{0 \dots 0}|^2 + |a'_{10 \dots 0}|^2}} \begin{pmatrix} a'_{00 \dots 0} & a'_{10 \dots 0} \\ a'_{10 \dots 0} & -a'_{00 \dots 0} \end{pmatrix} \otimes \mathbb{1} \otimes \dots \otimes \mathbb{1} \quad (2.36)$$

which leaves $|\langle 0|^{\otimes n} VU|\psi\rangle|^2 = \sqrt{|a'_{00 \dots 0}|^2 + |a'_{10 \dots 0}|^2}$. But, by assumption, $|\Phi\rangle$ maximized the overlap with $|\psi\rangle$ and we therefore have a contradiction which forces $a'_{10 \dots 0} = 0$. The same argument can simultaneously be made for the coefficients of other basis elements with a Hamming weight of 1. \square

Note that this argument only applies to the Hamming weights of 1 and $n - 1$. If we tried to use the same idea to eliminate $a'_{110 \dots 0}$, up to local unitaries we could certainly mix $a'_{00 \dots 0}$ and $a'_{110 \dots 0}$ in the overlap with $|0\rangle^{\otimes n}$, but not without also including $a'_{100 \dots 0}$ and $a'_{010 \dots 0}$, which in general will not always increase the inner product.

I will now prove that (2.32) is a canonical form for symmetric states using the same notation as in the proof of Lemma 1.

Proof. For a symmetric state $|\psi\rangle$, it was shown in [41] that one can always find a *symmetric*

product state, $|\Phi\rangle = |\phi\rangle^{\otimes n}$, which maximizes $\langle\Phi|\psi\rangle$ over product states. This implies that the U for which $U|\Phi\rangle = |0\rangle^{\otimes n}$ is also symmetric, and therefore $U|\psi\rangle$ is likewise symmetric. Following the arguments of the proof of Lemma 1, it follows that $a'_1 = 0$ because $|\mathcal{S}_1^{(n)}\rangle$ is a collection of basis elements with Hamming weights of 1. A final phasing local unitary can then be applied to leave a'_2 real. \square

One might wonder if such a canonical form can be applied to spaces with different symmetries, say for the translationally invariant states examined in the next chapter. Unfortunately, this is not the case, as one is not guaranteed to find a symmetric product state with maximal overlap for states with weaker symmetries [41].

2.2 Invariants of Three Qubit Symmetric States

Any multi-particle state has a set of polynomials in the coefficients of the state which are invariant under the action of various local operators [42]. In particular, a 3 qubit state, under the action of local unitaries, is known to have 5 algebraically independent polynomial invariants, as well as the state norm and \mathbb{Z}_2 invariants [43]. There is some freedom in choosing 5 generators of the algebra of invariant polynomials, as any polynomial in invariants is additionally an invariant of the state. One set of generators which is particularly convenient for 3 qubit states under local unitary operators is

$$\{\mathcal{C}_{1,2}, \mathcal{C}_{2,3}, \mathcal{C}_{3,1}, \tau, \kappa\}, \quad (2.37)$$

where $\mathcal{C}_{i,j}$ is the pairwise concurrence between parties i and j , τ is the three-tangle, and κ is the Kempe invariant [44]. which is defined for a 3 qubit state, $|\psi\rangle = \sum_{i,j,k=0}^1 a_{ijk} |ijk\rangle$, as

$$\kappa = a_{i_1 j_1 k_1} a_{i_2 j_2 k_2} a_{i_3 j_3 k_3} a_{i_1 j_2 k_3}^* a_{i_2 j_3 k_1}^* a_{i_3 j_1 k_2}^*. \quad (2.38)$$

Note that in the above expression I have adopted the convention of summing over repeated indices. This choice of invariants is particularly useful as it uses some of the most prevalent entanglement measures in the concurrence and three-tangle.

As mentioned in Chapter 1, the concurrence and three-tangle for 3 qubit states is constrained by (1.61), but no such constraints are known for all 5 invariants of arbitrary states. For symmetric states of 3 qubits, however, I was able to determine the full achievable space of the invariants [39]. Symmetric states offer a significant simplification to the picture of 3 qubit invariants. Clearly, if a state is symmetric under relabeling of parties, each of the two-party reduced density operators, $\rho_{i,j}$, will be identical. This then causes $\mathcal{C}_{1,2} = \mathcal{C}_{2,3} = \mathcal{C}_{3,1} = \mathcal{C}$ and effectively reduces the number of invariants to 3, which will be denoted,

$$\{\mathcal{C}, \tau, \kappa\}. \quad (2.39)$$

These invariants can be directly calculated from my version of the Mandilara canonical form (2.21). In terms of the parameters y , θ , and ϕ , the invariants are,

$$\tau = \frac{2y \sin^3 \frac{\theta}{2}}{1 + y^2 + 2y \cos^3 \frac{\theta}{2} \cos \phi}, \quad (2.40)$$

$$\mathcal{C} = \frac{y \sin \frac{\theta}{2} \sin \theta}{1 + y^2 + 2y \cos^3 \frac{\theta}{2} \cos \phi}, \quad (2.41)$$

$$\begin{aligned} \kappa = & \frac{1}{8(1 + y^2 + 2y \cos^3 \frac{\theta}{2} \cos \phi)} \times \\ & \left[(1 + y^2)(8 + 19y^2 + 8y^4 + 9y^2(4 \cos \theta + \cos 2\theta)) \right. \\ & + 24y \cos^3 \frac{\theta}{2} (2 + 3y^2 + 2y^4 + 3y^2 \cos \theta) \cos \phi \\ & \left. + 48y^2 (1 + y^2) \cos^6 \frac{\theta}{2} \cos 2\phi + 16y^3 \cos^9 \frac{\theta}{2} \cos 3\phi \right]. \end{aligned} \quad (2.42)$$

Figure 2.1 shows the invariants of 10^5 randomly generated symmetric 3 qubit states, where the states were generated by sampling randomly over the allowed values of y , θ , and ϕ . At a first glance, it is interesting to note that the three-tangle and Kempe invariants achieve their maximum values of 1 on the symmetric subspace, but the concurrence does not due its monogamy constraints [19]. A straightforward maximization over the state parameters reveals a maximum concurrence of $2/3$ in the symmetric subspace, which confirms the result of [21] for $n = 3$. The points of Figure 2.1 appear to lie almost on a surface, but closer inspection reveals that they in fact fill a narrow volume, the boundaries of which can be calculated. We can invert the expressions

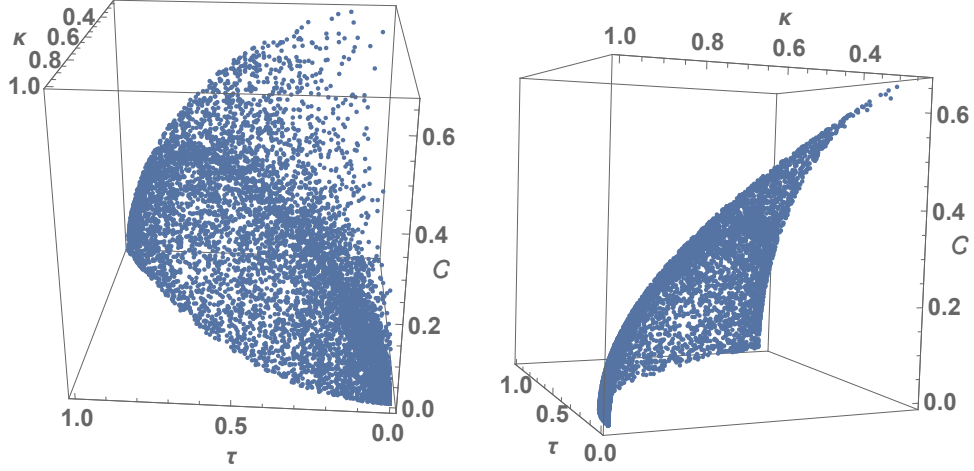


Figure 2.1: Scatterplot from two points of view of invariants of randomly generated symmetric 3 qubit states.

(2.40-2.42) by a Gröbner basis calculation to find,

$$\cos \frac{\theta}{2} = \frac{\mathcal{C}}{\sqrt{\mathcal{C}^2 + \tau^2}}, \quad (2.43)$$

$$\cos \phi = \frac{4 - 3\tau^2 - 9\mathcal{C}^2 - 4\kappa}{3\mathcal{C}^3}, \quad (2.44)$$

$$y = \frac{6\tau^2 + 9\mathcal{C}^2 + 4\kappa - 4}{3(\tau^2 + \mathcal{C}^2)^{3/2}} - \sqrt{\left(\frac{6\tau^2 + 9\mathcal{C}^2 + 4\kappa - 4}{3(\tau^2 + \mathcal{C}^2)^{3/2}}\right)^2 - 1}. \quad (2.45)$$

The constraints on the state parameters then provide constraints on these functions of the invariants.

The extrema of these constraints are the surfaces which form the boundaries of the invariant space.

The boundaries are formed when equality is achieved in the following relations,

$$0 \leq 4 - \tau^2 - 9\mathcal{C}^2 - 4\kappa + 3\mathcal{C}^3 \quad (2.46)$$

$$0 \geq 4 - \tau^2 - 9\mathcal{C}^2 - 4\kappa - 3\mathcal{C}^3 \quad (2.47)$$

$$0 \geq 4 - 6\tau^2 - 9\mathcal{C}^2 - 4\kappa + 3(\tau^2 + \mathcal{C}^2)^{3/2}. \quad (2.48)$$

These three surfaces, which are shown in Figure 2.2, form boundaries for the possible space of the invariants and serve as additional monogamy relations for symmetric 3 qubit entanglement. Note that the state parameter constraints lead to more constraints on the invariants, but (2.46-2.48) is the minimal set of constraints required to describe the region. Because there is

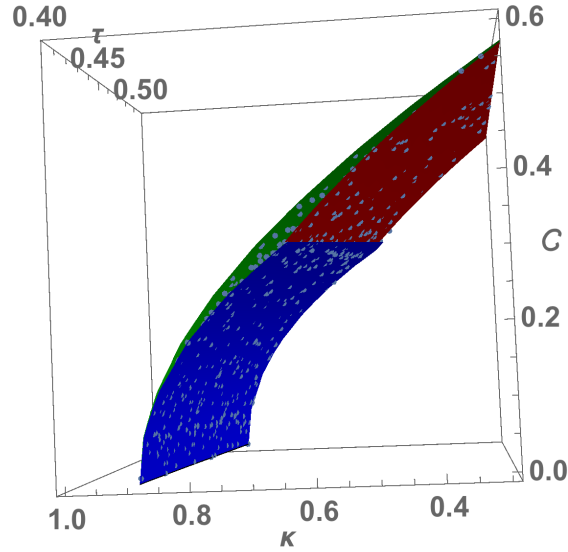


Figure 2.2: View of a slice of the boundaries of the volume of symmetric 3 qubit invariants superimposed over the points of Figure 2.1. The contour achieving equality in (2.46) is shown in green (the upper-left surface), (2.47) in blue (lower-left), and (2.48) in red (upper-right).

a bijective map between the invariants and the state parameters, each invariant triple which lies within the region satisfying (2.46-2.48) can be mapped to a 3 qubit symmetric state, and therefore the entire region is achievable.

We should at this point address the states which do not admit the use of the Mandilara canonical form, which are denoted as $\{|\bar{\psi}\rangle\}$. Recall that a state, $|\bar{\psi}\rangle$, has a degenerate Majorana root with degree 2 [38]. Thankfully, we can show that the invariants of the states in $\{|\bar{\psi}\rangle\}$ likewise satisfy (2.46-2.48). An arbitrary 3 qubit state with a degenerate Majorana root of degree 2 can be expressed in the Majorana representation as

$$|\bar{\psi}\rangle = \frac{1}{A} \sum_{\pi \in S_3} \pi |\phi_1\rangle \otimes |\phi_1\rangle \otimes |\phi_2\rangle, \quad (2.49)$$

We can again use local unitaries to simplify states of this form to

$$|\bar{\psi}'\rangle = \frac{1}{A} \sum_{\pi \in S_3} \pi |0\rangle \otimes |0\rangle \otimes |\theta\rangle, \quad (2.50)$$

where $|\theta\rangle$ is of the same form as (2.21). The invariants of (2.50) are

$$\tau = 0, \tag{2.51}$$

$$\kappa = \frac{2 + 48 \cos^2 \frac{\theta}{2} + 141 \cos^4 \frac{\theta}{2} + 52 \cos^6 \frac{\theta}{2}}{9(1 + 2 \cos^2 \frac{\theta}{2})^3}, \tag{2.52}$$

$$\mathcal{C} = \frac{2 - 2 \cos^2 \frac{\theta}{2}}{3 + 6 \cos^2 \frac{\theta}{2}}. \tag{2.53}$$

It is then easy to verify that (2.51-2.53) satisfy (2.46-2.48) for $\theta \in (0, \pi]$. This is perhaps unsurprising given that the states with a degenerate Majorana root of degree 2 are a limiting case of states which admit the canonical form. Now all 3 qubit symmetric states have been considered and it can be concluded that (2.46-2.48) do indeed describe the full achievable region for 3 qubit symmetric states.

A similar approach could be used to analyze the invariants of n qubits for the symmetric subspace. 3 qubits, in particular, can be fully analyzed and visualized because the number of invariants and state parameters is suitably low. Additionally, in the 3 qubit case, remarkably there is an invertible map between the state parameters and the invariants, allowing for our calculation of the achievable region. Turning to the $n > 3$ qubit case, [37] and [34] use the Majorana representation to examine the SLOCC classes and invariants of symmetric states, but the LU invariants remain less explored. The inner products of the vectors in the Majorana representation are themselves a set of $2n - 3$ LU invariants, as used in [37]. It would be interesting to find an alternate set of $2n - 3$ algebraically independent LU invariants which includes pertinent entanglement measures. That set of invariants could potentially then be calculated in terms of the $2n - 3$ state parameters. The remarkable fact that this map was invertible for 3 qubits will not necessarily be true in the n qubit case, though it is certainly worth examining.

2.3 Local Unitary Equivalence of Symmetric States

The results of the previous section well motivate the value of restricting entanglement calculations to the symmetric subspace. Those results need not *only* be applied to symmetric

states though, as the class of states which can be achieved by acting on symmetric states by local unitaries will have identical entanglement properties to those of symmetric states. This then begs the question: How can one identify whether or not a non-symmetric state, $|\psi\rangle$, can be rotated by local unitaries to a symmetric state? This concept of LU equivalence is one which has been well studied in the general case due to its implications not only to entanglement theory, but also to quantum communication and quantum algorithms, where the initial states can be freely transformed by local unitaries.

Necessary conditions for LU equivalence were found in [45] and admit an intuitive interpretation. Consider an n qubit state, $|\psi\rangle$, and its single particle reduced density matrices, $\{\rho_i\}$. The action of a local unitary, $U = \bigotimes_{i=1}^n U_i$ on $|\psi\rangle$ can, in part, be seen as the rotation of ρ_i by U_i . This is convenient because the single party density matrices and their rotations are easy to visualize thanks to their geometric interpretation through the ‘Bloch Ball’. Namely, $\rho_i = \frac{1}{2}\mathbb{1}_2 + \frac{1}{2}\vec{n}_i \cdot \vec{\sigma}$, where $\vec{\sigma}$ is the vector of Pauli matrices, and $\vec{n}_i \in \mathbb{R}^3$ is the Bloch vector for ρ_i and is constrained by $|\vec{n}_i| \leq 1$. It then follows that $U_i \rho_i U_i^\dagger = \frac{1}{2}\mathbb{1}_2 + \frac{1}{2}\vec{n}'_i \cdot \vec{\sigma}$, where \vec{n}'_i is the rotation of \vec{n}_i by the $O(3)$ representation of U_i and therefore $|\vec{n}_i| = |\vec{n}'_i|$. So acting on $|\psi\rangle$ by a local unitary simply rotates each of its single party Bloch vectors in \mathbb{R}^3 , which is considerably easier to interpret than unitary transformations on $(\mathbb{C}^2)^{\otimes n}$. The obvious necessary condition for unitary equivalence is then that $|\psi\rangle$ and $|\psi'\rangle$, with respective single party Bloch vectors, $\{\vec{n}_i\}$ and $\{\vec{n}'_i\}$, are equivalent to each other under local unitaries only if $|\vec{n}_i| = |\vec{n}'_i| \forall i$.

There is a notable limitation to the condition that $|\vec{n}_i| = |\vec{n}'_i| \forall i$, which prevents it from alone being a sufficient for LU equivalence. The limitation is that if $|\vec{n}_i| = |\vec{n}'_i| = 0$ for at least one party, then we lose not only the nice geometric interpretation of the action of U , but the sufficiency of this condition for LU equivalence. Resolutions to this issue are discussed in [45], but they leave the problem challenging analytically. Thankfully, for symmetric state of 3 qubits, we can resolve this issue and additionally we can reinterpret the LU equivalence condition in terms of entanglement.

For symmetric states, the single party Bloch vectors obey $\vec{n}_i = \vec{n} \forall i$, and therefore so too must any state which is LU equivalent to a symmetric state. In the case of 2 qubits, the Schmidt decomposition implies that any state is LU equivalent to a symmetric one. Moving to the 3 qubit case, consider an arbitrary state, $|\psi\rangle$, with single party Bloch vectors $\{\vec{n}_i\}$. In this setting I will now prove that $|\vec{n}_1| = |\vec{n}_2| = |\vec{n}_3|$ is a necessary and sufficient condition for $|\psi\rangle$ being LU equivalent to a symmetric state.

Proof. Start by acting on $|\psi\rangle$ by a local unitary which leaves it in the canonical form presented in [36],

$$|\psi'\rangle = a|000\rangle + b_1|100\rangle + b_2|010\rangle + b_3|001\rangle + ce^{i\phi}|111\rangle, \quad (2.54)$$

where $a, b_1, b_2, b_3, c > 0$ and $0 \leq \phi \leq \pi$. The single party reduced states of this state are then

$$\rho_1 = \begin{pmatrix} a^2 + b_1^2 + b_2^2 & ab_3 \\ ab_3 & b_3^2 + c^2 \end{pmatrix}, \quad (2.55)$$

$$\rho_2 = \begin{pmatrix} a^2 + b_1^2 + b_3^2 & ab_2 \\ ab_2 & b_2^2 + c^2 \end{pmatrix}, \quad (2.56)$$

$$\rho_3 = \begin{pmatrix} a^2 + b_2^2 + b_3^2 & ab_1 \\ ab_1 & b_1^2 + c^2 \end{pmatrix}. \quad (2.57)$$

To constrain the state such that $|\vec{n}_1| = |\vec{n}_2| = |\vec{n}_3|$, we can equivalently enforce that $\text{Tr}(\rho_1^2) = \text{Tr}(\rho_2^2) = \text{Tr}(\rho_3^2)$ because

$$\text{Tr}(\rho_i^2) = \frac{1}{2} + \frac{1}{2}|\vec{n}_i|^2. \quad (2.58)$$

This then results in the following set of conditions,

$$(b_i^2 - c^2)(b_j^2 - b_k^2) = 0, \quad (2.59)$$

for distinct i, j , and k . In satisfying (2.59), one may chose $b_1 = b_2 = b_3$, which is obviously already symmetric, or $b_i = b_j = c$ with b_k unconstrained. Without loss of generality, we can choose $b_1 = b$ and $b_2 = b_3 = c$, leaving the state as

$$|\psi'\rangle = a|000\rangle + b|100\rangle + c|010\rangle + c|001\rangle + ce^{i\phi}|111\rangle. \quad (2.60)$$

All that remains now is to find a local unitary which rotates this state to a symmetric one. Consider a local unitary, $U = U_1 \otimes U_2 \otimes U_3$. The symmetry between parties 2 and 3 in (2.60) implies that the suitable local unitary will obey $U_2 = U_3$. We can then factor out $U_2^{\otimes 3}$ from U , which leaves it in the form

$$U = (U_2^{\otimes 3})(U_2^\dagger U_1 \otimes \mathbb{1} \otimes \mathbb{1}) = (U_2^{\otimes 3})(U_1' \otimes \mathbb{1} \otimes \mathbb{1}). \quad (2.61)$$

We can then ignore the $U_2^{\otimes 3}$ component, as it simply rotates the state within the symmetric subspace. This leaves only the determination of U_1' , which can be parametrized as

$$U_1' = \begin{pmatrix} \cos \theta e^{i\alpha} & \sin \theta e^{i\beta} \\ -\sin \theta e^{-i\beta} & \cos \theta e^{-i\alpha} \end{pmatrix}. \quad (2.62)$$

To enforce that $|\psi''\rangle = U_1 \otimes \mathbb{1} \otimes \mathbb{1} |\psi'\rangle$ is symmetric we must require that $\langle 001 | \psi'' \rangle = \langle 010 | \psi'' \rangle = \langle 100 | \psi'' \rangle$ and $\langle 011 | \psi'' \rangle = \langle 110 | \psi'' \rangle = \langle 101 | \psi'' \rangle$, which evaluates to two complex conditions,

$$\cos \theta (b e^{-i\alpha} - c e^{i\alpha}) - a \sin \theta e^{-i\beta} = 0, \quad (2.63)$$

$$c \sin \theta (e^{i(\beta+\phi)} + e^{-i\beta}) = 0. \quad (2.64)$$

Examining (2.64) first, we must consider each solution. If $c = 0$, then the state is separable, and therefore trivially LU equivalent to a symmetric product state. If $\sin \theta = 0$, equation (2.63) would enforce $b = c$, which is symmetric. This leaves $\beta = \frac{\pi - \phi}{2}$. Using this to constrain (2.63) and solving its real and imaginary components yields the following solutions for θ and α .

$$\tan \alpha = \frac{c - b}{b + c} \tan \frac{\phi - \pi}{2}, \quad (2.65)$$

$$\tan \theta = \frac{(b - c) \cos \alpha}{a \cos \frac{\phi - \pi}{2}}. \quad (2.66)$$

These angles determine U_1' and leave $|\psi''\rangle$ symmetric. \square

As an aside, starting again from (2.54), one can determine the pairwise concurrences by using the following identity,

$$\sqrt{\alpha + \sqrt{\beta}} - \sqrt{\alpha - \sqrt{\beta}} = \sqrt{2\alpha - 2\sqrt{\alpha^2 - \beta}}. \quad (2.67)$$

From here, enforcing that $\mathcal{C}_{1,2} = \mathcal{C}_{2,3} = \mathcal{C}_{3,1}$ remarkably arrives again at (2.59). This implies that $\mathcal{C}_{1,2} = \mathcal{C}_{2,3} = \mathcal{C}_{3,1}$ is likewise a necessary and sufficient condition for $|\psi\rangle$ being LU equivalent

to a symmetric state.

Moving to states of more than three qubits, it can be shown that $|\vec{n}_i| = |\vec{n}_j| \forall i, j$ is no longer a sufficient condition for LU equivalence to symmetric states, nor is $\mathcal{C}_{i,j} = \mathcal{C}_{k,l} \forall i \neq j, k \neq l$. We can draw on a counterexample from the following theorem which was presented in [31],

Theorem 1. *The k particle reduced density matrices of a pure symmetric state of n qubits cannot be fully mixed for $2 \leq k < n$.*

This contradicts my proposed sufficient conditions for LU equivalence to symmetric states because we can examine the following unnormalized state,

$$|0_L\rangle = |00000\rangle + \sum_{\pi \in \mathbb{Z}_5} U_\pi (|11000\rangle - |10100\rangle - |01111\rangle), \quad (2.68)$$

whose single and two party reduced density matrices are each fully mixed [46]. This would then satisfy both of our proposed conditions for LU equivalence to symmetric states, but cannot be LU equivalent to a symmetric state according to Theorem 1.

While it is not the case that either $|\vec{n}_i| = |\vec{n}_j| \forall i, j$ or $\mathcal{C}_{i,j} = \mathcal{C}_{k,l} \forall i \neq j, k \neq l$ are sufficient conditions for LU equivalence to symmetric states, one might be able to make somewhat different statements regarding symmetric LU equivalence. It may be the case that $|\vec{n}_i| = |\vec{n}_j| \forall i, j$ is a sufficient condition for LU equivalence to translationally invariant states, a distinction which is made evident by considering the generalized Bloch vector representation detailed in Appendix C. Likewise, it may be that a state with translationally invariant pairwise concurrences is necessarily LU equivalent to a translationally invariant state. Alternatively it may be the case that $\mathcal{C}_{i,j} = \mathcal{C}_{k,l} \forall i \neq j, k \neq l$ is sufficient for LU equivalence to symmetric states so long as $\mathcal{C}_{i,j} > 0$. Each of these are open questions of great interest to me.

This work is, in part, a reprint of material from published work done in collaboration with David Meyer, as it appears in Physical Review A, as well as on the arXiv. Alexander Meill and David A. Meyer, ‘‘Symmetric 3 Qubit Invariants,’’ Phys. Rev. A **96**, 062310 (2017), arXiv:1702.07295. The dissertation author was the primary investigator and author of this material.

Chapter 3

Translationally Invariant States

Among the possible symmetries to enforce on a quantum state, translational invariance (TI) is a common and natural choice. This is due largely, in part, to their applications in physically relevant condensed matter systems with the same symmetry [47][48], such as 1-D spin chains with periodic boundary conditions [49]. Translationally invariant states have accordingly been a fruitful subject for entanglement theoretic research [50] and SLOCC class descriptions [47].

Translational invariance of quantum states can be defined in much the same way that we defined full permutation symmetry, with the only difference being that we only consider the cyclic subgroup of the full permutation group.

Definition 4. An n qubit state, $|\psi\rangle$ is *translationally invariant* if

$$U_\pi |\psi\rangle = |\psi\rangle \quad \forall \quad \pi \in \mathbb{Z}_n \subset S_n, \quad (3.1)$$

where U_π is the unitary representation of π on n qubits.

We can likewise define basis elements for translationally invariant states which mirror the Dicke basis for symmetric states. Let a normalized n qubit TI basis element be denoted with an overbrace,

$$\overbrace{|i_1 \dots i_n\rangle} = |\mathbb{Z}_n |i_1 \dots i_n\rangle|^{-\frac{1}{2}} \sum_{\pi \in \mathbb{Z}_n} U_\pi |i_1 \dots i_n\rangle, \quad (3.2)$$

where $|\mathbb{Z}_n |i_1 \dots i_n\rangle|$ denotes the cardinality of the orbit of $|i_1 \dots i_n\rangle$ under the action of the \mathbb{Z}_n cyclic permutation group. As an example, consider the 4 qubit basis element

$$\overbrace{|0011\rangle} = \frac{1}{2} \left[|0011\rangle + |1001\rangle + |1100\rangle + |0110\rangle \right], \quad (3.3)$$

which is notably different from the Dicke basis element $|S_2^{(4)}\rangle$, which symmetrizes $\overbrace{|0011\rangle}$ and $\overbrace{|0101\rangle}$. In this sense we can clearly see that translational invariance is a weaker symmetry than full permutation symmetry, and so the translationally invariant subspace is larger than the fully symmetric one. Likewise it offers a weaker constraint on pairwise entanglement, which we will exclusively examine via the pairwise concurrence in this chapter.

The cyclic symmetry implies that for any pairwise concurrence, $\mathcal{C}_{i,j}$, between parties i and j , $\mathcal{C}_{i,j} = \mathcal{C}_{i+k,j+k}$ for any $k \in \mathbb{Z}$, where the party label subscripts are to be evaluated mod n . So each allowable pairwise concurrence in a TI state corresponds to the spacing between party labelings. As a point of notation, define $\mathcal{C}_k^{(n)}$ to be the pairwise concurrence between parties k -away in an n qubit TI state. Note that k runs from 1 to $\lfloor \frac{n}{2} \rfloor$, as any $k > \frac{n}{2}$ is equivalent to the $n - k$ spacing. The $\lfloor \frac{n}{2} \rfloor$ distinct $\mathcal{C}_k^{(n)}$ is reduced from the $\binom{n}{2}$ distinct pairs in a general n qubit state.

The entanglement picture in TI states is further simplified by the fact that many $\mathcal{C}_k^{(n)}$ share the same properties. To see this, consider some m which is not a factor of n , and the associated permutation, $\pi \in S_n$,

$$\pi : i \mapsto mi \pmod n. \quad (3.4)$$

Note that π is invertible only when $m = 1$ or $m \nmid n$. Permuting the party labels of some TI state, $|\psi\rangle$, according to π^{-1} will leave the state in some new TI state, $|\chi\rangle = U_{\pi^{-1}} |\psi\rangle$, which obeys $\mathcal{C}_{i,j}(|\psi\rangle) = \mathcal{C}_{\pi(i),\pi(j)}(|\chi\rangle)$. This means that any properties of $\mathcal{C}_k^{(n)}$ will be shared by $\mathcal{C}_{mk}^{(n)}$ for each m which is not a factor of n . It then suffices to only examine the constraints on $\mathcal{C}_k^{(n)}$ for k which are factors of n .

These simplifications, along with the natural reduction in state parameters, makes an

analytic description of the entanglement of TI states more approachable. In this chapter I present a preliminary analysis of the allowed pairwise concurrences in TI states. Both maximal pairwise entanglement as well as monogamy constraints for shared entanglement are considered. Due to the extensive nature of the calculations, significant portions of analysis are relegated to Appendix A.

3.1 Maximal Pairwise Concurrence

A natural question when examining a subset of quantum states is; which states maximize entanglement within that subset, and what is that maximal entanglement? Within the translationally invariant subspace, we need only examine the maxima of $\mathcal{C}_k^{(n)}$ for $1 \leq k \leq \lfloor \frac{n}{2} \rfloor$ and $k|n$. Denote a state which maximizes $\mathcal{C}_k^{(n)}$ as $|\psi_k^{(n)}\rangle$. Finding the $|\psi_k^{(n)}\rangle$ and the associated maximal $\mathcal{C}_k^{(n)}$ is greatly simplified by the following theorem, which was the main result of my work in [51],

Theorem 2. For $k|n$, $\max \mathcal{C}_k^{(n)} = \max \mathcal{C}_1^{(n/k)}$, and a corresponding state which maximizes $\mathcal{C}_k^{(n)}$ can be constructed as

$$|\psi_k^{(n)}\rangle = \bigotimes_{i=0}^{k-1} |\psi_1^{(n/k)}\rangle_{k\{n/k\}+i}, \quad (3.5)$$

where $\{n/k\}$ represents the set of integers from 0 to $n/k - 1$. These integers, multiplied by k then incremented by i , indicate the party labelings in the overall state.

Proof. Consider some n qubit TI state, $|\psi^{(n)}\rangle = \sum_{\mathbf{i} \in \mathbb{Z}_2^n} a_{\mathbf{i}} |\mathbf{i}\rangle$, and some $k|n$. Examine the reduced density matrix,

$$\rho_{k\{n/k\}} = \text{Tr}_{k\{n/k\}} \left(|\psi^{(n)}\rangle \langle \psi^{(n)}| \right) \quad (3.6)$$

$$= \sum_{\mathbf{j} \in \mathbb{Z}_2^{n-n/k}} \sum_{\mathbf{x}, \mathbf{y} \in \mathbb{Z}_2^{n/k}} a_{\mathbf{j}, \mathbf{x}} |\mathbf{x}\rangle \langle \mathbf{y}| a_{\mathbf{j}, \mathbf{y}}^*, \quad (3.7)$$

where \mathbf{x} and \mathbf{y} indicate basis elements in the parties in $k\{n/k\}$, while \mathbf{j} indicates basis elements in the remaining $n - n/k$ parties. Notably, this reduced state obeys, by definition, $\mathcal{C}_1^{(n/k)}(\rho_{k\{n/k\}}) =$

$$\mathcal{E}_k^{(n)} \left(\left| \psi^{(n)} \right\rangle \right).$$

Now label any $\pi \in \mathbb{Z}_n \subset S_n$ as

$$\pi_m^{(n)} : i \mapsto i + m \pmod{n}. \quad (3.8)$$

We can then examine that for any m ,

$$U_{\pi_{n/k-m}^{(n/k)}} \rho_{k\{n/k\}} = \sum_{\mathbf{j}} \sum_{\mathbf{x}, \mathbf{y}} \psi_{\mathbf{j}, \pi_m^{(n/k)}(\mathbf{x})} |\mathbf{x}\rangle \langle \mathbf{y}| \psi_{\mathbf{j}, \mathbf{y}}^* \quad (3.9)$$

$$= \sum_{\mathbf{j}} \sum_{\mathbf{x}, \mathbf{y}} \psi_{\pi_{km}^{(n)}(\mathbf{j}, \mathbf{x})} |\mathbf{x}\rangle \langle \mathbf{y}| \psi_{\mathbf{j}, \mathbf{y}}^* \quad (3.10)$$

$$= \rho_{k\{n/k\}}, \quad (3.11)$$

where the first equality describes the action of a permutation on the parties in $k\{n/k\}$, the second extends that permutation to the n parties and rearranges using the sum over \mathbf{j} , and the third uses the cyclic symmetry of $\left| \psi^{(n)} \right\rangle$. And so for any $\pi \in \mathbb{Z}_{n/k}$,

$$U_\pi \rho_{k\{n/k\}} = \rho_{k\{n/k\}} U_\pi = \rho_{k\{n/k\}}. \quad (3.12)$$

Since $\rho_{k\{n/k\}}$ commutes with U_π for $\pi_1^{(n/k)}$, they can be simultaneously diagonalized into a basis $\{|\phi_j\rangle\}$. Since U_π for $\pi_1^{(n/k)}$ is unitary, its eigenvalues associated to each $|\phi_j\rangle$ can be labeled as $\lambda_j = e^{i\phi_j}$. We can then examine

$$U_\pi \rho_{k\{n/k\}} = \sum_j p_j U_\pi |\phi_j\rangle \langle \phi_j| \quad (3.13)$$

$$= \sum_j p_j e^{i\phi_j} |\phi_j\rangle \langle \phi_j|, \quad (3.14)$$

which, according to (3.12), must be equal to the original $\rho_{k\{n/k\}}$. This is only possible if $e^{i\phi_j} = 1$ for each j , implying that $|\phi_j\rangle$ are each TI states.

Lastly, order the eigenstates to be decreasing in $\mathcal{E}_1^{(n/k)}(|\phi_j\rangle)$. By the convexity of the pairwise concurrence, it then follows that

$$\mathcal{E}_1^{(n/k)}(\rho_{k\{n/k\}}) = \mathcal{E}_1^{(n/k)}\left(\sum_j p_j |\phi_j\rangle \langle \phi_j|\right) \quad (3.15)$$

$$\leq \sum_j p_j \mathcal{E}_1^{(n/k)}(|\phi_j\rangle) \quad (3.16)$$

$$\leq \mathcal{E}_1^{(n/k)}(|\phi_1\rangle) \quad (3.17)$$

$$\leq \mathcal{E}_1^{(n/k)}\left(\left|\psi_1^{(n/k)}\right\rangle\right), \quad (3.18)$$

with the inequality being saturated by the state, (3.5). \square

Interestingly, convexity was the only property of the concurrence used in the proof of Theorem 2, meaning that any convex entanglement measure would obey an analogous statement in TI states.

Notably, (3.5) also agrees with the monogamy behavior examined in the next section, as each of $\mathcal{C}_{j \neq k}^{(n)} \left(\left| \psi_k^{(n)} \right\rangle \right) = 0$. As a result of Theorem 2, all that remains is to find $\mathcal{C}_1^{(n)}$ for each n . For $n \leq 3$, the TI subspace is equivalent to the totally symmetric one, where the maxima have previously been determined. This leads to $\max \mathcal{C}_1^{(2)} = 1$ with $\left| \psi_1^{(2)} \right\rangle = \frac{1}{\sqrt{2}}(|00\rangle + |11\rangle)$ and $\max \mathcal{C}_1^{(3)} = \frac{2}{3}$ with $\left| \psi_1^{(3)} \right\rangle = \frac{1}{\sqrt{3}}(|001\rangle + |010\rangle + |100\rangle)$ [21].

Turning to $n \geq 4$, no precise results are known, though a lower bound on maximal entanglement was presented in [50]. I was able to improve this bound for $n = 4$ and $n = 5$ in [51].

Consider arbitrary normalized 4 and 5 qubit TI states,

$$\left| \psi^{(4)} \right\rangle = a|0000\rangle + b\overbrace{|0001\rangle} + c\overbrace{|0011\rangle} + d\overbrace{|0101\rangle} + e\overbrace{|0111\rangle} + f|1111\rangle, \quad (3.19)$$

$$\begin{aligned} \left| \psi^{(5)} \right\rangle = & a|00000\rangle + b\overbrace{|00001\rangle} + c\overbrace{|00011\rangle} + d\overbrace{|00101\rangle} \\ & + e\overbrace{|00111\rangle} + f\overbrace{|01011\rangle} + g\overbrace{|01111\rangle} + h|11111\rangle. \end{aligned} \quad (3.20)$$

Unfortunately, even calculating $\mathcal{C}_1^{(4)}$ and $\mathcal{C}_1^{(5)}$ for arbitrary states is analytically challenging, let alone maximizing over that space. Instead, the calculation will be performed on the even-X state subspaces for $n = 4$ and $n = 5$. Even-X states (abbreviated X states), introduced in [52], are superpositions of only computational basis elements with even Hamming weight. Notably, the set of states TI states examined in [50] are a subset of the TIX states. Arbitrary 4 and 5 qubit TIX states then take the form,

$$\left| \psi_X^{(4)} \right\rangle = a|0000\rangle + c\overbrace{|0011\rangle} + d\overbrace{|0101\rangle} + f|1111\rangle, \quad (3.21)$$

$$\left| \psi_X^{(5)} \right\rangle = a|00000\rangle + c\overbrace{|00011\rangle} + d\overbrace{|00101\rangle} + g\overbrace{|01111\rangle}. \quad (3.22)$$

The X state subspace is a useful one as concurrence calculations on the space are rather simple.

Two qubit reduced density matrices of X states were shown in [52] to be of the form

$$\rho = \begin{pmatrix} \alpha & 0 & 0 & \nu \\ 0 & \beta & \mu & 0 \\ 0 & \mu^* & \gamma & 0 \\ \nu^* & 0 & 0 & \delta \end{pmatrix}. \quad (3.23)$$

The square roots of the eigenvalues of $\rho\tilde{\rho}$, as in the concurrence definition. are the following,

$$\lambda_i = \left\{ \sqrt{\beta\gamma} + |\mu|, \sqrt{\beta\gamma} - |\mu|, \sqrt{\alpha\delta} + |\nu|, \sqrt{\alpha\delta} - |\nu| \right\}. \quad (3.24)$$

Either the first or third term is the largest eigenvalue, so the X state concurrence is then

$$\mathcal{C}(|\psi_X\rangle) = 2 \max \left\{ 0, |\nu| - \sqrt{\beta\gamma}, |\mu| - \sqrt{\alpha\delta} \right\}. \quad (3.25)$$

Let $\mathcal{C}_{k,\mu}^{(n)}$ and $\mathcal{C}_{k,\nu}^{(n)}$ indicate the possible non-zero expressions for TIX concurrence involving μ and ν respectively. Following this notation, the concurrences of arbitrary 4 and 5 qubit TIX states can be calculated to be,

$$\mathcal{C}_{1,\mu}^{(4)} = \frac{|cd^* + dc^*|}{\sqrt{2}} - 2\sqrt{\left(|a|^2 + \frac{|c|^2}{4}\right) \left(\frac{|c|^2}{4} + |f|^2\right)} \quad (3.26)$$

$$\mathcal{C}_{1,\nu}^{(4)} = |ac^* + cf^*| - \frac{1}{2}|c|^2 - |d|^2 \quad (3.27)$$

$$\mathcal{C}_{2,\mu}^{(4)} = |c|^2 - 2\sqrt{\left(|a|^2 + \frac{|d|^2}{2}\right) \left(\frac{|d|^2}{2} + |f|^2\right)} \quad (3.28)$$

$$\mathcal{C}_{2,\nu}^{(4)} = \sqrt{2}|ad^* + df^*| - |c|^2 \quad (3.29)$$

$$\mathcal{C}_{1,\mu}^{(5)} = \frac{2}{5} \left(|dc^* + cd^*| + |d|^2 + |g|^2 - \sqrt{(5|a|^2 + 2|c|^2 + |d|^2)(|c|^2 + 3|g|^2)} \right) \quad (3.30)$$

$$\mathcal{C}_{1,\nu}^{(5)} = \frac{2}{5} \left(\left| \sqrt{5}ac^* + 2cg^* + dg^* \right| - |c|^2 - 2|d|^2 - |g|^2 \right) \quad (3.31)$$

$$\mathcal{C}_{2,\mu}^{(5)} = \frac{2}{5} \left(|dc^* + cd^*| + |c|^2 + |g|^2 - \sqrt{(5|a|^2 + |c|^2 + 2|d|^2)(|d|^2 + 3|g|^2)} \right) \quad (3.32)$$

$$\mathcal{C}_{2,\nu}^{(5)} = \frac{2}{5} \left(\left| \sqrt{5}ad^* + 2dg^* + cg^* \right| - 2|c|^2 - |d|^2 - |g|^2 \right). \quad (3.33)$$

In determining the maximum of $\mathcal{C}_1^{(4)}$ and $\mathcal{C}_1^{(5)}$ over the X state subspace, the maximization will need to be performed over both the μ and ν terms with the overall maximum being the larger of the two resulting maxima. These maximizations are easily performed after setting all the coefficient phases equal to 0. This phase treatment maximizes each absolute value in (3.26)-(3.33)

and simplifies the maximizations enough to readily calculate. The results are compiled in the table below. The overall maximum of $\mathcal{C}_1^{(4)} = \frac{1}{2}$ occurs when $d = 0$ and $a = c = f = \frac{1}{\sqrt{3}}$, while

Table 3.1: Maximum concurrences of 4 and 5 qubit CSX states. The analytic results for $n = 5$ are the roots of complicated polynomials, so their rounded numerical values are reported instead.

Concurrence	Maximum
$\mathcal{C}_{1,\mu}^{(4)}$	$\frac{1}{4}$
$\mathcal{C}_{1,\nu}^{(4)}$	$\frac{1}{2}$
$\mathcal{C}_{1,\mu}^{(5)}$	≈ 0.468
$\mathcal{C}_{1,\nu}^{(5)}$	≈ 0.366

the $\mathcal{C}_1^{(5)} \approx 0.468$ maximum occurs at $a = g = 0$ and $c \approx 0.298$ $d \approx 0.955$. These maxima, while calculated only over the TIX subspace, agree with the apparent maxima in numerical results for general TI states, as shown in Figure 3.3 in the next section. This $\mathcal{C}_1^{(5)}$ maximum is also a notable improvement over the lower bound established in [50].

For $n > 5$, the TIX state concurrences can be calculated, but the spaces prove too large and complicated to maximize over analytically. A possible future direction for this work is to bound the maximal $\mathcal{C}_1^{(n)}$ in the large n limit.

3.2 Constraints on Shared Pairwise Concurrence

We know that the space of allowable pairwise concurrences, $\{\mathcal{C}_{i,j}\}$, in arbitrary n qubit states is constrained by monogamy relations. Within the translationally invariant subspace we would analogously expect monogamy relations for the set of $\{\mathcal{C}_k^{(n)}\}$. I examined such monogamy relations for 4 and 5 qubit TI states in [51]. Shown in Figure 3.1 are the $k = 1$ and $k = 2$ concurrences for 10^5 randomly generated 4 and 5 qubit TI states.

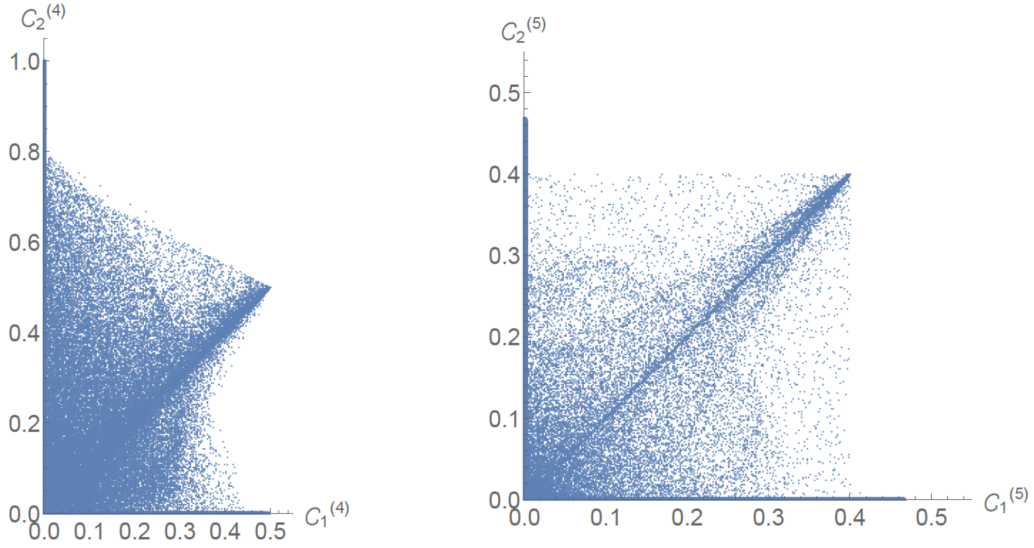


Figure 3.1: Pairwise concurrences of 10^5 randomly generated 4 and 5 qubit TI states.

This first numerical examination demonstrates the peculiar monogamous relationship between pairwise concurrences in TI states. It appears that for both $n = 4$ and $n = 5$, above some threshold concurrence the other concurrence must be equal to 0. This differs from typical monogamy relations [19][53], which also suggest that the maximally entangled states minimize entanglement with other parties, but allow for states with slightly less entanglement than the maximum to share other entanglements.

The following theorem provides some analytical context to the TI state monogamy.

Theorem 3. *The neighborhood of states around any $|\psi_2^{(4)}\rangle$ have $\mathcal{C}_1^{(4)} = 0$.*

Proof. Consider the state,

$$|\psi_2^{(4)}\rangle = |\psi_1^{(2)}\rangle_{1,3} \otimes |\psi_1^{(2)}\rangle_{2,4}, \quad (3.34)$$

The pure 2 qubit states with concurrence equal to 1 are equivalent to each other under local unitaries, so the set of $|\psi_2^{(4)}\rangle$ are likewise equivalent. This implies that the entanglement properties of any $|\psi_2^{(4)}\rangle$ can be determined by examining those of (3.34). Now consider altering (3.34) by some infinitesimal perturbation of the form of (3.19),

$$|\psi'\rangle = |\psi_2^{(4)}\rangle + \varepsilon |\psi^{(4)}\rangle, \quad (3.35)$$

where $\varepsilon \ll 1$. To show $\mathcal{C}_1^{(4)} = 0$ for the above state regardless of the perturbation, we first calculate the reduced density matrix between adjacent parties,

$$\rho_r = \frac{\mathbb{1}}{4} + \frac{\varepsilon}{2} \Re \left[\begin{pmatrix} 2a & b & b & c \\ b & \sqrt{2}d & c & e \\ b & c & \sqrt{2}d & e \\ c & e & e & 2f \end{pmatrix} \right] + \mathcal{O}(\varepsilon^2). \quad (3.36)$$

It is clear that only the real part of the perturbation will affect the concurrence, so continue assuming the coefficients of the perturbation are real. For simplicity, absorb ε into the perturbation coefficients. Continuing in the concurrence calculation,

$$\rho_r \tilde{\rho}_r = \frac{\mathbb{1}}{16} + \frac{1}{8} \begin{pmatrix} 2a+2f & b-e & b-e & 2c \\ b-e & 2\sqrt{2}d & 2c & e-b \\ b-e & 2c & 2\sqrt{2}d & e-b \\ 2c & e-b & e-b & 2a+2f \end{pmatrix} + \mathcal{O}(\varepsilon^2). \quad (3.37)$$

The square roots of the eigenvalues of this matrix are all $\lambda_i = \frac{1}{4} \sqrt{1 + \mathcal{O}(\varepsilon) + \mathcal{O}(\varepsilon^2)}$. therefore, the sum $\lambda_1 - \lambda_2 - \lambda_3 - \lambda_4$ will certainly be negative, so the concurrence is 0. \square

The monogamy of TI states is more clearly observed by examining the subconcurrence, defined as

$$s\mathcal{C} = \lambda_1 - \lambda_2 - \lambda_3 - \lambda_4, \quad (3.38)$$

where λ_i are the square roots of the eigenvalues of $\rho \tilde{\rho}$ in descending magnitude, as in the concurrence definition. More simply, the subconcurrence has the same definition as the concurrence, except it doesn't map negative sums of λ_i to 0. The subconcurrences of randomly generated 4 and 5 qubit TI states are displayed in Figure 3.2.

Figure 3.2 clearly demonstrates the apparent thresholds in 4 and 5 qubits. For both $n = 4$ and $n = 5$, it appears that above some $k = 2$ subconcurrence, the $k = 1$ subconcurrence must be negative. Due to the symmetry discussed at the beginning of the previous section, in 5-qubits, states with $k = 1$ subconcurrences above the same threshold will have negative $k = 2$

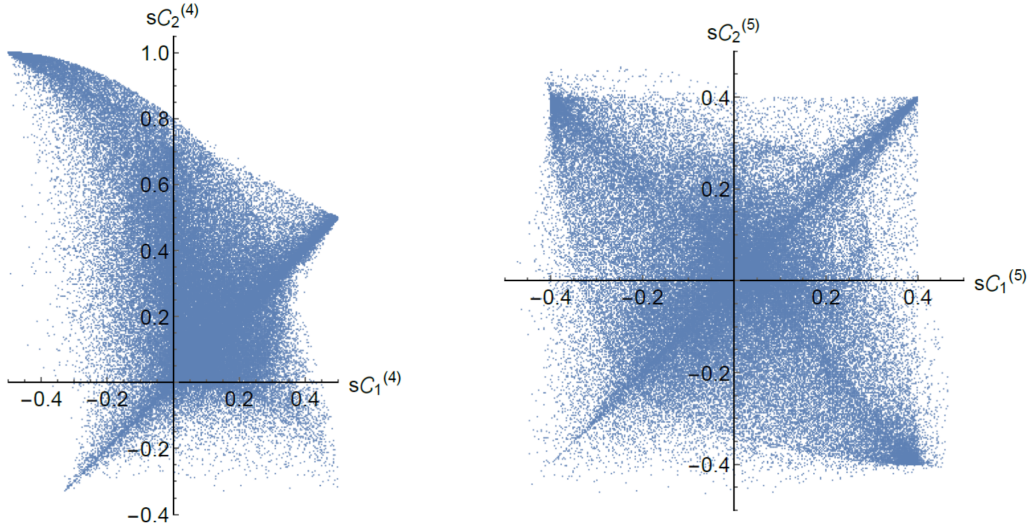


Figure 3.2: Pairwise subconcurrences of 10^5 randomly generated 4 and 5 qubit TI states.

subconcurrence. For $n = 4$, however, the totally symmetric state, $|W\rangle = \overbrace{|0001\rangle}$ has the same $s\mathcal{C}_1^{(4)}$ as (3.34) while also having $s\mathcal{C}_2^{(4)} = \frac{1}{2}$.

The analytic description of these monogamy thresholds will again be performed on the X state subspace, where the calculations are much simpler. Shown in Figure 3.3 are the subconcurrences of randomly generated TIX states overlaid on general TI state subconcurrences. Based on these numerical results, it appears that TIX states share the same monogamy thresholds and maximum concurrences as TI states, making them a relevant subset for analysis.

Looking only at TIX states, we found the achievable concurrence boundaries in both 4 and 5 qubits. The full analysis is presented in Appendix A, but the boundaries allow for a quick determination of the concurrence thresholds in the X state subspace. The thresholds are compiled in Table 3.2 on the next page. Note that the $s\mathcal{C}_1^{(4)}$ threshold only fully holds for TIX states. Also recall that the concurrence symmetry in 5 qubits implies that $s\mathcal{C}_1^{(5)}$ and $s\mathcal{C}_2^{(5)}$ have the same threshold.

This work is, in part, a reprint of material from published work done in collaboration with David Meyer, as it appears on the arXiv. Alexander Meill and David A. Meyer, “Pairwise Concurrence in Cyclically Symmetric Quantum States,” arXiv:1802.06877. The dissertation

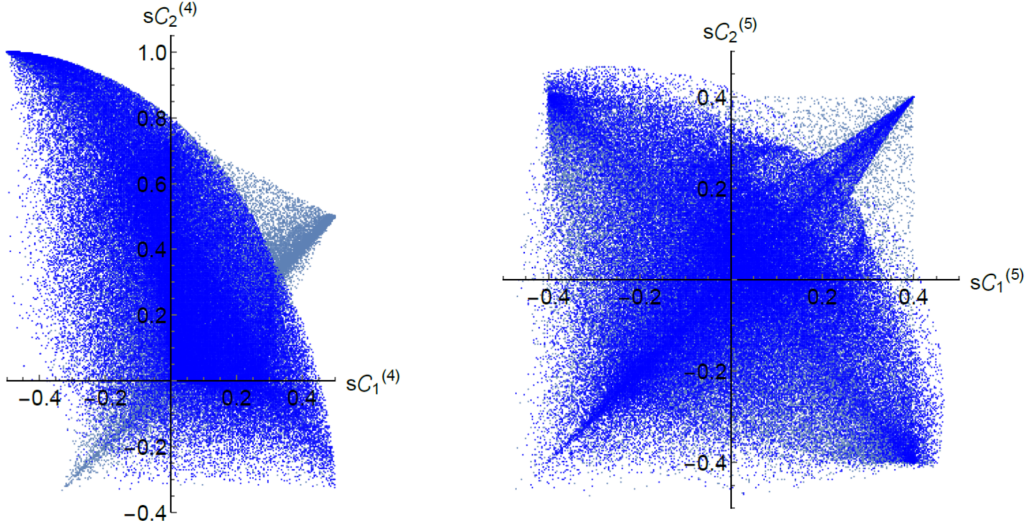


Figure 3.3: Pairwise subconcurrences of 10^5 randomly generated 4 and 5 qubit TI and TIX (darker blue) states.

Table 3.2: Threshold concurrences of 4 and 5 qubit TIX states. The analytic result for $n = 5$ are the roots of complicated polynomials, so the rounded numerical value is reported instead.

Concurrence	Threshold
$s\mathcal{C}_1^{(4)}$	$\frac{2\sqrt{2}-1}{4}$
$s\mathcal{C}_2^{(4)}$	$\frac{4}{5}$
$s\mathcal{C}_k^{(5)}$	≈ 0.418

author was the primary investigator and author of this material.

Chapter 4

Symmetric Matrix Product States

The results of the previous chapter are somewhat surprising when put into context. Theorem 2 implies that maximal entanglement in translationally invariant states *increases* with the spacing between the party labels. This, at a first glance, is in stark contradiction with the classical intuition - that classical correlations *decay* with spacing in translationally invariant systems [54] [55]. This contradiction is resolved by the fact that label spacing, in states which are only constrained by translational invariance, has no immediate physical meaning. As discussed in the previous chapter, permuting the parties of a TI state equates pairwise correlations along any spacing to that of a factor of the number of parties, n . The most apparent example of this is prime n , which leads to each spacing being essentially equivalent. So this then begs the question: If translational invariance alone is not enough, what further symmetry or state structure is required to convey physical separation in translationally invariant systems?

One potential approach is the ‘Matrix Product State’ (MPS) structure, which is ubiquitous in the study of condensed matter spin systems [56] [57] [58] as well as in high energy theory, as it pertains to the holographic principle in the study of anti-de Sitter space/conformal field theory [59] [60]. A matrix product state is constructed by assigning a set of matrices, $\{A_i^{[j]}\} \in M_{D_j \times D_{j+1}}$, to each particle, where j is the party label and $i = 1, \dots, d_j$. The trace of the product of these

matrices determine the computational basis coefficients of the overall state,

$$|\psi\rangle = \sum_{i_1=1}^{d_1} \dots \sum_{i_n=1}^{d_n} \text{Tr} \left(A_{i_1}^{[1]} \dots A_{i_n}^{[n]} \right) |i_1 \dots i_n\rangle. \quad (4.1)$$

One interpretation of matrix product states, which in part led to their initial conception in the AKLT model [58], begins by assigning to party j a pair of virtual spins of dimension D_j and D_{j+1} . The virtual spins of neighboring parties, j and $j+1$, are taken to be in a maximally entangled bond, which, upon being measured in a basis corresponding to the matrices $A_i^{[j]}$, leave the physical spins in the actual state, $|\psi\rangle$. In this sense, the entangling of neighboring spins adds a notion of locality to the state. The dimension of the virtual spins, D_j , are referred to as the “Bond Dimension”, and convey some notion of interaction scale for the state. Physically this notion is formalized by the fact that one can always construct a parent Hamiltonian which acts non-trivially on $L \sim 2 \log D / \log d$ neighboring parties, for which that MPS is a ground state [56]. If the bond dimensions are sufficiently large, any state may be represented as an MPS [61]. To make use of the interaction length interpretation, however, we generally seek the smallest bond dimension which admits a MPS representation of the state. MPS representations of a given bond dimension then form a non-trivial subset of the overall Hilbert space with physically relevant properties.

This restriction to matrix product states allows us to further constrain the translationally invariant space of states in such a manner that enforces a physical length scale. A translationally invariant MPS is one which assigns the same set of matrices, $\{A_i\} \in M_{D \times D}$, to each party. This alone is enough to yield translational invariance because cycling the parties merely cycles the A matrices, which, due to the cyclic invariance of the trace, leaves the state unchanged. Returning to the problem of growing pairwise entanglement with party spacing in TI states, one would expect that the entanglement grows at the cost of bond dimension, D . While there is yet no formal proof of such a statement, it is nonetheless interesting to ask what kind of entanglement can be achieved when D is fixed, and preferably, small. In this chapter I answer this question for fully symmetric matrix product states and develop an LU canonical form for TI matrix product states as a tool for future entanglement analysis.

4.1 Translationally Invariant MPS LU Canonical Form

As discussed in Chapter 2, LU canonical forms are a powerful tool in entanglement analysis because they simplify the state space while leaving the entanglement properties unchanged. MPS's are particularly difficult to expand into the computational basis, so any reduction in the parameter space is valuable in that pursuit. Other work has examined reducing the degrees of freedom in exact representation of MPS's [35] [62], but none have yet exploited the action of local unitaries to further simplify the state. I was able to develop an LU canonical form for translationally invariant matrix product states of n qubits with $D = 2$, which leaves the state with only 1 real and 2 complex degrees of freedom, with probable room for additional reduction. What follows is a derivation of that LU canonical form.

Begin by considering an n qubit TI MPS,

$$|\psi\rangle = \sum_{i_1=0}^1 \dots \sum_{i_n=0}^1 \text{Tr}(A_{i_1} \dots A_{i_n}) |i_1 \dots i_n\rangle. \quad (4.2)$$

A standard canonical form for such states was introduced in [62] which involves merely changing the structure of the A_i matrices, while maintaining the exact original state. They identified the key property that, without changing the bond dimension, D , one can achieve the original state with a set of matrices A_i which obey

$$\sum_{i=0}^1 A_i A_i^\dagger = \mathbb{1}_D. \quad (4.3)$$

This form is referred to as 'left normalized', while the same constraint for $A_i^\dagger A_i$ is referred to as the 'right normalized' canonical form. For $D > 2$, the canonical form can be additionally constrained with a block structure, but we will restrict to $D = 2$ where (4.3) is sufficient.

In the search for an LU canonical form on TI MPS's it will be important to observe that a state which obeys (4.3) will continue to do so under LU evolution. To see this, consider a symmetric local unitary operator, $U = U_1^{\otimes n}$ acting on $|\psi\rangle$, resulting in a new set of matrices,

$$A'_i = \sum_{j=0}^1 \{U_1\}_{i,j} A_j. \quad (4.4)$$

We can then show that these new matrices are still in the left normalized canonical form,

$$\sum_{i=0}^1 A'_i A_i{}^\dagger = \sum_{i,j,k=0}^1 \{U_1\}_{i,k}^* \{U_1\}_{i,j} A_j A_k{}^\dagger \quad (4.5)$$

$$= \sum_{i,j,k=0}^1 \{U_1^\dagger\}_{k,i} \{U_1\}_{i,j} A_j A_k{}^\dagger \quad (4.6)$$

$$= \sum_{j,k=0}^1 \{U_1^\dagger U_1\}_{k,j} A_j A_k{}^\dagger \quad (4.7)$$

$$= \sum_{j,k=0}^1 \delta_{k,j} A_j A_k{}^\dagger \quad (4.8)$$

$$= \sum_{i=0}^1 A_i A_i{}^\dagger \quad (4.9)$$

$$= \mathbb{1}_D. \quad (4.10)$$

This fact allows us to freely apply LU operators while continuing to enforce (4.3). Consider, then, parametrizing

$$U_1 = \begin{pmatrix} \cos \theta e^{i\mu} & -\sin \theta e^{iv} \\ \sin \theta e^{-iv} & \cos \theta e^{-i\mu} \end{pmatrix}, \quad (4.11)$$

and examine

$$\{A'_0\}_{0,1} = \cos \theta e^{i\mu} \{A_0\}_{0,1} - \sin \theta e^{iv} \{A_1\}_{0,1}. \quad (4.12)$$

We can choose U_1 so that $\{A'_0\}_{0,1} = 0$ by setting

$$\tan \theta e^{i(v-\mu)} = \frac{\{A_0\}_{0,1}}{\{A_1\}_{0,1}}. \quad (4.13)$$

At this point we can express A'_0 as,

$$A'_0 = \begin{pmatrix} \alpha & 0 \\ \gamma & \beta \end{pmatrix}, \quad (4.14)$$

where $\alpha \in \mathbb{R}$ and $\beta, \gamma \in \mathbb{C}$.

We can now enforce (4.3) to constrain A'_1 ,

$$A'_1 A_1{}^\dagger = \mathbb{1} - A'_0 A_0{}^\dagger = \begin{pmatrix} 1 - \alpha^2 & \alpha \gamma^* \\ \alpha \gamma & 1 - |\gamma|^2 - |\beta|^2 \end{pmatrix}. \quad (4.15)$$

In examining the parametrization of A'_1 , the following Lemma will be useful.

Lemma 2. *If $A, B \in M(D)$ satisfy $AA^\dagger = BB^\dagger$, then $A = BV$ for some $V \in U(D)$.*

Proof. Let $U_A \Sigma_A V_A^\dagger = A$ and $U_B \Sigma_B V_B^\dagger = B$ be the singular value decompositions of A , and B . Note that $AA^\dagger = BB^\dagger$ implies $U_A = U_B = U$ and $\Sigma_A = \Sigma_B = \Sigma$. Then if $V = V_B V_A^\dagger$,

$$BV = U \Sigma V_B^\dagger V_B V_A^\dagger = U \Sigma V_A^\dagger = A. \quad (4.16)$$

□

Lemma 2, in conjunction with the Cholesky decomposition of (4.15), gives the following parametrization of A'_1 ,

$$A'_1 = \begin{pmatrix} \sqrt{1-\alpha^2} & 0 \\ \frac{\alpha\gamma}{\sqrt{1-\alpha^2}} & \sqrt{1-|\beta|^2-|\gamma|^2-\frac{\alpha^2|\gamma|^2}{1-\alpha^2}} \end{pmatrix} V, \quad (4.17)$$

where V is an arbitrary unitary matrix. These two matrices, A'_0 and A'_1 , form an LU canonical form for any TI MPS with $D = 2$.

This canonical form is potentially useful in parametrizing states of $D = 2$, but the process could potentially extend to $D > 2$. One would simply eliminate the desired entries in A_0 through LU evolution, then parametrize A_1 with (4.3) and the Cholesky decomposition. There are some notable choices made in the derivation of my canonical form, which could be altered to suit the needs of any particular application. One could eliminate a different entry in A_0 , and one could choose an expansion of $A_1 A_1^\dagger$ other than the Cholesky decomposition. Additionally, numerical evidence suggests that β can likely be constrained to be real by further manipulation.

4.2 Fully Symmetric Representations and Entanglement

While the primary application of the MPS structure has been to TI systems, fully permutation symmetric states have also been examined in the MPS context [35] [63]. When expressing a symmetric state as an MPS, one could opt for a non-symmetric matrix structure. The W -state, $|W\rangle = \overbrace{|0\dots 01\rangle}$, for instance, can be achieved with only $D = 2$ by the *almost* symmetric set of matrices, $(A_0^{[j]}, A_1^{[j]}) = (|0\rangle\langle 1|, \mathbb{1})$ for $j < n$ and $(A_0^{[n]}, A_1^{[n]}) = (|0\rangle\langle 1| \sigma_x, \sigma_x)$ [62]. If one wanted a more symmetric choice of matrices, the obvious choice is to enforce that A_i are diagonal

and independent of party. Much like party independence of A_i being sufficient for translational invariance due to the cyclic invariance of the trace, having A_i be diagonal allows for arbitrary shuffling of the (now commuting) matrices leaving the state unchanged. With this matrix structure, the W -state requires a minimal bond dimension of $D = n$, and is given by the matrices,

$$A_0 \propto \text{diag} \left\{ 0, 1, e^{i\alpha}, e^{2i\alpha}, \dots, e^{(n-2)i\alpha} \right\} \quad (4.18)$$

$$A_1 \propto \text{diag} \left\{ (1-n)^{\frac{1}{n}}, 1, e^{(n-1)i\beta}, e^{(n-2)i\beta}, \dots, e^{2i\beta} \right\}, \quad (4.19)$$

where $\alpha = 2\pi/n(n-1)$ and $\beta = 2\pi/n$ [35]. While the W -state has a provably minimal bond dimension of $D = n$, I was able to show that the MPS, $|W_\varepsilon\rangle$, described by the matrices,

$$A_0 = \begin{pmatrix} 1 & 0 \\ 0 & e^{\frac{i\pi}{n}} \end{pmatrix} \quad (4.20)$$

$$A_1 = \varepsilon \begin{pmatrix} 0 & 0 \\ 0 & e^{-\frac{i(n-1)\pi}{n}} \end{pmatrix}, \quad (4.21)$$

obeys $\langle W|W_\varepsilon\rangle = 1 - \mathcal{O}(\varepsilon)$. This example is notable from an entanglement perspective, for the W -state maximizes pairwise concurrence in symmetric states of n qubits [21]. This implies that for a bond dimension of only $D = 2$, one can get arbitrary close to a maximally entangled symmetric state, which is quite valuable as an information resource.

The previous example of approximating the W -state with a low bond dimension state generalizes to the entire symmetric subspace. It was shown in [35] that an arbitrary symmetric state of n qubits can be exactly described by a diagonal MPS of bond dimension $D \leq n + 1$. The state is constructed by first observing, as was introduced in Chapter 2, that a symmetric state can be expressed as a superposition of symmetric product states,

$$|\psi\rangle = \sum_{j=1}^D x_j |\phi_j\rangle^{\otimes n}. \quad (4.22)$$

This state then admits a diagonal MPS representation with the matrices,

$$A_i = \sum_{j=1}^D x_j^{1/n} \langle i|\phi_j\rangle |j\rangle\langle j|. \quad (4.23)$$

This map from symmetric state to diagonal MPS is also invertible. Given the matrices,

$$A_i = \sum_{j=1}^D r_j^{(i)} |j\rangle\langle j|, \quad (4.24)$$

we can expand this state into the form of (4.22) with

$$x_j = \sqrt{\sum_{i=0}^1 |r_j^{(i)}|^2} \quad (4.25)$$

$$\langle i|\chi_j\rangle = \frac{r_j^{(i)}}{x_j}. \quad (4.26)$$

It seems as if we can do much better than $D \leq n + 1$, however, given our knowledge of the Mandilara canonical form, which states that almost every symmetric state can be expressed as a superposition of $D \leq \lceil \frac{n}{2} \rceil$ symmetric product states. The exceptions, which do not admit such an expansion, are states with at least one Majorana root degenerate to degree $2 \leq \mathcal{D} \leq n - 1$. The W -state is a prime example of such an exception, having one non-degenerate root and one root degenerate to degree $\mathcal{D} = n - 1$. The obvious question then is; if we perturb the degenerate roots to infinitesimally break that degeneracy, do we maintain near unit overlap with the original state? If the answer to this question is yes, then we would be able to approximate *any* symmetric state with a diagonal MPS with bond dimension $D \leq \lceil \frac{n}{2} \rceil$ with infinitesimal error. I confirmed that this is indeed possible, as described by the following theorem.

Theorem 4. *Given a symmetric state of n qubits in the Majorana representation,*

$$|\psi\rangle = \frac{1}{\sqrt{A}} \sum_{\pi \in S_n} U_\pi \bigotimes_{j=1}^n |\phi_j\rangle, \quad (4.27)$$

and the perturbed state

$$|\psi'\rangle = \frac{1}{\sqrt{A}} \sum_{\pi \in S_n} U_\pi |\phi'_1\rangle \bigotimes_{j=2}^n |\phi_j\rangle, \quad (4.28)$$

which obeys $|\langle \phi_1 | \phi'_1 \rangle| = \cos \varepsilon \approx 1 - \frac{1}{2} \varepsilon^2$, then the overlap between these two states is bounded from below by $\langle \psi | \psi' \rangle \geq 1 - 2(n!) \varepsilon$.

The proof of this theorem can be found in Appendix B. Note that the overlap, $|\langle \phi_1 | \phi'_1 \rangle| = \cos \varepsilon$, was chosen to represent a perturbation of the according Majorana star by an angle of 2ε .

The above theorem and its implications are exciting, particularly in the context of entangle-

ment. We now know that we can get arbitrarily close to highly entangled symmetric states while keeping the bond dimension low. We should confirm, though, that those approximate states have approximately the same pairwise concurrence. Say $|\psi'\rangle = |\psi\rangle + \varepsilon |\psi^\perp\rangle$, where $\langle \psi | \psi^\perp \rangle = 0$.

We want to show that

$$\left| \mathcal{C}(|\psi'\rangle) - \mathcal{C}(|\psi\rangle) \right| \leq \mathcal{O}(\varepsilon).$$

To do so, we will find the square roots of eigenvalues of the usual $\rho' \tilde{\rho}'$, or, equivalently, the fourth roots of $\rho' \tilde{\rho}' \tilde{\rho}' \rho'$. To first order in ε we have

$$\rho' \tilde{\rho}' \tilde{\rho}' \rho' = \rho \tilde{\rho} \tilde{\rho} \rho + \varepsilon G,$$

where

$$G = H \tilde{\rho} \tilde{\rho} \rho + \rho \tilde{H} \tilde{\rho} \rho + \rho \tilde{\rho} \tilde{H} \rho + \rho \tilde{\rho} \tilde{\rho} H,$$

where

$$H = |\psi\rangle\langle\psi^\perp| + |\psi^\perp\rangle\langle\psi|.$$

Importantly, $\rho \tilde{\rho} \tilde{\rho} \rho$ and G are Hermitian, so in finding the eigenvalues of the Hermitian $\rho' \tilde{\rho}' \tilde{\rho}' \rho'$ we can use the usual quantum error propagation. Namely, to first order in ε ,

$$\lambda'_i = \lambda_i + \varepsilon \langle \lambda_i | G | \lambda_i \rangle,$$

unless some of the λ'_i 's are degenerate. In that case, the corrections to λ'_i are the eigenvalues of $\varepsilon \langle \lambda_j | G | \lambda_k \rangle$. Since $\langle \lambda_j | G | \lambda_k \rangle$ are finite, so too is the $\mathcal{O}(\varepsilon)$ correction to λ'_i . And so, finally, the perturbed concurrence is

$$\mathcal{C}(|\psi'\rangle) = \max \left\{ 0, (\lambda_1)^{\frac{1}{4}} - (\lambda_2)^{\frac{1}{4}} - (\lambda_3)^{\frac{1}{4}} - (\lambda_4)^{\frac{1}{4}} \right\} = \mathcal{C}(|\psi\rangle) + \mathcal{O}(\varepsilon).$$

To give some final context to these results, I will find the full space of $D = 2$ matrix product states and show how the W -state lies infinitely close to that space. Start by exploiting the inverse map from a $D = 2$ diagonal MPS to a superposition of 2 symmetric product states,

$$|\psi\rangle = x_1 |\phi_1\rangle^{\otimes n} + x_2 |\phi_2\rangle^{\otimes n}. \quad (4.29)$$

I will describe the achievable subspace of symmetric states using the Majorana representation, and to do so we will find the Majorana roots of this state, then see what is achievable. Note that

the action of LU operators is easily visualized in the Majorana representation as rotations of the Bloch-sphere. This will be helpful, as I will use LU operators to simplify the state as much as possible before calculating the Majorana roots, and it will then be understood that the set of achievable Majorana representations includes all rotations of the ones found.

Now, to simplify the state and find its Majorana representation, start by using local unitaries to leave the state as

$$|\psi\rangle' = x_1 |0\rangle^{\otimes n} + x_2 (r_0 |0\rangle + r_1 |1\rangle)^{\otimes n}, \quad (4.30)$$

where $r_i \in \mathbb{R}$. Now let $x = -(x_2 r_1 / x_1)^n$ and $y = -r_0 / r_1$ and express the (now unnormalized) state as

$$|\psi\rangle' \propto |0\rangle^{\otimes n} - x^{-n} (-y |0\rangle + |1\rangle)^{\otimes n}. \quad (4.31)$$

Note that in computing the Majorana roots, the normalization of the state does not matter, so the roots will entirely depend on the unbounded $x \in \mathbb{C}$ and $y \in \mathbb{R}$. Moving forward in calculating the Majorana roots, we define the unnormalized state

$$|\alpha\rangle = (|0\rangle + \alpha^* |1\rangle)^{\otimes n}, \quad (4.32)$$

where α is an unbounded complex number. The Majorana roots are then the solutions in α to $\langle \alpha | \psi \rangle' = 0$, which can be expressed as,

$$1 - x^{-n} (\alpha - y)^n = 0 \quad (4.33)$$

$$\alpha - y = x e^{2\pi i m / n} \quad (4.34)$$

$$\alpha = y + x e^{2\pi i m / n}. \quad (4.35)$$

where $m \in \mathbb{Z}$. To finish the computation of the Majorana representation we would perform a stereographic projection of these n roots to the Bloch-sphere, then use points directly opposite these projections as the points of the Majorana representation. So, to summarize this result, the roots in the complex plane lie in a circle of radius $|x|$ centered at y , and are evenly spaced around this circle with starting angle, $\arg(x)$. The W -state, in particular, is approached by taking the limits, $|x| \rightarrow \infty$ and $y \rightarrow \infty$. This places a single star at the origin, with the remaining $n - 1$ points

out approaching infinity. This projects to one point at the $|1\rangle$ pole, with the remaining points project infinitely close to the $|0\rangle$ pole.

Chapter 5

Party-Site Symmetric States

The final symmetry examined in this thesis is motivated by the dynamics of identical particles whose motion is constrained to the discrete sites of a complete graph. Consider n particles evolving on a complete graph of d sites. To describe the state of such a system, we can index the site position of particle j by i_j , and therefore the overall state can be described by n qudits, or, a vector in $\mathbb{C}_d^{\otimes n}$,

$$|\psi\rangle = \sum_{i_1=1}^d \dots \sum_{i_n=1}^d a_{i_1 \dots i_n} |i_1 \dots i_n\rangle. \quad (5.1)$$

To this state we would then want to enforce constraints which reflect the symmetries of both:

- *Party*: Because the particles in question are identical, we want to enforce that any permutation of their labels leaves the state unchanged.
- *Site*: Because the particles are walking on a *complete* graph, the sites themselves of that graph are identical, and any permutation of their labels would leave the graph, and therefore the state, unchanged.

We have encountered party symmetry before, as it is the familiar full permutation symmetry which was the focus of Chapter 2, but site symmetry is a new consideration. We can formalize these combined symmetries in the following definition,

Definition 5. A state,

$$|\psi\rangle = \sum_{i_1=1}^d \dots \sum_{i_n=1}^d a_{i_1 \dots i_n} |i_1 \dots i_n\rangle, \quad (5.2)$$

is *party-site symmetric (PSS)* if

$$U_\mu |\psi\rangle = |\psi\rangle \quad \forall \quad \mu \in S_n \quad (5.3)$$

$$V_{\mathbf{v}}^{\otimes n} |\psi\rangle = |\psi\rangle \quad \forall \quad \mathbf{v} \in S_d, \quad (5.4)$$

where U_μ is the unitary representation of μ , which permutes the party labels,

$$U_\mu |i_1 \dots i_N\rangle = |\mu(i_1 \dots i_N)\rangle, \quad (5.5)$$

while $V_{\mathbf{v}}$ is the unitary representation of \mathbf{v} , which permutes the basis (site) labels,

$$V_{\mathbf{v}} |i\rangle = |\mathbf{v}(i)\rangle. \quad (5.6)$$

The individual symmetries associated to party (5.3) and site (5.4) will be referred to as U and V symmetries respectively. For PSS states we expect that many of the coefficients, $a_{i_1 \dots i_n}$, are constrained to be equal by the U and V symmetries, leaving some much smaller basis for the subspace. The U symmetry implies that the ordering of i_1 - i_n does not matter, so we can equate groups of the $a_{i_1 \dots i_n}$ under common labels, where each of the i_1 - i_n are arranged so that like indices are adjacent. For example, $a_{1,2,2,3,4,2,3}$ would be equal to and can be labeled as $a_{1,2,2,2,3,3,4}$. Furthermore, the indices can be arranged in decreasing number of like indices. This would equate and relabel $a_{1,2,2,2,3,3,4}$ to $a_{2,2,2,3,3,1,4}$. The V symmetry then implies that the collective index values themselves can be freely permuted, so $a_{2,2,2,3,3,1,4}$ could be labeled as any $a_{i_1, i_1, i_1, i_2, i_2, i_3, i_4}$, so long as i_1 - i_4 are distinct. Given that freedom, the only actually distinguishing feature of $a_{i_1, i_1, i_1, i_2, i_2, i_3, i_4}$, and the elements it is grouped with, is the partitioning of shared indices, meaning we can label the grouped elements by $a_{3,2,1,1}$, where now the subscripts denote the number of elements who share a given index. One can recognize that such a grouping and labeling can be expressed in a young diagram,

$$\begin{array}{|c|c|c|c|} \hline \square & \square & \square & \square \\ \hline \square & \square & & \\ \hline \square & & & \\ \hline \end{array} = \left\{ \mu \left(\mathbf{v}(1), \mathbf{v}(2), \mathbf{v}(2), \mathbf{v}(3), \mathbf{v}(4), \mathbf{v}(2), \mathbf{v}(3)) \right) \mid \mu \in S_n, \mathbf{v} \in S_d \right\}$$

In general, the number of rows in a Young diagram indicates that each of the elements in the set has that many distinct indices. The number of blocks in a row indicates how many parties share that index. Naturally, the total number of blocks is n , and there can be at most d rows in a Young diagram. With the interpretation of Young diagrams established, we then find that they serve as an orthonormal basis for pure PSS states,

$$|\psi\rangle = \sum_{y \in \mathcal{Y}(n,d)} a_y |y\rangle, \quad (5.7)$$

where $\mathcal{Y}(n,d)$ is the set of Young diagrams with n blocks and at most d rows, and $|y\rangle$ is a normalized equal superposition of computational basis elements belonging to the set described by the Young diagram, y .

The symmetries of PSS states clearly offer a significant reduction to the state space, but they do so while maintaining notable physical relevance. PSS states are a natural starting point for the description of quantum random walks of identical particles on the complete graph. Such walks have been shown to be a candidate model for quantum search algorithms which achieve the same $\mathcal{O}(\sqrt{N})$ speedup as Grover's algorithm [64]. While the marking of a site (or sites) to search for does break the site symmetry slightly, the fully symmetric case offers a baseline for describing the entanglement properties of the more general walks [65]. In particular, we would like to examine whether or not the PSS symmetry alone is enough to validate a mean field approximation,

$$\rho_2 \approx \rho_1 \otimes \rho_1, \quad (5.8)$$

where ρ_1 and ρ_2 are the one- and two-party reduced density matrices respectively, which, thanks to the U symmetry, are independent of party labels. The purpose for examining such an assumption, as detailed in the next section, is that it is a key step in potentially approximating the dynamics of quantum random walks with non-linear equations of motion which result in conditional $\mathcal{O}(N^{1/4})$ speedup of quantum search [66].

At first glance, the mean field approximation seems like a reasonable one for the PSS setting. It is certainly *not* true for an entangled state, so presumably the more entangled the state, the bigger the violation. But, as we have seen previously, the symmetry of the state forces

any entanglement to be shared among each party, and therefore should decrease with n due to monogamy. In this chapter I will further motivate the relevance of the mean field approximation for PSS states, then examine its validity more precisely.

5.1 The Gross-Pitaevskii Equation

To appreciate the need for the mean field approximation we have to make a slight diversion into continuous space equations of motion. In particular, we will examine the derivation of the Gross-Pitaevskii Equation [67], which is a widely use tool in the study of Bose-Einstein condensates [68]. The derivation begins with the exact equations of motion, which are described by the multi-particle Schrödinger Equation,

$$i\hbar \partial_t \psi(t, x_1, \dots, x_n) = \left[\sum_{j=1}^n \frac{|p_j|^2}{2m} + \frac{1}{n} \sum_{1 \leq j < k \leq n} V(x_j - x_k) \right] \psi(t, x_1, \dots, x_n), \quad (5.9)$$

where the particle interactions are merely pairwise and described by the potential, $V(x_j - x_k)$, which is independent of party labels. If one were to trace over each party but the first to find the equations of motion for reduced state of the first particle, ρ_1 , one would arrive at the BBGKY Hierarchy,

$$\begin{aligned} -i\hbar \partial_t \rho_1(t, x_1; x'_1) &= \left(\frac{|p_1|^2}{2m} - \frac{|p'_1|^2}{2m} \right) \rho_1(t, x_1; x'_1) \\ &+ \frac{1}{n} \sum_{j=2}^n \int [V(x_1 - x_j) - V(x'_1 - x_j)] \rho_{1,j}(t, x_1, x_j; x'_1, x_j) dx_j. \end{aligned} \quad (5.10)$$

The main obstacle in the use of the BBGKY Hierarchy is the fact that the dynamics of ρ_1 are coupled to the dynamics of each of the two party reduced states, $\rho_{1,j}$, which, in turn, are coupled to the dynamics of the three party reduced states, and so on, forming a hierarchy of coupled differential equations. To break the hierarchy and decouple the equations of motion we must make a set of assumptions. First, we assume party symmetry, an assumption natural given that the intent is to describe the motion of identical bosons. Party symmetry allows the sum to be

evaluated, leaving,

$$\begin{aligned}
-i\hbar \partial_t \rho_1(t, x_1; x'_1) &= \left(\frac{|p_1|^2}{2m} - \frac{|p'_1|^2}{2m} \right) \rho_1(t, x_1; x'_1) \\
&+ \frac{n-1}{n} \int [V(x_1 - x_2) - V(x'_1 - x_2)] \rho_2(t, x_1, x_2; x'_1, x_2) dx_2,
\end{aligned} \tag{5.11}$$

where now ρ_1 and ρ_2 label the reduced states of any single particle or pair of particles respectively. Next we assume many particles, $1 \ll n$, and suitably short range interactions such that $V(x) \approx \lambda \delta(x)$. These make the integration easy to perform and leaves us with the Gross-Pitaevskii Hierarchy,

$$-i\hbar \partial_t \rho_1(t, x_1; x'_1) = \left(\frac{|p_1|^2}{2m} - \frac{|p'_1|^2}{2m} \right) \rho_1(t, x_1; x'_1) + \lambda [\rho_2(t, x_1, x_1; x'_1, x_1) - \rho_2(t, x_1, x'_1; x'_1, x'_1)]. \tag{5.12}$$

To this point, the assumptions have been minor and natural. The assumption which breaks the hierarchy, though, is somewhat unique to the Bose-Einstein condensate setting. In the large n limit, the state of any two particles in a Bose-Einstein condensate decouples and can be described by the tensor product of the individual state [68],

$$\rho_2(t, x_1, x_2; x'_1, x'_2) \approx \rho_1(t, x_1; x'_1) \otimes \rho_1(t, x_2; x'_2), \tag{5.13}$$

which is exactly the continuous space version of the mean field approximation, (5.8). This approximation breaks the hierarchy and arrives at Non-Linear Schrödinger Equation,

$$-i\hbar \partial_t \rho_1(t, x_1; x'_1) = \left(\frac{|p_1|^2}{2m} - \frac{|p'_1|^2}{2m} + \lambda [\rho_1(t, x_1; x_1) - \rho_1(t, x'_1; x'_1)] \right) \rho_1(t, x_1; x'_1). \tag{5.14}$$

The final necessary assumption, which is also appropriate in the Bose-Einstein condensate setting, is that $\rho_1(t, x_1; x'_1) = \psi(t, x_1) \psi^*(t, x'_1)$ is pure. This alters the equations of motion from describing the dynamics of a density matrix, ρ_1 to a pure wavefunction, ψ , and is the final form of the Gross-Pitaevskii Equation,

$$-i\hbar \partial_t \psi(t, x) = \left(\frac{|p|^2}{2m} + \lambda |\psi(t, x)|^2 \right) \psi(t, x). \tag{5.15}$$

The Gross-Pitaevskii equation is notably non-linear, but results in decoupled equations of motion.

It is that non-linearity which, in the complete graph quantum search setting,

$$-i\hbar \partial_t |\psi(t)\rangle = \left[\mathcal{H}_0 + g \sum_j |\langle j | \psi(t) \rangle|^2 |j\rangle \langle j| \right] |\psi(t)\rangle, \quad (5.16)$$

enables the conditional speedup over Grover's algorithm, which is provably optimal in the linear setting [69]. Clearly, though, in order to use (5.16), we need to show that the mean field approximation, (5.8), is a reasonable one. Examining that assertion in the fully symmetric PSS setting is the clear first step.

5.2 Measuring Mean Field Approximation Validity

There are two main challenges in measuring the validity of mean field approximation, (5.8), for a general PSS state, (5.1). The first is performing the partial trace to find ρ_1 and ρ_2 , and the second is evaluating how similar ρ_2 and $\rho_1 \otimes \rho_1$ are by some metric. There are many options for measuring the distance between two matrices. Two methods which make use of the generalized Bloch vector representation of the state are described in Appendix C, but the primary metric of choice for this thesis is the matrix Fidelity [70],

$$F(A, B) = \left[\text{Tr} \sqrt{\sqrt{A} B \sqrt{A}} \right]^2. \quad (5.17)$$

The fidelity is a common choice in quantum information theory [71] as a generalization of the pure state inner product to mixed states. As applied to the task at hand, let us label, for a PSS state, $|\psi\rangle$,

$$F(|\psi\rangle) = \left[\text{Tr} \sqrt{\sqrt{\rho_1 \otimes \rho_1} \rho_2 \sqrt{\rho_1 \otimes \rho_1}} \right]^2. \quad (5.18)$$

Before determining $F(|\psi\rangle)$ for a selection of PSS states, it will be useful to examine some properties of PSS states, their reductions, and the fidelity measure applied to those reductions. First, let us examine the reduced state, ρ_k , of any $k < n$ parties from the overall PSS state, and find how the U and V symmetries translate to the symmetries of that reduced state. Begin by

tracing out the last $n - k$ parties to find

$$\rho_k = \text{Tr}_{\bar{k}}(|\psi\rangle\langle\psi|) \quad (5.19)$$

$$= \sum_{l_{k+1}\dots l_N} \sum_{i_1\dots i_k} \sum_{j_1\dots j_k} a_{i_1\dots i_k l_{k+1}\dots l_N} |i_1\dots i_k\rangle\langle j_1\dots j_k| a_{j_1\dots j_k l_{k+1}\dots l_N}^* \quad (5.20)$$

Now consider $V_{\mathbf{v}-1}$ for some $\mathbf{v} \in S_d$, acting on ρ_k ,

$$V_{\mathbf{v}-1} \rho_k V_{\mathbf{v}-1}^\dagger = \sum_{i,j,l} a_{\mathbf{v}(i_1)\dots\mathbf{v}(i_k)l_{k+1}\dots l_N} |i_1\dots i_k\rangle\langle j_1\dots j_k| a_{\mathbf{v}(j_1)\dots\mathbf{v}(j_k)l_{k+1}\dots l_N}^* \quad (5.21)$$

$$= \sum_{i,j,l} a_{\mathbf{v}(i_1)\dots\mathbf{v}(i_k)\mathbf{v}(l_{k+1})\dots\mathbf{v}(l_N)} |i_1\dots i_k\rangle\langle j_1\dots j_k| a_{\mathbf{v}(j_1)\dots\mathbf{v}(j_k)\mathbf{v}(l_{k+1})\dots\mathbf{v}(l_N)}^* \quad (5.22)$$

$$= \sum_{i,j,l} a_{i_1\dots i_k l_{k+1}\dots l_N} |i_1\dots i_k\rangle\langle j_1\dots j_k| a_{j_1\dots j_k l_{k+1}\dots l_N}^* \quad (5.23)$$

$$= \rho_k. \quad (5.24)$$

Likewise consider $U_{\mu-1}$ for $\mu \in S_k$. We can also extend $\mu \otimes \mathbb{1}_{n-k} \in S_n$ as the permutation which acts on the first k parties by μ and leaves the traced over parties fixed. Now examine

$$U_{\mu-1} \rho_k U_{\mu-1}^\dagger = \sum_{i,j,l} a_{\mu(i_1\dots i_k)l_{k+1}\dots l_N} |i_1\dots i_k\rangle\langle j_1\dots j_k| a_{\mu(j_1\dots j_k)l_{k+1}\dots l_N}^* \quad (5.25)$$

$$= \sum_{i,j,l} a_{\mu \otimes \mathbb{1}_{N-k}(i_1\dots i_k l_{k+1}\dots l_N)} |i_1\dots i_k\rangle\langle j_1\dots j_k| a_{\mu \otimes \mathbb{1}_{N-k}(j_1\dots j_k l_{k+1}\dots l_N)}^* \quad (5.26)$$

$$= \sum_{i,j,l} a_{i_1\dots i_k l_{k+1}\dots l_N} |i_1\dots i_k\rangle\langle j_1\dots j_k| a_{j_1\dots j_k l_{k+1}\dots l_N}^* \quad (5.27)$$

$$= \rho_k. \quad (5.28)$$

Even more interesting is that acting on only one side by U would likewise leave ρ_k invariant because μ can be freely extended to $\mu \otimes \mathbb{1}_{N-k}$ for either the bra or the ket individually. This is not true for the V symmetry, where absorbing \mathbf{v} into the sum in l has to affect both the bra and the ket simultaneously. Altogether then we have

$$U \rho_k = \rho_k U = \rho_k \quad (5.29)$$

$$V \rho_k V^\dagger = \rho_k. \quad (5.30)$$

These symmetries allow us to greatly constrain the elements of ρ_1 and ρ_2 , leaving us with a fairly simple parametrization of the two matrices. Starting with ρ_1 , the V symmetry implies that $\{\rho_1\}_{i,j} = \{\rho_1\}_{\mathbf{v}(i),\mathbf{v}(j)}$ for any $\mathbf{v} \in S_d$. This then equates all the diagonal elements as $\{\rho_1\}_{i,i} = \frac{1}{d}$ and the off diagonal elements as $\{\rho_1\}_{i,j} = A$ for all $i \neq j$. Since the V symmetry

equates $\{\rho_1\}_{i,j} = \{\rho_1\}_{j,i}$, the hermiticity of ρ_1 then implies that $A \in \mathbb{R}$. The same application of the U and V symmetries along with hermiticity constrain the following elements of ρ_2 , in which it is implied that i, j, k , and l are distinct,

$$\{\rho_2\}_{ij,kl} = B_1 \quad (5.31)$$

$$\{\rho_2\}_{ii,kl} = B_2 \quad (5.32)$$

$$\{\rho_2\}_{ij,il} = \{\rho_2\}_{ij,li} = \{\rho_2\}_{ji,il} = \{\rho_2\}_{ji,li} = B_3 \quad (5.33)$$

$$\{\rho_2\}_{ii,kk} = B_4 \quad (5.34)$$

$$\{\rho_2\}_{ii,il} = \{\rho_2\}_{ii,li} = B_5 \quad (5.35)$$

$$\{\rho_2\}_{ij,ij} = \{\rho_2\}_{ij,ji} = \frac{1}{d^2} + C \quad (5.36)$$

$$\{\rho_2\}_{ii,ii} = \frac{1}{d^2} - (d-1)C, \quad (5.37)$$

where B_1, B_3, B_4 , and C are real, while B_2 and B_5 are complex. Notably, we can relate A to the parameters of ρ_2 by

$$A = \{\rho_1\}_{i,j} \quad (5.38)$$

$$= \{\text{Tr}_2(\rho_2)\}_{i,j} \quad (5.39)$$

$$= \sum_{k=1}^d \{\rho_2\}_{ik,jk} \quad (5.40)$$

$$= (d-2)B_3 + B_5 + B_5^* \quad (5.41)$$

$$= (d-2)B_3 + 2\Re(B_5). \quad (5.42)$$

The symmetries of ρ_1 and ρ_2 aid in the determination of $M := \sqrt{\rho_1 \otimes \rho_1} \rho_2 \sqrt{\rho_1 \otimes \rho_1}$ and its square root for the purpose of calculating $F(|\psi\rangle)$. First, we can confirm that

$$\begin{aligned} \sqrt{\rho_1} &= \frac{(d-1)\sqrt{1-Ad} + \sqrt{1+Ad(d-1)}}{d^{\frac{3}{2}}} \mathbb{1}_d \\ &+ \frac{\sqrt{1+Ad(d-1)} - \sqrt{1-Ad}}{d^{\frac{3}{2}}} \sum_{i \neq j} |i\rangle\langle j|, \end{aligned} \quad (5.43)$$

by recognizing that

$$\begin{aligned} \left\{ \sqrt{\rho_1^2} \right\}_{i,i} &= \left(\frac{(d-1)\sqrt{1-Ad} + \sqrt{1+Ad(d-1)}}{d^{\frac{3}{2}}} \right)^2 \\ &+ (d-1) \left(\frac{\sqrt{1+Ad(d-1)} - \sqrt{1-Ad}}{d^{\frac{3}{2}}} \right)^2 = \frac{1}{d}, \end{aligned} \quad (5.44)$$

and

$$\begin{aligned} \left\{ \sqrt{\rho_1^2} \right\}_{i,j} &= 2 \left(\frac{(d-1)\sqrt{1-Ad} + \sqrt{1+Ad(d-1)}}{d^{\frac{3}{2}}} \right) \left(\frac{\sqrt{1+Ad(d-1)} - \sqrt{1-Ad}}{d^{\frac{3}{2}}} \right) \\ &+ (d-2) \left(\frac{\sqrt{1+Ad(d-1)} - \sqrt{1-Ad}}{d^{\frac{3}{2}}} \right)^2 = A, \end{aligned} \quad (5.45)$$

for $i \neq j$. From this we can see that $\sqrt{\rho_1}$ has the same symmetries as ρ_1 . We can extend this notion and show that M , as well as its square root, have all the same symmetries as ρ_2 . To see this, begin by noting that

$$\left\{ \sqrt{\rho_1 \otimes \rho_1} \right\}_{ij,kl} = \left\{ \sqrt{\rho_1} \right\}_{i,k} \left\{ \sqrt{\rho_1} \right\}_{j,l}. \quad (5.46)$$

This allows us to confirm that $\sqrt{\rho_1 \otimes \rho_1}$ has V symmetry,

$$\left\{ V \sqrt{\rho_1 \otimes \rho_1} V^\dagger \right\}_{ij,kl} = \left\{ \sqrt{\rho_1} \right\}_{V(i),V(k)} \left\{ \sqrt{\rho_1} \right\}_{V(j),V(l)} \quad (5.47)$$

$$= \left\{ \sqrt{\rho_1} \right\}_{i,k} \left\{ \sqrt{\rho_1} \right\}_{j,l} \quad (5.48)$$

$$= \left\{ \sqrt{\rho_1 \otimes \rho_1} \right\}_{ij,kl}. \quad (5.49)$$

The same is not true for the full U symmetry, however, which we can see if we consider U as the swap operator and the following family of entries,

$$\left\{ U \sqrt{\rho_1 \otimes \rho_1} \right\}_{ij,il} = \left\{ \sqrt{\rho_1} \right\}_{j,i} \left\{ \sqrt{\rho_1} \right\}_{i,l} \quad (5.50)$$

$$\neq \left\{ \sqrt{\rho_1} \right\}_{i,i} \left\{ \sqrt{\rho_1} \right\}_{j,l}. \quad (5.51)$$

It is true, however, that

$$\left\{ U \sqrt{\rho_1 \otimes \rho_1} U^\dagger \right\}_{ij,kl} = \left\{ \sqrt{\rho_1} \right\}_{j,l} \left\{ \sqrt{\rho_1} \right\}_{i,k} \quad (5.52)$$

$$= \left\{ \sqrt{\rho_1 \otimes \rho_1} \right\}_{ij,kl}. \quad (5.53)$$

This finally allows us to show that

$$V\sqrt{\rho_1 \otimes \rho_1}\rho_2\sqrt{\rho_1 \otimes \rho_1}V^\dagger = V\sqrt{\rho_1 \otimes \rho_1}V^\dagger V\rho_2V^\dagger V\sqrt{\rho_1 \otimes \rho_1}V^\dagger \quad (5.54)$$

$$= \sqrt{\rho_1 \otimes \rho_1}\rho_2\sqrt{\rho_1 \otimes \rho_1}, \quad (5.55)$$

and

$$U\sqrt{\rho_1 \otimes \rho_1}\rho_2\sqrt{\rho_1 \otimes \rho_1} = U\sqrt{\rho_1 \otimes \rho_1}U^\dagger U\rho_2\sqrt{\rho_1 \otimes \rho_1} \quad (5.56)$$

$$= \sqrt{\rho_1 \otimes \rho_1}\rho_2\sqrt{\rho_1 \otimes \rho_1}, \quad (5.57)$$

with of course the same being true for a right application of U . The same symmetries then apply to \sqrt{M} , a fact which is easily shown through the singular value decomposition.

The fact that \sqrt{M} has the same symmetries as ρ_2 means that we can associate a set of B_1 - B_5 to its off-diagonal elements. We can then let $\sqrt{M}^2 = M$ provide a set of constraints of those B_1 - B_5 , which, in the large d limit evaluate to

$$\{M\}_{\ddot{ii},\ddot{ii}} = \left\{ \sqrt{M} \right\}_{\ddot{ii},\ddot{ii}}^2 + d^2 B_2^2 + dB_4^2 + 2d|B_5|^2 \quad (5.58)$$

$$\{M\}_{ij,ij} = 2 \left\{ \sqrt{M} \right\}_{ij,ij}^2 + d^2 B_1^2 + d|B_2|^2 + 4dB_3^2 + |B_5|^2 \quad (5.59)$$

$$\{M\}_{\ddot{ii},jj} = 2 \left\{ \sqrt{M} \right\}_{\ddot{ii},\ddot{ii}} B_4 + d^2 |B_2|^2 + 2dB_2 B_5^* + 2dB_2^* B_5 + 2|B_5|^2 + dB_4^2 \quad (5.60)$$

$$\{M\}_{\ddot{ii},ij} = \left\{ \sqrt{M} \right\}_{\ddot{ii},\ddot{ii}} B_5 + B_4 B_5 + 2 \left\{ \sqrt{M} \right\}_{ij,ij} B_5 + dB_3 B_5 \quad (5.61)$$

$$+ dB_3 B_5^* + dB_2 B_3 + dB_2^* B_3 + d^2 B_2 B_1 + dB_2 B_4$$

$$\{M\}_{\ddot{ii},jk} = \left\{ \sqrt{M} \right\}_{\ddot{ii},\ddot{ii}} B_2 + B_4 B_5 + B_4 B_5^* + 2B_3 B_5 + 2B_3 B_5^* + dB_2 B_4 \quad (5.62)$$

$$+ \left\{ \sqrt{M} \right\}_{ij,ij} B_2 + dB_1 B_5 + B_1 B_5^* + 2dB_2 B_3 + 2B_2^* B_3 + d^2 B_1 B_2$$

$$\{M\}_{ij,ik} = 4 \left\{ \sqrt{M} \right\}_{ij,ij} B_3 + B_2^* B_5 + B_2 B_5^* + d|B_2|^2 + |B_5|^2 + 2dB_3^2 + 4dB_1 B_3 + d^2 B_1^2 \quad (5.63)$$

$$\{M\}_{ij,kl} = 4 \left\{ \sqrt{M} \right\}_{ij,ij} B_1 + 2B_2^* B_5 + 2B_2 B_5^* + 8B_3^2 + d|B_2|^2 + 8dB_1 B_3 + d^2 B_1^2. \quad (5.64)$$

With these symmetries, properties, and constraints in tow, we can turn to finding $F(|\psi\rangle)$ for PSS states.

5.2.1 Exact Fidelity Analysis

For the most general PSS state,

$$|\psi\rangle = \sum_{y \in \mathcal{Y}(n,d)} a_y |y\rangle, \quad (5.65)$$

the resulting matrix, M , is analytically challenging to diagonalize or find the square root of for the purpose of finding the fidelity. In some simple cases, however, the fidelity can be determined exactly. Consider the following set of PSS states described by single, rectangular Young diagram basis elements,

$$y(k) = k \left\{ \begin{array}{c} \begin{array}{ccc} \square & \square & \dots & \square & \square \\ \square & & & & \square \\ \vdots & & & & \vdots \\ \square & & & & \square \\ \square & \square & \dots & \square & \square \end{array} \\ \underbrace{\hspace{10em}}_{\frac{n}{k}} \end{array} \right.$$

Expressed as a state in the computational basis,

$$|y(k)\rangle = \mathcal{A}_k^{-\frac{1}{2}} \sum_{\mu \in \mathcal{S}_n} \sum_{i_1 < \dots < i_k} U_\mu \bigotimes_{j=1}^k |i_j\rangle^{\otimes \frac{n}{k}}, \quad (5.66)$$

where \mathcal{A}_k is a normalization constant equal to the number of computational basis elements present in $|y(k)\rangle$. It evaluates to

$$\mathcal{A}_k = \binom{d}{k} \frac{n!}{\left[\left(\frac{n}{k}\right)!\right]^k} = \left(\frac{k!(d-k)! \left[\left(\frac{n}{k}\right)!\right]^k}{d!n!} \right)^{-1}. \quad (5.67)$$

The first step in calculating $F(|y(k)\rangle)$ is the determination of the components of ρ_2 and ρ_1 .

Consider first

$$\rho_1 = \mathcal{A}_k^{-1} \sum_{i, k_2 \dots k_n \in y} \sum_{j, k_2 \dots k_n \in y} |i\rangle \langle j| \quad (5.68)$$

$$= \mathcal{A}_k^{-1} \sum_{i,j} \mathcal{N}_{i,j}^{(y)} |i\rangle \langle j|, \quad (5.69)$$

where $\mathcal{N}_{i,j}^{(y)}$ is the number of strings, $(k_2 \dots k_n)$, for which both $(ik_2 \dots k_n)$ and $(jk_2 \dots k_n)$ are contained in the set associated to y . We can analogously define $\mathcal{N}_{ij,kl}^{(y)}$ such that

$$\rho_2 = \mathcal{A}_k^{-1} \sum_{i,j,k,l} \mathcal{N}_{ij,kl}^{(y)} |ij\rangle \langle kl|. \quad (5.70)$$

Determining each of the \mathcal{N} for the family of $y(k)$ is a simple counting/combinatorics exercise.

The results are the following, where it is assumed that i, j, k , and l are distinct,

$$\mathcal{N}_{i,j}^{(y(k))} = \delta(k-n) \frac{(d-2)!}{(d-n-1)!} \quad (5.71)$$

$$\mathcal{N}_{ii,ii}^{(y(k))} = \begin{cases} 0 & k = n \\ \binom{d-1}{k-1} \frac{(n-2)!}{\left(\binom{n}{k-2}\right)! \left[\left(\binom{n}{k}\right)!\right]^{k-1}} & k \neq n \end{cases} \quad (5.72)$$

$$\mathcal{N}_{ij,ij}^{(y(k))} = \binom{d-2}{k-2} \frac{(n-2)!}{\left[\left(\binom{n}{k-1}\right)!\right]^2 \left[\left(\binom{n}{k}\right)!\right]^{k-2}} \quad (5.73)$$

$$\mathcal{N}_{ii,jj}^{(y(k))} = \delta\left(k - \frac{n}{2}\right) \binom{d-2}{\frac{n}{2}-1} \frac{(n-2)!}{2^{\frac{n}{2}-1}} \quad (5.74)$$

$$\mathcal{N}_{ij,ik}^{(y(k))} = \delta(k-n) \frac{(d-3)!}{(d-n-1)!} \quad (5.75)$$

$$\mathcal{N}_{ij,kl}^{(y(k))} = \delta(k-n) \frac{(d-4)!}{(d-n-2)!}, \quad (5.76)$$

while $\mathcal{N}_{ii,ij}^{(y(k))} = \mathcal{N}_{ii,jk}^{(y(k))} = 0$. Dividing by \mathcal{A}_k then finally gives the components of each reduced density matrix,

$$A = \delta(k-n) \frac{d-n}{d(d-1)} \quad (5.77)$$

$$\{\rho_2\}_{ii,ii} = \frac{n-k}{dk(n-1)} \quad (5.78)$$

$$\{\rho_2\}_{ij,ij} = \frac{n(k-1)}{d(d-1)k(n-1)} \quad (5.79)$$

$$B_4 = \delta\left(k - \frac{n}{2}\right) \frac{d - \frac{n}{2}}{d(d-1)(n-1)} \quad (5.80)$$

$$B_3 = \delta(k-n) \frac{d-n}{d(d-1)(d-2)} \quad (5.81)$$

$$B_1 = \delta(k-n) \frac{(d-n)(d-n-1)}{d(d-1)(d-2)(d-3)} \quad (5.82)$$

$$B_2 = B_5 = 0 \quad (5.83)$$

From here there are three major cases to consider: $k < n/2$, $k = n/2$, and $k = n$. Starting with the

$k < n/2$ case we have

$$\rho_1 = \frac{1}{d} \mathbb{1}_d \quad (5.84)$$

$$\sqrt{\rho_1 \otimes \rho_1} = \frac{1}{d} \mathbb{1}_{d^2} \quad (5.85)$$

$$\rho_2 = \frac{1}{dk(n-1)} \left[(n-k) \sum_i |ii\rangle\langle ii| + \frac{n(k-1)}{d-1} \sum_{i \neq j} |ij\rangle\langle ij| + |ij\rangle\langle ji| \right] \quad (5.86)$$

$$M = \frac{1}{d^3k(n-1)} \left[(n-k) \sum_i |ii\rangle\langle ii| + \frac{n(k-1)}{d-1} \sum_{i \neq j} |ij\rangle\langle ij| + |ij\rangle\langle ji| \right]. \quad (5.87)$$

Given that we will be tracing this matrix after finding its square root, we can jointly reorder the rows and columns together. Doing so yields the convenient representation,

$$M = \frac{n(k-1)}{d^4k(n-1)} \left[\begin{pmatrix} 1 & 1 \\ 1 & 1 \end{pmatrix}^{\oplus d(d-1)/2} \oplus \frac{d(n-k)}{n(k-1)} \mathbb{1}_d \right], \quad (5.88)$$

which we be easily diagonalized,

$$M = \frac{n(k-1)}{d^4k(n-1)} \left[\begin{pmatrix} 2 & 0 \\ 0 & 0 \end{pmatrix}^{\oplus d(d-1)/2} \oplus \frac{d(n-k)}{n(k-1)} \mathbb{1}_d \right], \quad (5.89)$$

and then we can take the square root,

$$\sqrt{M} = \sqrt{\frac{n(k-1)}{d^4k(n-1)}} \left[\begin{pmatrix} \sqrt{2} & 0 \\ 0 & 0 \end{pmatrix}^{\oplus d(d-1)/2} \oplus \sqrt{\frac{d(n-k)}{n(k-1)}} \mathbb{1}_d \right]. \quad (5.90)$$

And finally we can find $F(|y(k < n/2)\rangle)$,

$$F(|y(k < n/2)\rangle) = \left(\text{Tr} \sqrt{M} \right)^2 \quad (5.91)$$

$$= \left(\sqrt{\frac{n(k-1)}{d^4k(n-1)}} \left(\frac{d(d-1)}{\sqrt{2}} + \sqrt{\frac{d^3(n-k)}{n(k-1)}} \right) \right)^2 \quad (5.92)$$

$$= \frac{\left((d-1)\sqrt{n(k-1)} + \sqrt{2d(n-k)} \right)^2}{2d^2k(n-1)}. \quad (5.93)$$

This is a nice exact result, but $F()$ as $d \rightarrow \infty$ simplifies to

$$F(|y(k < n/2)\rangle) = \frac{n(k-1)}{2k(n-1)}. \quad (5.94)$$

Moving to the $k = n/2$ case, the same analysis arrives at

$$M = \frac{1}{d^2(n-1)} \left[\frac{2(n-2)}{d(d-1)} \begin{pmatrix} 1 & 0 \\ 0 & 0 \end{pmatrix}^{\oplus d(d-1)/2} \oplus \left(\frac{1}{d} \mathbb{1}_d + \frac{d-\frac{n}{2}}{d(d-1)} \sum_{i \neq j} |i\rangle\langle j| \right) \right]. \quad (5.95)$$

In computing \sqrt{M} , we can recognize that the final block component of M is of the same form of ρ_1 , which we have computed the square root of in (5.43). This allows us to find

$$\begin{aligned} \sqrt{M} = & \sqrt{\frac{1}{d^2(n-1)}} \left[\sqrt{\frac{2(n-2)}{d(d-1)}} \begin{pmatrix} 1 & 0 \\ 0 & 0 \end{pmatrix}^{\oplus d(d-1)/2} \right. \\ & \left. \oplus \left(\frac{\sqrt{2+2d-n} + \sqrt{(d-1)(n-2)}}{\sqrt{2d^3}} \mathbb{1}_d + \frac{\sqrt{2+2d-n} - \sqrt{\frac{n-1}{d-1}}}{\sqrt{2d^3}} \sum_{i \neq j} |i\rangle\langle j| \right) \right]. \end{aligned} \quad (5.96)$$

And now we can find

$$F(|y(k = n/2)\rangle) = \frac{\left(\sqrt{2+2d-n} + (d+1)\sqrt{(d-1)(n-2)} \right)^2}{2d^3(n-1)}, \quad (5.97)$$

which, as $d \rightarrow \infty$, evaluates to

$$F(|y(k = n/2)\rangle) = \frac{n-2}{2(n-1)}. \quad (5.98)$$

Lastly we have the $k = n$ case, in which only three cases lead to simple analysis: $n = d$, $n = d - 1$, and $n \ll d$. For $n = d$ we find that

$$M = \frac{2}{d^3(d-1)} \begin{pmatrix} 1 & 0 \\ 0 & 0 \end{pmatrix}^{\oplus d(d-1)/2}. \quad (5.99)$$

This makes determining the fidelity rather straightforward,

$$F(|y(k = n = d)\rangle) = \frac{d-1}{2d}, \quad (5.100)$$

which is equal to $1/2$ in the large d limit. Now for the $n = d - 1$ case, we start with

$$\rho_1 = \frac{1}{d} \mathbb{1}_d + \frac{1}{d^2} \sum_{i \neq j} |i\rangle\langle j| \quad (5.101)$$

$$\begin{aligned} \rho_2 = & \frac{1}{d^2} \sum_{i \neq j} |ij\rangle\langle ij| + |ij\rangle\langle ji| \\ & + \frac{1}{d^3} \sum_{\text{distinct } i,j,k} |ij\rangle\langle ik| + |ij\rangle\langle ki| + |ji\rangle\langle ik| + |ji\rangle\langle ki|. \end{aligned} \quad (5.102)$$

From here we can find M , whose symmetric entries in the large d limit are

$$\{M\}_{ii,ii} = \frac{24 - 16\sqrt{2}}{d^5} \quad (5.103)$$

$$\{M\}_{ij,ij} = \frac{1}{d^4} \quad (5.104)$$

$$B_1 = \frac{14 - 4\sqrt{2}}{d^6} \quad (5.105)$$

$$B_2 = B_4 = \frac{16\sqrt{2} - 18}{d^6} \quad (5.106)$$

$$B_3 = \frac{3}{d^5} \quad (5.107)$$

$$B_5 = \frac{8 - 4\sqrt{2}}{d^5}. \quad (5.108)$$

These allow for us to solve (5.58)-(5.64) to find the components of \sqrt{M} , a calculation which is not at daunting as it seems thanks to the large d limit. The result is that

$$\{\sqrt{M}\}_{ij,ij} = \mathcal{O}\left(d^{-\frac{5}{2}}\right) \quad (5.109)$$

$$\{\sqrt{M}\}_{ij,ij} = \frac{1}{\sqrt{2}d^2} + \mathcal{O}\left(d^{-\frac{5}{2}}\right), \quad (5.110)$$

and therefore $F(|y(k = n = d - 1)\rangle) = \frac{1}{2}$ in the large d limit. Lastly, moving to the $n \ll d$ case, we actually have that in the large d limit,

$$\rho_1 \approx \frac{1}{d} \sum_{i,j} |i\rangle\langle j|, \quad (5.111)$$

which is pure, and therefore $\rho_2 = \rho_1 \otimes \rho_1$ and $F(|y(k = n \ll d)\rangle) = 1$.

The results of these calculations are somewhat surprising given our intuitions regarding monogamy constraints on the symmetric sharing of entanglement. We had expected a heuristic connection between entanglement in the state and violation of the mean field approximation. This notion was only partially correct though, as the mean field approximation is a stronger assumption than the separability of ρ_2 . Recall that a mixed state is separable if

$$\rho = \sum_i^r p_i \rho_i^{(1)} \otimes \rho_i^{(2)}, \quad (5.112)$$

for some decomposition, in which r is unbounded. The mean field approximation, however, demands $r = 1$, which is therefore only true for a subset of separable states. So it is then unsurprising that we were able to find PSS states for which $F(|\psi\rangle)$ was not close to 1, as the

entanglement decaying with n due to the symmetry implies that the state merely approaches a separable one, not one for which the mean field approximation is a necessarily good one.

The example of rectangular Young diagrams raises an important intuition regarding the validity of the mean field approximation. The results of this section can be summarized as larger k leading to better agreement with the mean field approximation. Physically, small k corresponds to more compact grouping of the particles. Therefore we are led to believe that the more spread out the particles are, the better the mean field approximation gets. This notion is given further context in the next section, where we conclude that the only way to get good agreement with the mean field approximation is to have isolated particles. This intuition does give hope to the use of the Gross-Pitaevskii Equation in quantum search. The initial state for that algorithm is the uniform superposition,

$$|\psi_0\rangle = \left(\sum_{i=1}^d |i\rangle \right)^{\otimes n}, \quad (5.113)$$

which we know is approximately the $|y(k=n)\rangle$ state in the $n \ll d$ limit, and approaches perfect agreement with the mean field approximation. Left to evolve, we would expect that the particles would stay mostly spread because that is both entropically and energetically favored. This intuition would need to be examined in the case of PSS states with marked sites, however.

5.2.2 Bounded Fidelity Analysis

The previous section introduced the intuition that isolated particles make for better agreement with the mean field approximation. In this section I will confirm that notion by proving that good fidelity is *impossible* without isolated particles. The following theorem will be instrumental in that endeavor,

Theorem 5. *As $d \rightarrow \infty$, if a PSS state, $|\psi\rangle$, has $A \leq \mathcal{O}(d^{-2})$, then $F(|\psi\rangle) \leq 1/2$.*

Proof. Begin by noting that the normalization of ρ_2 implies that $\{\rho_2\}_{ii,ii} \leq \mathcal{O}(d^{-1})$ and $\{\rho_2\}_{ij,ij} \leq \mathcal{O}(d^{-2})$ for $i \neq j$. This then constrains each of $|B_1| - |B_5|$ by the positivity of ρ_2 . The simplest

constraint comes from enforcing that the minors with a single B_i and its associated diagonal elements is positive. This gives

$$|B_1| \leq \mathcal{O}(d^{-2}) \quad (5.114)$$

$$|B_3| \leq \mathcal{O}(d^{-2}) \quad (5.115)$$

$$|B_2| \leq \mathcal{O}(d^{-\frac{3}{2}}) \quad (5.116)$$

$$|B_5| \leq \mathcal{O}(d^{-\frac{3}{2}}) \quad (5.117)$$

$$|B_4| \leq \mathcal{O}(d^{-1}). \quad (5.118)$$

We know that, as $d \rightarrow \infty$, $A = dB_3 + 2\Re(B_5)$. This tightens the constraint on B_3 to $|B_3| \leq \mathcal{O}(d^{-5/2})$. The final required constraint is a tighter bound on B_1 , which will be achieved by considering the larger minor of ρ_2 defined by,

$$\rho_{\square} = \sum_{i \neq j} \sum_{k \neq l} \{\rho_2\}_{ij,kl} |ij\rangle \langle kl|. \quad (5.119)$$

I will now show that the following are eigenvectors of ρ_{\square} ,

$$|\lambda_1\rangle = \sum_{i \neq j} |ij\rangle \quad (5.120)$$

$$|\lambda_2\rangle = |12\rangle + |21\rangle + \frac{d-4}{d-2} \sum_{i>2} |2i\rangle + |i2\rangle - \frac{2}{d-2} \sum_{i \neq j > 2} |ij\rangle. \quad (5.121)$$

Starting with $|\lambda_1\rangle$ we have,

$$\rho_{\square} |\lambda_1\rangle = \sum_{i \neq j} \sum_{k \neq l} \{\rho_{\square}\}_{ij,kl} |ij\rangle. \quad (5.122)$$

And therefore

$$\langle ij | \rho_{\square} |\lambda_1\rangle = \sum_{k \neq l} \{\rho_{\square}\}_{ij,kl} \quad (5.123)$$

$$= 2\{\rho_2\}_{ij,ij} + 4(d-2)B_3 + (d-2)(d-3)B_1. \quad (5.124)$$

This implies that the associated eigenvalue is

$$\lambda_1 = 2\{\rho_2\}_{ij,ij} + 4(d-2)B_3 + (d-2)(d-3)B_1. \quad (5.125)$$

Moving to $|\lambda_2\rangle$ we have,

$$\rho_{\square} |\lambda_2\rangle = \sum_{i \neq j} \left(2\{\rho_{\square}\}_{ij,12} + 2\frac{d-4}{d-2} \sum_{k>2} \{\rho_{\square}\}_{ij,k2} - \frac{2}{d-2} \sum_{k \neq l > 2} \{\rho_{\square}\}_{ij,kl} \right) |ij\rangle. \quad (5.126)$$

Element by element we can confirm that

$$\langle 12 | \rho_{\square} | \lambda_2 \rangle = 2 \{ \rho_2 \}_{ij,ij} + 2(d-4)B_3 - 2(d-3)B_1 \quad (5.127)$$

$$= \langle 21 | \rho_{\square} | \lambda_2 \rangle, \quad (5.128)$$

and for $i > 2$,

$$\langle i2 | \rho_{\square} | \lambda_2 \rangle = 2B_3 + 2 \frac{d-4}{d-2} \left(\{ \rho_2 \}_{ij,ij} + (d-3)B_3 \right) \quad (5.129)$$

$$\begin{aligned} & - \frac{2}{d-2} (2(d-3)B_3 + (d-3)(d-4)B_1) \\ & = \frac{d-4}{d-2} \left(2 \{ \rho_2 \}_{ij,ij} + 2(d-4)B_3 - 2(d-3)B_1 \right) \end{aligned} \quad (5.130)$$

$$= \langle 2i | \rho_{\square} | \lambda_2 \rangle \quad (5.131)$$

$$\langle i1 | \rho_{\square} | \lambda_2 \rangle = 2B_3 + 2 \frac{d-4}{d-2} (B_3 + (d-3)B_1) \quad (5.132)$$

$$\begin{aligned} & - \frac{2}{d-2} (2(d-3)B_3 + (d-3)(d-4)B_1) \\ & = 0 \end{aligned} \quad (5.133)$$

$$= \langle 2i | \rho_{\square} | \lambda_2 \rangle, \quad (5.134)$$

and for $i \neq j > 2$,

$$\langle ij | \rho_{\square} | \lambda_2 \rangle = 2B_1 + 2 \frac{d-4}{d-2} (2B_3 + (d-4)B_1) \quad (5.135)$$

$$\begin{aligned} & - \frac{2}{d-2} \left(2 \{ \rho_2 \}_{ij,ij} + 4(d-4)B_3 + (d-4)(d-5)B_1 \right) \\ & = - \frac{2}{d-2} \left(2 \{ \rho_2 \}_{ij,ij} + 2(d-4)B_3 - 2(d-3)B_1 \right), \end{aligned} \quad (5.136)$$

which implies that the associated eigenvalue is

$$\lambda_2 = 2 \{ \rho_2 \}_{ij,ij} + 2(d-4)B_3 - 2(d-3)B_1. \quad (5.137)$$

To enforce that $\rho_{\square} \geq 0$, we must have that $\lambda_1 \geq 0$ and $\lambda_2 \geq 0$. In the large d limit this evaluates to the following constraints on B_1 ,

$$B_3 \geq 0 \quad \rightarrow \quad - \frac{2 \{ \rho_2 \}_{ij,ij}}{d^2} - \frac{4B_3}{d} \leq B_1 \leq \frac{\{ \rho_2 \}_{ij,ij}}{d} + B_3 \quad (5.138)$$

$$B_3 \leq 0 \quad \rightarrow \quad - \frac{\{ \rho_2 \}_{ij,ij}}{d^2} \leq B_1 \leq \frac{\{ \rho_2 \}_{ij,ij}}{d} \quad (5.139)$$

which can be combined to $|B_1| \leq \max \{ \mathcal{O}(d^{-3}), \mathcal{O}(B_3) \}$, which in this case gives $|B_1| \leq \mathcal{O}(d^{-5/2})$.

With the magnitudes of the off-diagonal elements of ρ_2 so constrained, the matrix multiplication to find M reveals that

$$\{M\}_{ii,ii} = \frac{\{\rho_2\}_{ii,ii}}{d^2} + \mathcal{O}\left(d^{-\frac{7}{2}}\right) \quad (5.140)$$

$$\{M\}_{ij,ij} = \frac{\{\rho_2\}_{ij,ij}}{d^2} + \mathcal{O}\left(d^{-\frac{9}{2}}\right). \quad (5.141)$$

We can then turn (5.58) and (5.59) into the following inequalities,

$$\left\{\sqrt{M}\right\}_{ii,ii} \leq \frac{\sqrt{\{\rho_2\}_{ii,ii}}}{d} \quad (5.142)$$

$$\left\{\sqrt{M}\right\}_{ij,ij} \leq \frac{\sqrt{\{\rho_2\}_{ij,ij}}}{\sqrt{2}d}. \quad (5.143)$$

If we parametrize the diagonal elements of ρ_2 with $d \rightarrow \infty$ as $\{\rho_2\}_{ii,ii} = \cos^2 \theta / d$ and $\{\rho_2\}_{ij,ij} = \sin^2 \theta / d^2$ for $i \neq j$, we can finally evaluate

$$F(|\psi\rangle) = \left(d \left\{\sqrt{M}\right\}_{ii,ii} + d^2 \left\{\sqrt{M}\right\}_{ij,ij} \right)^2 \quad (5.144)$$

$$\leq \left(\frac{\cos \theta}{\sqrt{d}} + \frac{\sin \theta}{2} \right)^2 \quad (5.145)$$

$$\leq \frac{1}{2}. \quad (5.146)$$

□

Theorem 5 allows us to identify any PSS state with $A \leq \mathcal{O}(d^{-2})$ as one for which the mean field approximation is not valid. In finding sets of PSS states with such A , it will be important to establish notation which allows us to describe an arbitrary Young diagram, y , and its corresponding state vector, $|y\rangle$. First, as before, label the number of rows as $k^{(y)}$, but now denote the number of distinct row lengths as $p^{(y)}$. Denote the length of the q^{th} distinct row from the bottom as $M_q^{(y)}$. Denote the number of rows of length $M_q^{(y)}$ as $l_q^{(y)}$. These labels are constrained by $p^{(y)} < k^{(y)} < d$ and $\sum_{q=1}^{p^{(y)}} l_q^{(y)} M_q^{(y)} = n$. Finally, this notation allows us to determine the normalization coefficient, \mathcal{A}_y , for a single Young diagram basis element,

$$\mathcal{A}_y = \frac{d! n!}{(d - k^{(y)})! \Pi_y}, \quad (5.147)$$

where

$$\Pi_y = \prod_{q=1}^{p^{(y)}} l_q! \left[M_q^{(y)}! \right]^{l_q^{(y)}}. \quad (5.148)$$

To confirm the intuition of the previous section, that isolated particles are required for good fidelity, let us start by considering the fidelity for single basis element states. In particular, let us examine Young diagrams which contain *no* isolated particles, and denote the set of such Young diagrams as $\mathcal{Y}_{>}$,

$$\mathcal{Y}_{>} = \left\{ y \in \mathcal{Y}(n, d) \mid M_1^{(y)} \geq 2 \right\}, \quad (5.149)$$

for example,

$$y \in \mathcal{Y}_{>} = \begin{array}{c} \begin{array}{ccc} \square & \square & \dots & \square & \square & \square & \dots & \square & \square & \square \\ \square & & & & & & & & & \\ \vdots & & & & & & & & & \end{array} \\ \underbrace{\begin{array}{ccc} \square & & \square \\ \square & \square & \dots & \square & \square \\ \square & & & & \end{array}}_{\geq 2} \end{array} .$$

We can then confirm that A for any $|y\rangle$ such that $y \in \mathcal{Y}_{>}$ obeys $A \leq \mathcal{O}(d^{-2})$, and therefore, by Theorem 5, $F(|y\rangle) \leq 1/2$. To see this, start by performing the partial trace on $|y\rangle$ to find ρ_1 and ρ_2 , which amounts to finding the set of $\mathcal{N}^{(y)}$. The thought process for finding a particular $\mathcal{N}^{(y)}$ is relatively consistent, so take $\mathcal{N}_{i,j}^{(y)}$ as an example. Obviously, if $M_1^{(y)} = 1$, there will be a contribution to $\mathcal{N}_{i,j}^{(y)}$ which is proportional to $l_1^{(y)}$. But for $M_1^{(y)} \geq 2$, the only way to contribute to $\mathcal{N}_{i,j}^{(y)}$ is if i and j are in row blocks q and $q+1$, and $M_q^{(y)} + 1 = M_{q+1}^{(y)}$. To add some intuition to that statement, we can only add to $\mathcal{N}_{i,j}^{(y)}$ if, after removing a single block from y , there are at least two places (one for i and one for j) to put that block back to return to y . All that remains is to sum over the possible arrangements and selections of the remaining indices which construct an element in y ,

$$\mathcal{N}_{i,j}^{(y)} = \frac{(d-2)!(n-1)!}{(d-k^{(y)})!\Pi_y} \left(\delta(M_1^{(y)} - 1) l_1^{(y)} (d - k^{(y)}) + 2 \sum_{q=2}^{p^{(y)}} \Delta^{(y)}(q, 1) l_q^{(y)} l_{q-1}^{(y)} M_q^{(y)} \right), \quad (5.150)$$

where $\Delta^{(y)}(q, r) = \delta(M_q^{(y)} - M_{q-1}^{(y)} - r)$. The same intuition applies to the remaining $\mathcal{N}^{(y)}$, and

we can fully specify them all as

$$\mathcal{N}_{ii,ii}^{(y)} = \frac{(d-1)!(n-2)!}{(d-k^{(y)})!\Pi_y} \sum_{q=1}^{p^{(y)}} l_q^{(y)} M_q^{(y)} (M_q^{(y)} - 1) \quad (5.151)$$

$$\mathcal{N}_{ij,ij}^{(y)} = \frac{(d-2)!(n-2)!}{(d-k^{(y)})!\Pi_y} \left(\sum_{q \neq m} l_q^{(y)} l_m^{(y)} M_q^{(y)} M_m^{(y)} + \sum_{q=1}^{p^{(y)}} l_q^{(y)} (l_q^{(y)} - 1) (M_q^{(y)})^2 \right) \quad (5.152)$$

$$\mathcal{N}_{ii,jj}^{(y)} = 2 \frac{(d-2)!(n-2)!}{(d-k^{(y)})!\Pi_y} \left((d-k^{(y)}) \sum_{q=1}^2 \delta(M_q^{(y)} - 2) l_q^{(y)} + \sum_{q=2}^{p^{(y)}} \Delta^{(y)}(q, 2) l_q^{(y)} l_{q-1}^{(y)} M_q^{(y)} (M_q^{(y)} - 1) \right) \quad (5.153)$$

$$\mathcal{N}_{ij,ik}^{(y)} = \frac{(d-3)!(n-2)!}{(d-k^{(y)})!\Pi_y} \left(\delta(M_1^{(y)} - 1) l_1^{(y)} (l_1^{(y)} - 1) (d-k^{(y)}) \right) \quad (5.154)$$

$$\begin{aligned} & + 2 \sum_{q \neq \{m-1, m\}} \Delta^{(y)}(m, 1) l_q^{(y)} l_m^{(y)} l_{m-1}^{(y)} M_q^{(y)} M_m^{(y)} \\ & + 2 \sum_{q=2}^{p^{(y)}} \Delta^{(y)}(q, 1) l_q^{(y)} l_{q-1}^{(y)} M_q^{(y)} \left((l_q^{(y)} - 1) M_q^{(y)} + (l_{q-1}^{(y)} - 1) M_{q-1}^{(y)} \right) \end{aligned}$$

$$\mathcal{N}_{ij,kl}^{(y)} = \frac{(d-4)!(n-2)!}{(d-k^{(y)})!\Pi_y} \left(\delta(M_1^{(y)} - 1) l_1^{(y)} (l_1^{(y)} - 1) (d-k^{(y)}) (d-k^{(y)} - 1) \right) \quad (5.155)$$

$$\begin{aligned} & + 8 \sum_{q \neq \{m-1, m, m+1\}} \Delta^{(y)}(q, 1) \Delta^{(y)}(m, 1) l_q^{(y)} l_{q-1}^{(y)} l_m^{(y)} l_{m-1}^{(y)} M_q^{(y)} M_m^{(y)} \\ & + 8 \sum_{q=3}^{p^{(y)}-1} \Delta^{(y)}(q, 1) l_q^{(y)} l_{q-1}^{(y)} M_q^{(y)} \left[\Delta^{(y)}(q+1, 1) l_{q+1}^{(y)} (l_q^{(y)} - 1) M_{q+1}^{(y)} \right. \\ & \left. + (l_q^{(y)} - 1) (l_{q-1}^{(y)} - 1) M_q^{(y)} + \Delta^{(y)}(q-1, 1) (l_{q-1}^{(y)} - 1) l_{q-2}^{(y)} M_{q-1}^{(y)} \right] \end{aligned}$$

$$\mathcal{N}_{ii,ij}^{(y)} = \mathcal{N}_{ii,jk}^{(y)} = 0. \quad (5.156)$$

From here we can use $\mathcal{N}_{i,j}^{(y)}$ for $M_1^{(y)} \geq 2$ to determine A, and find the following bounds,

$$A = \frac{2}{d^2 n} \sum_{q=2}^{p^{(y)}} \Delta^{(y)}(q, 1) l_q^{(y)} l_{q-1}^{(y)} M_q^{(y)} \quad (5.157)$$

$$\leq \frac{2}{d^2 n} \sum_{q=2}^{p^{(y)}} l_q^{(y)} l_{q-1}^{(y)} M_q^{(y)} \quad (5.158)$$

$$< \frac{2k^{(y)}}{d^2 n} \sum_{q=2}^{p^{(y)}} l_q^{(y)} M_q^{(y)} \quad (5.159)$$

$$< \frac{2k^{(y)}}{d^2}. \quad (5.160)$$

So indeed, $A \leq \mathcal{O}(d^{-2})$ so long as $k^{(y)} = \mathcal{O}(1)$, and therefore $F(|y\rangle) \leq 1/2$ for $y \in \mathcal{Y}_>$.

Now let us consider the bigger picture by returning to an arbitrary PSS state,

$$|\psi\rangle = \sum_{y \in \mathcal{Y}(n,d)} a_y |y\rangle, \quad (5.161)$$

with $\sum_y |a_y|^2 = 1$. From this state, we would like to trace down to ρ_1 and examine A , for the potential use of Theorem 5. So let us perform that partial trace, which I have broken up into three components,

$$A = \sum_y \left[A_{>}^{(y)} + A_1^{(y)} \right] + \sum_{y \neq z} A_{\times}^{(y,z)}, \quad (5.162)$$

where, before defining them formally, the components can be described as $A_{>}^{(y)}$ and $A_1^{(y)}$ being the contributions from the $M_1^{(y)} > 1$ and $M_1^{(y)} = 1$ components respectively for each y , and $A_{\times}^{(y,z)}$ being the cross terms from different Young diagram basis elements. Now, in more detail, we can start with the familiar terms,

$$A_{>}^{(y)} = 2 \frac{|a_y|^2}{\mathcal{A}_y} \frac{(d-2)!}{(d-k^{(y)})!} \frac{(n-1)!}{\Pi_y} \sum_{q=2}^{p^{(y)}} \Delta^{(y)}(q,1) l_q^{(y)} l_{q-1}^{(y)} M_q^{(y)} \quad (5.163)$$

$$= \frac{2|a_y|^2}{d(d-1)n} \sum_{q=2}^{p^{(y)}} \Delta^{(y)}(q,1) l_q^{(y)} l_{q-1}^{(y)} M_q^{(y)} \quad (5.164)$$

$$A_1^{(y)} = \delta(M_1^{(y)} - 1) \frac{|a_y|^2}{\mathcal{A}_y} \frac{(d-2)!}{(d-k^{(y)}-1)!} \frac{(n-1)!}{\Pi_y} l_1^{(y)} \quad (5.165)$$

$$= \delta(M_1^{(y)} - 1) \frac{|a_y|^2 (d-k^{(y)}) l_1^{(y)}}{d(d-1)n}. \quad (5.166)$$

The new term in the calculation is the cross term, $A_{\times}^{(y,z)}$, arising from the fact that $|\psi\rangle$ is now a superposition of Young diagram basis elements. But not all cross terms are going to appear in the partial trace. Two Young diagrams, y and z , will only contribute to $A_{\times}^{(y,z)}$ if $|ik_2 \dots k_n\rangle$ is in $|y\rangle$ and $|jk_2 \dots k_n\rangle$ is in $|z\rangle$ or vice versa. This then implies that Young diagrams, y and z , differ by only one block placement. Possibly a clearer way to describe this is that removing a single block from y and from z will arrive at the same Young diagram, or, more precisely, they are connected to a common vertex with $n-1$ blocks in Young's lattice. This leads us to define the 'compatibility function', $G(y,z)$, which evaluates to 1 if y and z are connected to a common vertex with $n-1$

blocks in Young's lattice, and evaluates to 0 otherwise. The size of $A_{\times}^{(y,z)}$ will then depend on the number permutations of the remaining $k_2 \dots k_n$ which are consistent with y and z . To quantify this, let $m_1^{(y)}$ indicate the row cluster from which the block is taken in y and moved to the row cluster $m_2^{(y)}$ in y to create z . We can analogously define $m_1^{(z)}$ and $m_2^{(z)}$. We could then choose which diagram, y or z , to index the sum over the $k_2 \dots k_n$. Rather than committing to one, we will do both simultaneously, relying on the following identity for compatible y and z ,

$$\frac{l_{m_1}^{(y)} l_{m_2}^{(y)} M_{m_1}^{(y)}}{\Pi_y} = \frac{l_{m_1}^{(z)} l_{m_2}^{(z)} M_{m_1}^{(z)}}{\Pi_z} = \sqrt{\frac{l_{m_1}^{(y)} l_{m_2}^{(y)} M_{m_1}^{(y)}}{\Pi_y} \frac{l_{m_1}^{(z)} l_{m_2}^{(z)} M_{m_1}^{(z)}}{\Pi_z}}. \quad (5.167)$$

From here we can finally determine

$$A_{\times}^{(y,z)} = \frac{a_y a_z^*}{\sqrt{\mathcal{A}_y \mathcal{A}_z}} G(y,z) \frac{(d-2)}{(d-k^{(y,z)})!} (n-1)! \sqrt{\frac{l_{m_1}^{(y)} l_{m_2}^{(y)} M_{m_1}^{(y)}}{\Pi_y} \frac{l_{m_1}^{(z)} l_{m_2}^{(z)} M_{m_1}^{(z)}}{\Pi_z}} \quad (5.168)$$

$$= \frac{a_y a_z^*}{d(d-1)n} G(y,z) \frac{\sqrt{(d-k^{(y)})!(d-k^{(z)})!}}{(d-k^{(y,z)})!} \sqrt{l_{m_1}^{(y)} l_{m_2}^{(y)} M_{m_1}^{(y)} l_{m_1}^{(z)} l_{m_2}^{(z)} M_{m_1}^{(z)}}, \quad (5.169)$$

where $k^{(y,z)} = \max\{k^{(y)}, k^{(z)}\}$. The $k^{(y,z)}$ distinction is required if only one of $M_{m_1}^{(y)} = 1$ or $M_{m_1}^{(z)} = 1$, which causes $k^{(y)}$ and $k^{(z)}$ to differ by 1. If this is the case, we arrive at an overall factor of $\sqrt{d-k^{(y,z)}}$ in $A_{\times}^{(y,z)}$, if not, that whole first fraction cancels.

Now consider a PSS state which is an arbitrary superposition of only Young diagram basis states in $\mathcal{Y}_{>}$,

$$|\psi_{>}\rangle = \sum_{y \in \mathcal{Y}_{>}} a_y |y\rangle. \quad (5.170)$$

For such a state, the $A_1^{(y)}$ term disappears, and the $A_{\times}^{(y,z)}$ term needs no $k^{(y,z)}$ distinction, as none of the $y \in \mathcal{Y}_{>}$ have isolated blocks. We can then bound the sums over the remaining terms, starting

with that over $A_{>}^{(y)}$

$$\sum_y A_{>}^{(y)} = \frac{2}{d(d-1)n} \sum_y |a_y|^2 \sum_{q=2}^{p^{(y)}} \Delta^{(y)}(q, 1) l_q^{(y)} l_{q-1}^{(y)} M_q^{(y)} \quad (5.171)$$

$$< \frac{2}{d(d-1)} \sum_y |a_y|^2 \sum_{q=1}^{p^{(y)}} l_q^{(y)} \quad (5.172)$$

$$\leq \frac{n}{d(d-1)} \sum_y |a_y|^2 \quad (5.173)$$

$$= \frac{n}{d(d-1)}, \quad (5.174)$$

which is clearly still $\leq \mathcal{O}(d^{-2})$ so long as $n \ll d$. We can then turn our attention to bounding the sum over $A_{\times}^{(y,z)}$,

$$\sum_{y \neq z} A_{\times}^{(y,z)} = \frac{1}{d(d-1)n} \sum_{y \neq z} a_y a_z^* G(y, z) \sqrt{l_{m_1}^{(y)} l_{m_2}^{(y)} M_{m_1}^{(y)} l_{m_1}^{(z)} l_{m_2}^{(z)} M_{m_1}^{(z)}} \quad (5.175)$$

$$< \frac{n}{2d(d-1)} \sum_{y \neq z} a_y a_z^* G(y, z) \quad (5.176)$$

$$= \frac{n}{4d(d-1)} \sum_{y \neq z} (a_y a_z^* + a_z a_y^*) G(y, z) \quad (5.177)$$

$$\leq \frac{n}{2d(d-1)} \sum_{y \neq z} |a_y| |a_z| G(y, z) \quad (5.178)$$

$$\leq \frac{n}{d(d-1)} \sum_y |a_y| \sum_{z \leq y} |a_z| G(y, z), \quad (5.179)$$

where $z \leq y$ if $|a_z| \leq |a_y|$. Continuing on,

$$\sum_{y \neq z} A_{\times}^{(y,z)} \leq \frac{n}{d(d-1)} \sum_y |a_y|^2 \sum_{z \leq y} G(y, z) \quad (5.180)$$

$$< \frac{n}{d(d-1)} \sqrt{\frac{n}{2}} \sum_y |a_y|^2 \quad (5.181)$$

$$= \frac{n}{d(d-1)} \sqrt{\frac{n}{2}}, \quad (5.182)$$

which is likewise $\leq \mathcal{O}(d^{-2})$ so long as $n\sqrt{n} \ll d$. These two together imply that $A \leq \mathcal{O}(d^{-2})$, and therefore, by Theorem 5, $F(|\psi_{>} \rangle) \leq 1/2$.

The cumulative work of this chapter is limited to concluding that isolated particles are required for good agreement with the mean field approximation in PSS states. I have not yet been able to say more than this, however. In particular, if $A > \mathcal{O}(d^{-2})$, then the resulting M

matrix, while easy enough to calculate, proves to be too difficult to analyze further in a fidelity calculation. For single basis elements, $|y\rangle$, I would ideally be able to bound $F(|y\rangle)$ as a function of the ratio of isolated particles to non-isolated. Those bounds could then be extended to arbitrary superpositions. Then, of course, the entire analysis would need to be repeated with marked sites.

Chapter 6

Conclusion and Future Directions

The whole of this thesis can be summed up by the general approach of making difficult calculations in the fields of quantum entanglement and state representations more tractable by restricting to symmetric subsets of the overall Hilbert space. In Chapter 2 I did just this for the totally symmetric subspace of multi-qubit states. Comparing and constraining different entanglement measures is generally difficult and, even in the three qubit case, cannot be done fully. But restricting to symmetric states allowed the full invariant space to be analyzed exactly. Likewise, the question of LU equivalence, while only partially understood in general, was shown to be fully understood in the symmetric subspace in three qubits. The result that equal pairwise concurrence in three qubits guaranteed LU equivalence to a symmetric state is a powerful result, and I would like to find its analogue in more qubits.

In Chapter 3 I shifted both to more qubits and translational invariance - a weaker symmetry. Rather than attempt to constrain all entanglement in this larger setting, however, I narrowed the entanglement picture to just pairwise entanglement as measured by the pairwise concurrence. I showed that pairwise entanglement in translationally invariant systems is entirely described by spacing of particles, but that spacing does not have the same physical interpretation one would expect in a translationally invariant system. Two parties being ‘adjacent’ does not reflect some

physical interaction length, but rather establishes some periodicity in the ring of parties, periodicity which changes when the spacing between parties is a factor of the number of parties. This allowed for the search for maximal pairwise concurrence to be restricted to maximal entanglement between adjacent parties in those smaller periodic cycles. Performing that maximization, as well as finding constraints on simultaneous entanglement of different spacings, could not be done in general and required restricting to the X state subspace in 4 and 5 qubits. The most notable unanswered question at this point is how the maximal adjacent entanglement decays with n in translationally invariant systems. Even if an exact answer remains out of reach, I would at least like to bound the scaling with n in the large n limit.

In Chapter 4 I addressed the matrix product state structure and how it adds the physical interpretation of spacing and interaction length in physical systems. Unfortunately, I was unable to do any entanglement calculations in the translationally invariant space, but I was able to come up with a novel canonical form for those states. In the fully symmetric space, however, I connected the Mandilara canonical form to the matrix product state space as a low bond dimensional approximation and demonstrated how maximal pairwise concurrence is achievable with only $D = 2$. Moving forward, I would like to find how the pairwise concurrence for $D = 2$ translationally invariant matrix product states decays with spacing, potentially in the large n limit.

Finally, in Chapter 5, I examined the assumptions required for non-linear dynamics in party-site symmetric systems and found that the mean field approximation is a poor one if the particles are not isolated. It remains to be shown, though, to what degree isolated particles give good agreement with the mean field approximation. The main hurdle to overcome in that analysis is the evaluation of the matrix fidelity for matrices with arbitrary dimension. If possible, that analysis would then need to be extended to the case where the complete graph is not fully symmetric, but has a subset of marked sites, partitioning the sites into marked and unmarked, while remaining symmetric in those sets. This would mean the basis elements are now pairs of Young diagrams, for marked and unmarked sites. An interesting tangential idea worth exploring

is what kinds of dynamics can be derived if separability, rather than the stronger mean field approximation, is assumed. We expect separability to be a more reasonable assumption in the PSS setting, so it would be safe to use the resultant equations of motion and to see what can be accomplished with the quantum random walk search in that setting.

The theory of entanglement has proven to be a fruitful medium to apply concepts of symmetry. Tools such as Young diagrams and the Majorana representation were invaluable in understanding state representations in the symmetric subspace, and the symmetrized matrices made otherwise impossible analysis doable. These benefits need not be limited to entanglement theory, though. Both in quantum mechanics and abroad, my study of symmetry will hopefully allow for future problems to find partial solutions in the symmetric subspace.

Appendix A

TIX State Achievable Pairwise Subconcurrence Boundaries

To find the boundary for TIX state subconcurrences, the boundaries of each of the pairs $(s\mathcal{C}_{1,\mu(v)}^{(n)}, s\mathcal{C}_{2,\mu(v)}^{(n)})$ need be found, with the overall boundary being a combination of the outermost boundaries from each pairing. To simplify the search for the boundaries, note that for any 4 or 5 qubit TIX state, the subconcurrence terms (3.26)-(3.33) are strictly increased by setting the coefficient phases to 0. This implies that the boundaries can be searched for among 4 and 5 qubit TIX states with purely real coefficients.

A.1 4 Qubits

Consider an arbitrary 4 qubit TIX state, (3.21), with real coefficients. The corresponding normalized state

$$|\bar{\Psi}\rangle = \frac{1}{\sqrt{a^2 + c^2 + f^2}} \left(a|0000\rangle + c\overbrace{|1100\rangle} + f|1111\rangle, \right) \quad (\text{A.1})$$

has both larger or equal $s\mathcal{C}_{1,v}^{(4)}$ and larger or equal $s\mathcal{C}_{2,\mu}^{(4)}$. To show this, consider either subconcurrency, \mathcal{C} , for which it is then true that

$$\mathcal{C}(|\bar{\psi}\rangle) \geq \mathcal{C}(|\bar{\psi}\rangle) \Big|_{d=0} = \mathcal{C}(|\psi\rangle) \Big|_{d=0} \geq \mathcal{C}(|\psi\rangle). \quad (\text{A.2})$$

All of which implies that the boundary of the $(s\mathcal{C}_{1,v}^{(4)}, s\mathcal{C}_{2,\mu}^{(4)})$ pairs can be looked for among states with $d = 0$. Likewise the state

$$|\bar{\psi}\rangle = \sqrt{\frac{a^2 + f^2}{2}} (|0000\rangle + |1111\rangle) + c \overbrace{|1100\rangle} + d \overbrace{|1010\rangle}, \quad (\text{A.3})$$

has larger or equal $s\mathcal{C}_{1,\mu}^{(4)}$, $s\mathcal{C}_{1,v}^{(4)}$, and $s\mathcal{C}_{2,v}^{(4)}$, meaning the boundaries of the $(s\mathcal{C}_{1,\mu}^{(4)}, s\mathcal{C}_{2,v}^{(4)})$ and $(s\mathcal{C}_{1,v}^{(4)}, s\mathcal{C}_{2,\mu}^{(4)})$ pairs can be found among states where $a = f$. And lastly the state

$$|\bar{\psi}\rangle = \frac{1}{\sqrt{c^2 - d^2}} \left(c \overbrace{|1100\rangle} + d \overbrace{|1010\rangle} \right), \quad (\text{A.4})$$

has larger or equal $s\mathcal{C}_{1,\mu}^{(4)}$ and $s\mathcal{C}_{2,\mu}^{(4)}$, so the boundary of the $(s\mathcal{C}_{1,\mu}^{(4)}, s\mathcal{C}_{2,\mu}^{(4)})$ pairs can be found among states where $a = f = 0$.

Using these simplified states, the remaining coefficients can be expressed using the following spherical parametrizations,

$$\{a, c, f\} \rightarrow \{\sin \theta \cos \phi, \cos \theta, \sin \theta \sin \phi\} \quad (\text{A.5})$$

$$\{a, c, d\} \rightarrow \{\cos \alpha, \sin \alpha \cos \beta, \sin \alpha \sin \beta\} \quad (\text{A.6})$$

$$\{c, d\} \rightarrow \{\cos \zeta, \sin \zeta\}, \quad (\text{A.7})$$

associated with the $(s\mathcal{C}_{1,v}^{(4)}, s\mathcal{C}_{2,\mu}^{(4)})$, $(s\mathcal{C}_{1,\mu(v)}^{(4)}, s\mathcal{C}_{2,v}^{(4)})$, and $(s\mathcal{C}_{1,\mu}^{(4)}, s\mathcal{C}_{2,\mu}^{(4)})$ pairs respectively, where $\{\theta, \phi, \alpha, \beta, \zeta\} \in [0, \pi/2]$. In these parametrizations, we can define the maps,

$$\mathcal{C}_{v,\mu} : \{\theta, \phi\} \rightarrow \{s\mathcal{C}_{1,v}^{(4)}, s\mathcal{C}_{2,\mu}^{(4)}\} \quad (\text{A.8})$$

$$\mathcal{C}_{\mu(v),v} : \{\alpha, \beta\} \rightarrow \{s\mathcal{C}_{1,\mu(v)}^{(4)}, s\mathcal{C}_{2,v}^{(4)}\} \quad (\text{A.9})$$

$$\mathcal{C}_{\mu,\mu} : \zeta \rightarrow \{s\mathcal{C}_{1,\mu}^{(4)}, s\mathcal{C}_{2,\mu}^{(4)}\}, \quad (\text{A.10})$$

according to the expressions (3.26)-(3.29). The boundaries of the images of these maps correspond to the boundaries of the domains, as well as the zeroes of the determinant of the Jacobians for each map. The result of all these boundary determinations leave the following two outermost

boundaries,

$$s\mathcal{C}_{2,X}^{(4)} \leq \begin{cases} \frac{2}{5} \left(8\sqrt{1 - 2s\mathcal{C}_{1,X}^{(4)} - 4(s\mathcal{C}_{1,X}^{(4)})^2} - s\mathcal{C}_{1,X}^{(4)} + 1 \right), & -\frac{1}{2} \leq s\mathcal{C}_{1,X}^{(4)} \leq \frac{63}{226} \\ \frac{1}{9} \left(8\sqrt{1 - s\mathcal{C}_{1,X}^{(4)} - 2(s\mathcal{C}_{1,X}^{(4)})^2} - 4s\mathcal{C}_{1,X}^{(4)} - 1 \right), & \frac{63}{226} \leq s\mathcal{C}_{1,X}^{(4)} \leq \frac{1}{2} \end{cases}, \quad (\text{A.11})$$

which came from the $(s\mathcal{C}_{1,\nu}^{(4)}, s\mathcal{C}_{2,\mu}^{(4)})$ pairs. These boundaries are displayed in the Figure A.1.

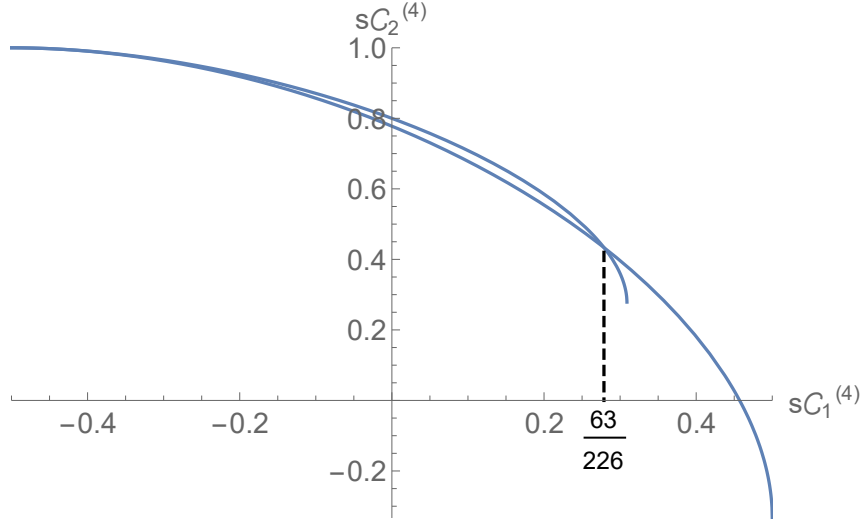


Figure A.1: The 4 qubit TIX state subconcurrence boundaries.

A.2 5 Qubits

Following the methods from the previous section, start by considering an arbitrary 5 qubit TIX state, (3.22), with real coefficients. The corresponding normalized state,

$$|\bar{\psi}\rangle = \frac{1}{\sqrt{c^2 + d^2 + g^2}} \left(c \overbrace{|00011\rangle} + d \overbrace{|00101\rangle} + g \overbrace{|01111\rangle} \right), \quad (\text{A.12})$$

has larger or equal $s\mathcal{C}_{1,\mu}^{(5)}$, and $s\mathcal{C}_{2,\mu}^{(5)}$, so therefore the boundary of the $(s\mathcal{C}_{1,\mu}^{(5)}, s\mathcal{C}_{2,\mu}^{(5)})$ pairs can be searched for among states with $a = 0$. For the other pairs, we will bound their subconcurrences by a sequence of lines which lie within the $(s\mathcal{C}_{1,\mu}^{(5)}, s\mathcal{C}_{2,\mu}^{(5)})$ boundary.

We can now parametrize the remaining coefficients of (A.12) as

$$\{c, d, g\} \rightarrow \{\sin \theta \cos \phi, \sin \theta \sin \phi, \cos \theta\}, \quad (\text{A.13})$$

and define the map

$$\mathcal{C}_{\mu,\mu} : \{\theta, \phi\} \rightarrow \left\{ s\mathcal{C}_{1,\mu}^{(5)}, s\mathcal{C}_{2,\mu}^{(5)} \right\}, \quad (\text{A.14})$$

according to (3.30) and (3.32). By analyzing the boundaries of the domain and the zeroes of the determinant of the Jacobian of this map, three boundaries make up a maximal set, and are plotted in Figure A.2. These three boundaries are parametrized by $\theta = \frac{\pi}{2}$, $\phi = 0$, and $\phi = \frac{\pi}{2}$. The exact polynomials in $s\mathcal{C}_{1,X}^{(5)}$ and $s\mathcal{C}_{2,X}^{(5)}$ which describe these boundaries are easily determined by a Gröbner basis calculation, but the results are quite lengthy.

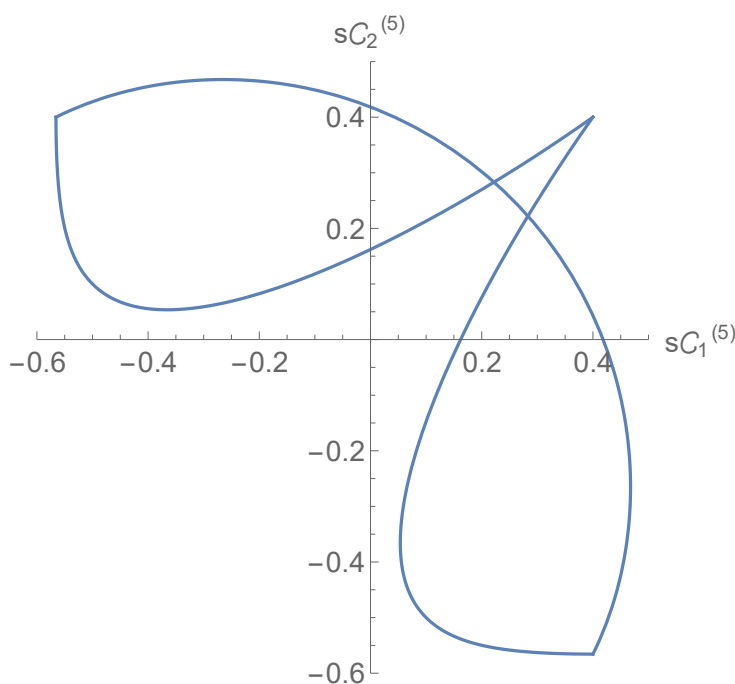


Figure A.2: The 5 qubit TIX state subconcurrence boundaries.

Turning now to the remaining subconcurrence pairings. It was shown in Table 3.1 that $\mathcal{C}_{1(2),v}^{(5)} \leq 0.366$. Another simple maximization shows that $s\mathcal{C}_{1,v}^{(5)} + s\mathcal{C}_{2,v}^{(5)} \leq \frac{2}{5}$. These three conditions bound the $(s\mathcal{C}_{1,v}^{(5)}, s\mathcal{C}_{2,v}^{(5)})$ pairs to a region well within the previous boundary, as shown in Figure A.3.

Lastly, the remaining two pairs, $(s\mathcal{C}_{1,\mu(v)}^{(5)}, s\mathcal{C}_{2,v(\mu)}^{(5)})$ can be handled together due to the symmetry in 5 qubits. Similar to the previous pair boundary, we will find a set of lines which

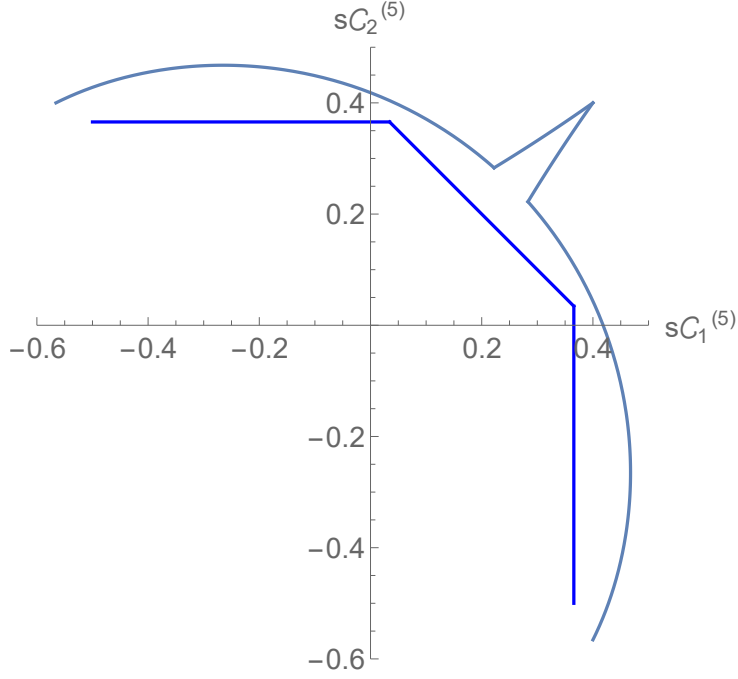


Figure A.3: The bounding conditions on the $(s\mathcal{C}_{1,v}^{(5)}, s\mathcal{C}_{2,v}^{(5)})$ pairs (darker blue) with the overall boundary.

bound the $(s\mathcal{C}_{1,\mu}^{(5)}, s\mathcal{C}_{2,v}^{(5)})$ pairs. We can again take advantage of $s\mathcal{C}_{2,v}^{(5)} \leq 0.366$, as well as the following two new maximizations,

$$s\mathcal{C}_{2,v}^{(5)} + s\mathcal{C}_{1,\mu}^{(5)} \leq \frac{47}{100} \quad (\text{A.15})$$

$$s\mathcal{C}_{2,v}^{(5)} + 2s\mathcal{C}_{1,\mu}^{(5)} \leq \frac{4}{5} \quad (\text{A.16})$$

These three conditions bound the $(s\mathcal{C}_{1,\mu}^{(5)}, s\mathcal{C}_{2,v}^{(5)})$ pairs within the original boundary for $0 \leq s\mathcal{C}_{1,\mu}^{(5)}$ and $0 \leq s\mathcal{C}_{2,v}^{(5)}$, as shown in Figure A.4. Note that these conditions on the $(s\mathcal{C}_{1,\mu}^{(5)}, s\mathcal{C}_{2,v}^{(5)})$ do not actually fall within the original boundary for regions in $0.4 \leq s\mathcal{C}_{1,\mu}^{(5)}$ and $s\mathcal{C}_{2,v}^{(5)} \leq 0$. But given that $s\mathcal{C}_{2,v}^{(5)} \leq 0$ for that region, the actual concurrences would be mapped to $\mathcal{C}_2^{(5)} = 0$, where the boundaries would then agree.

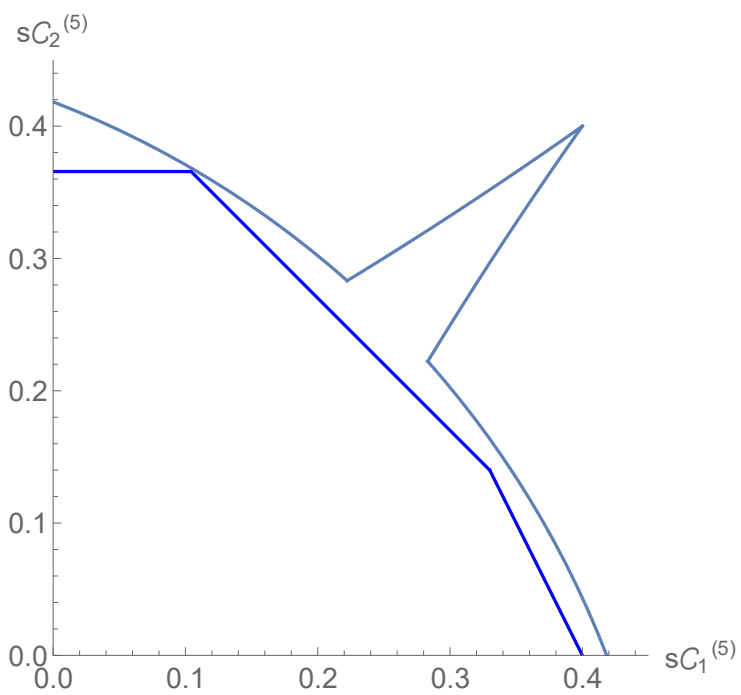


Figure A.4: The bounding conditions on the $(s\mathcal{C}_{1,\mu}^{(5)}, s\mathcal{C}_{2,\nu}^{(5)})$ pairs (darker blue) with the overall boundary.

Appendix B

Proof of Theorem 4

Proof. To show this analytically, start by considering an arbitrary n qubit symmetric state in the Majorana representation,

$$|\psi\rangle = \frac{1}{\sqrt{A}} \sum_{\pi \in \mathcal{S}_n} U_\pi \bigotimes_{j=1}^n |\phi_j\rangle, \quad (\text{B.1})$$

where again we have,

$$A = n! \sum_{\pi \in \mathcal{S}_n} \prod_{j=1}^n \langle \phi_j | \phi_{\pi(j)} \rangle. \quad (\text{B.2})$$

Consider perturbing one of the single qubit states, $|\phi_1\rangle$, to $|\phi'_1\rangle$ by rotating its Majorana star away by an angle 2ε such that $\langle \phi_1 | \phi'_1 \rangle = \cos \varepsilon \approx 1 - \frac{1}{2}\varepsilon^2$. The new overall state, $|\psi'\rangle$, would have a new normalization coefficient, A' . Let us start by putting bounds on A' in ε .

For any $j > 2$, let $2\theta_j$ be the relative angle between Majorana stars 1 and j , so that $|\langle \phi_1 | \phi_j \rangle| = \cos \theta_j$. The new relative angles, $2\theta'_j$, are bounded by

$$|2\theta_j - 2\theta'_j| \leq 2\varepsilon.$$

Likewise the inner products, $\langle \phi_j | \phi'_1 \rangle$, are then bounded by

$$\left| \langle \phi_j | \phi_1 \rangle - \langle \phi_j | \phi'_1 \rangle \right| \leq \varepsilon.$$

Notably, this does imply that the inner product could be negative if $\langle \phi_j | \phi_1 \rangle = 0$ for some j .

Now consider the upper bound on A' in ε . Start by labeling

$$A'_\pi = \prod_{j=1}^n \langle \phi'_j | \phi'_{\pi(j)} \rangle, \quad (\text{B.3})$$

where $|\phi'_j\rangle = |\phi_j\rangle$ for $j \neq 1$. Now $A' = n! \sum_{\pi \in S_n} A'_\pi$. We can then bound,

$$|A'_\pi| \leq \left| \left(\langle \phi_1 | \phi_{\pi(1)} \rangle + \varepsilon \right) \left(\langle \phi_{\pi^{-1}(1)} | \phi_1 \rangle + \varepsilon \right) \prod_{j \neq \{1, \pi^{-1}(1)\}} \langle \phi_j | \phi_{\pi(j)} \rangle \right| \quad (\text{B.4})$$

$$\leq |A_\pi| + \varepsilon \left| \langle \phi_1 | \phi_{\pi(1)} \rangle + \langle \phi_{\pi^{-1}(1)} | \phi_1 \rangle \right| \left| \prod_{j \neq \{1, \pi^{-1}(1)\}} \langle \phi_j | \phi_{\pi(j)} \rangle \right| + \mathcal{O}(\varepsilon^2) \quad (\text{B.5})$$

$$\leq |A_\pi| + 2\varepsilon + \mathcal{O}(\varepsilon^2). \quad (\text{B.6})$$

Notably, for the set of π for which $\pi(1) = 1$, $A'_\pi = A_\pi$ and the above condition is still true, though possibly unnecessary. We then have, to first order in ε ,

$$A' = n! \sum_{\pi \in S_n} A'_\pi \leq n! \left[\sum_{\pi \in S_n} (A_\pi + 2\varepsilon) \right] = A + 2(n!)^2 \varepsilon. \quad (\text{B.7})$$

Now turn to finding a lower bound for A' in ε . Consider, first, an A_π which is not equal to 0. We could repeat the analysis above to find that

$$|A'_\pi| \geq |A_\pi| - 2\varepsilon + \mathcal{O}(\varepsilon^2). \quad (\text{B.8})$$

Then, for $A_\pi = 0$, the magnitude of A_π could only increase, so the above expression still holds.

This then allows us to compute the full bounds on A' ,

$$A - 2(n!)^2 \varepsilon \leq A' \leq A + 2(n!)^2 \varepsilon. \quad (\text{B.9})$$

We can now turn our attention to bounding $|\langle \psi' | \psi \rangle|$. Start by examining

$$\begin{aligned} |\langle \psi | \psi' \rangle| &= \frac{n!}{\sqrt{A'A}} \left| \sum_{\pi \in S_n} \prod_{j=1}^n \langle \phi'_j | \phi_{\pi(j)} \rangle \right| \\ &= \frac{n!}{\sqrt{A'A}} \left| \sum_{\pi \in S_n} B_\pi \right|, \end{aligned}$$

where

$$B_\pi = \prod_{j=1}^n \langle \phi'_j | \phi_{\pi(j)} \rangle. \quad (\text{B.10})$$

We can extremize,

$$\begin{aligned} |B_\pi| &\geq \left| \left(\langle \phi_1 | \phi_{\pi(1)} \rangle - \varepsilon \right) \prod_{j=2}^n \langle \phi_j | \phi_{\pi(j)} \rangle \right| \\ &\geq |A_\pi| - \varepsilon. \end{aligned}$$

So then

$$\begin{aligned} |\langle \psi | \psi' \rangle| &\geq \frac{n!}{\sqrt{A'A}} \left[\frac{A}{n!} - (n!) \varepsilon \right] \\ &= \sqrt{\frac{A}{A!}} - (n!)^2 \frac{\varepsilon}{\sqrt{A'A}}. \end{aligned}$$

To give the most extreme lower bound, we would want to minimize the first term and maximize the second. Examining the first term,

$$\begin{aligned} \sqrt{\frac{A}{A!}} &\geq \sqrt{\frac{A}{A + 2(n!)^2 \varepsilon}} \\ &\approx 1 - \frac{(n!)^2}{A} \varepsilon + \mathcal{O}(\varepsilon^2). \end{aligned}$$

And the second term,

$$\begin{aligned} \frac{\varepsilon}{\sqrt{A'A}} &\leq \frac{\varepsilon}{\sqrt{A^2 - 2A(n!)^2 \varepsilon}} \\ &\approx \frac{\varepsilon}{A} + \mathcal{O}(\varepsilon^2). \end{aligned}$$

Combined we have

$$|\langle \psi | \psi' \rangle| \geq 1 - 2 \frac{(n!)^2}{A} \varepsilon. \quad (\text{B.11})$$

All that remains is to examine the minimum possible value of A , which we can show to be bounded from below by $A \geq 1$. I will prove this by induction, starting with the $n = 1$ case, as well as the $n = 2$ to be thorough. If $n = 1$,

$$A = \langle \phi_1 | \phi_1 \rangle = 1. \quad (\text{B.12})$$

For $n = 2$,

$$A = 2 \left(\langle \phi_1 | \phi_1 \rangle \langle \phi_2 | \phi_2 \rangle + \langle \phi_1 | \phi_2 \rangle \langle \phi_2 | \phi_1 \rangle \right) \quad (\text{B.13})$$

$$= 2 \left(1 + |\langle \phi_1 | \phi_2 \rangle|^2 \right) \quad (\text{B.14})$$

$$\geq 1. \quad (\text{B.15})$$

We must now prove the induction condition, or that

$$\sum_{\pi \in S_{n-1}} \prod_{j=1}^{n-1} \langle \phi_j | \phi_{\pi(j)} \rangle \geq 1 \implies \sum_{\pi \in S_n} \prod_{j=1}^n \langle \phi_j | \phi_{\pi(j)} \rangle \geq 1. \quad (\text{B.16})$$

To show this, start by partitioning S_n into two disjoint subsets,

$$\mathcal{X} = \{\pi \in S_n | \pi : 1 \mapsto 1\} \quad (\text{B.17})$$

$$\mathcal{Y} = S_n - \mathcal{X}. \quad (\text{B.18})$$

So \mathcal{X} are the permutations which fix party 1, and \mathcal{Y} are the remaining permutations in S_n .

Using these partitions, split the sum in A into

$$A = \sum_{\alpha \in \mathcal{X}} \prod_{j=1}^n \langle \phi_j | \phi_{\alpha(j)} \rangle + \sum_{\beta \in \mathcal{Y}} \prod_{j=1}^n \langle \phi_j | \phi_{\beta(j)} \rangle. \quad (\text{B.19})$$

All the permutations in the first sum fix party 1, but freely permute the remaining $n-1$ parties.

$$\sum_{\alpha \in \mathcal{X}} \prod_{j=1}^n \langle \phi_j | \phi_{\alpha(j)} \rangle = \langle \phi_1 | \phi_1 \rangle \sum_{\pi \in S_{n-1}} \prod_{j=2}^n \langle \phi_j | \phi_{\pi(j)} \rangle \quad (\text{B.20})$$

$$\geq \langle \phi_1 | \phi_1 \rangle \quad (\text{B.21})$$

$$= 1, \quad (\text{B.22})$$

where the first inequality is true by the induction condition.

Now examine the second sum. Consider a permutation, $\pi \in \mathcal{Y}$, which sends party 1 to party, $p \neq 1$, and sends some $q \neq p$ to 1. The product of inner products, A_π , for such a permutation would look like

$$\langle \phi_1 | \phi_p \rangle \langle \phi_p | \phi_l \rangle \dots \langle \phi_m | \phi_q \rangle \langle \phi_q | \phi_1 \rangle. \quad (\text{B.23})$$

Also in \mathcal{Y} would be permutation which has all the same mappings for parties except 1, p , and q , but now acts as a swap on parties 1 and p , and sends q to l . This corresponding A_π for this permutation would look like

$$\langle \phi_1 | \phi_p \rangle \langle \phi_q | \phi_l \rangle \dots \langle \phi_m | \phi_q \rangle \langle \phi_p | \phi_1 \rangle. \quad (\text{B.24})$$

And also in \mathcal{Y} would be the two permutations which merely exchange the roles of p and q in the

previous two permutations. If we sum the A_π of these four permutations we get

$$\begin{aligned}
& \langle \phi_1 | \phi_p \rangle \langle \phi_p | \phi_l \rangle \dots \langle \phi_m | \phi_q \rangle \langle \phi_q | \phi_1 \rangle \\
& + \langle \phi_1 | \phi_p \rangle \langle \phi_q | \phi_l \rangle \dots \langle \phi_m | \phi_q \rangle \langle \phi_p | \phi_1 \rangle \\
& + \langle \phi_1 | \phi_q \rangle \langle \phi_q | \phi_l \rangle \dots \langle \phi_m | \phi_p \rangle \langle \phi_p | \phi_1 \rangle \\
& + \langle \phi_1 | \phi_q \rangle \langle \phi_p | \phi_l \rangle \dots \langle \phi_m | \phi_p \rangle \langle \phi_q | \phi_1 \rangle.
\end{aligned} \tag{B.25}$$

Now define $\gamma_p = \langle \phi_1 | \phi_p \rangle$ and $|\chi_{p,q}\rangle = \gamma_q |\phi_p\rangle + \gamma_p |\phi_q\rangle$. Using these definitions, the previous sum becomes,

$$\langle \chi_{p,q} | \phi_l \rangle \dots \langle \phi_m | \chi_{p,q} \rangle. \tag{B.26}$$

Note that this new single effective permutation on $n - 2$ qubits makes no constraint on the permutation on parties other than 1, p , and q . This means that, in summing over all permutations in \mathcal{Y} , the set of permutations of the form in (B.25) will include all effective permutations in S_{n-2} .

Altogether, this means that we can reduce the second sum in A to

$$\begin{aligned}
\sum_{\beta \in \mathcal{Y}} \prod_{j=1}^n \langle \phi_j | \phi_{\beta(j)} \rangle &= \sum_{p>q>1}^n \sum_{\pi \in S_{n-2}} \left(\langle \chi_{p,q} | \bigotimes_{j \neq 1,p,q}^n \langle \phi_j | \right) U_\pi \left(|\chi_{p,q}\rangle \bigotimes_{j \neq 1,p,q}^n \langle \phi_j | \right) \\
&\geq \sum_{p>q>1}^n |\langle \chi_{p,q} | \chi_{p,q} \rangle|^2 \\
&\geq 0.
\end{aligned}$$

Together this finally implies that $A \geq 1$.

We then finally have that

$$|\langle \psi | \psi' \rangle| \geq 1 - 2(n!) \varepsilon. \tag{B.27}$$

□

Obviously, this bound could likely be tightened, but it is sufficient for my purposes.

Appendix C

Matrix Norms on PSS Bloch Vectors

While the Fidelity is the matrix norm of choice in quantum information theory, other norms do exist and are less challenging analytically to evaluate due to not needing to find the eigenvalues of large matrices. The two norms discussed in this Appendix, the Hilbert-Schmidt distance [72] and the Super-Fidelity [73], are relatively simple analytically and also make convenient use of the generalized Bloch vector representation [74] of PSS states.

C.1 Bloch Vectors of PSS Reductions

A two qubit pure state,

$$|\psi\rangle = \cos\left(\frac{\theta}{2}\right)|0\rangle + \sin\left(\frac{\theta}{2}\right)e^{i\phi}|1\rangle, \quad (\text{C.1})$$

can be mapped to unit length vector in \mathbb{R}_3 by the Bloch vector representation [75],

$$|\psi\rangle\langle\psi| = \frac{1}{2}\mathbb{1} + \frac{1}{2}\vec{n} \cdot \vec{\sigma}, \quad (\text{C.2})$$

where $\vec{\sigma}$ is a vector of the Pauli matrices and

$$\vec{n} = (\sin\theta \cos\phi, \sin\theta \sin\phi, \cos\theta), \quad (\text{C.3})$$

is the unit length Bloch vector of the state, $|\psi\rangle$. This representation likewise extends to mixed two qubit states,

$$\rho = \frac{1}{2}\mathbb{1} + \frac{1}{2}\vec{r} \cdot \vec{\sigma}, \quad (\text{C.4})$$

where now $|\vec{r}| \leq 1$. The Bloch vector, \vec{r} , lends to the ‘Bloch Ball’ illustration of 2 qubit quantum states - that any 2 qubit state can be represented as a point within the unit ball in \mathbb{R}_3 , with pure states lying at the surface and mixed states in the interior. Beyond being a useful visualization of the state, the Bloch vector representation also forms an orthonormal basis for 2 qubit density matrices. To see this, begin by expressing ρ as

$$\rho = \sum_{i=0}^3 c_i \sigma_i, \quad (\text{C.5})$$

where $\sigma_0 = \mathbb{1}_2$, $\sigma_1 = \sigma_x$, $\sigma_2 = \sigma_y$, and $\sigma_3 = \sigma_z$. This representation relies on the orthonormality of σ_i , namely that

$$\text{Tr}(\sigma_i \sigma_j) = 2\delta_{i,j}, \quad (\text{C.6})$$

to find that

$$c_i = \frac{1}{2}\text{Tr}(\rho \sigma_i). \quad (\text{C.7})$$

The normalization of ρ then implies that $c_0 = \frac{1}{2}$, while the hermiticity of ρ implies that the remaining $c_i \in \mathbb{R}$, which agrees with the idea that $\vec{r} \in \mathbb{R}_3$. These properties will be critical as the Bloch vector representation is extended to multi-qubit states.

The multi-qubit extension of the Bloch vector representation has been shown to be a powerful tool in the analysis of symmetries and quantum marginals [31]. A multi-qubit state, pure or mixed, can be expressed as

$$\rho = \sum_{i_1 \dots i_n} c_{i_1 \dots i_n} \sigma_{i_1 \dots i_n}, \quad (\text{C.8})$$

where

$$\sigma_{i_1 \dots i_n} = \bigotimes_{j=1}^n \sigma_{i_j}. \quad (\text{C.9})$$

The properties of σ_i again allow us to determine

$$c_{i_1 \dots i_n} = \frac{1}{2^n} \text{Tr}(\rho \sigma_{i_1 \dots i_n}). \quad (\text{C.10})$$

The normalization of ρ then implies that $c_{0\dots 0} = 2^{-n}$, while the hermiticity of ρ again implies that each of $c_{i_1\dots i_n}$ are real. The positivity of ρ enforces an additional constraint on the vector components, but the constraint has no convenient form. If the state is pure, however, we can find an additional constraint by enforcing $\text{Tr}\rho^2 = \text{Tr}\rho$, which, after performing the trace, gives the following

$$\frac{1 - 2^{-N}}{2^N} = \sum_{i_1\dots i_N \in \hat{\mathbb{Z}}} c_{i_1\dots i_N}^2. \quad (\text{C.11})$$

The multi-qubit Bloch vector representation greatly simplifies the determination of reduced density matrices of an overall state. Consider tracing over the last $n - k$ parties of ρ ,

$$\rho_k = \text{Tr}_{i_{k+1}\dots i_n} \left(\sum_{i_1\dots i_n} c_{i_1\dots i_n} \sigma_{i_1\dots i_n} \right) \quad (\text{C.12})$$

$$= \sum_{i_1\dots i_n} c_{i_1\dots i_n} \sigma_{i_1\dots i_k} \text{Tr}(\sigma_{i_{k+1}\dots i_n}). \quad (\text{C.13})$$

But of the $\sigma_{i_{k+1}\dots i_n}$, the identity, $\sigma_{0\dots 0}$, is the only element with a non-zero trace, leaving

$$\rho_k = \sum_{i_1\dots i_k} c_{i_1\dots i_k 0\dots 0} \sigma_{i_1\dots i_k} \text{Tr}(\sigma_{0\dots 0}) \quad (\text{C.14})$$

$$= 2^{n-k} \sum_{i_1\dots i_k} c_{i_1\dots i_k 0\dots 0} \sigma_{i_1\dots i_k}. \quad (\text{C.15})$$

For short hand, we will denote the Bloch vector components of the reduced state, ρ_k , as $c_{i_1\dots i_k}$ where the other indices are implied to be 0.

In order to apply this representation to PSS states, we need to extend σ_i to higher dimensional particles. That would require a set of d^2 Hermitian matrices which are again orthonormal under the trace inner product. The generalized Gell-Mann matrices are exactly such a set and can be denoted, for $\alpha = 1, \dots, d - 1$ and $\beta > \alpha$, as

$$\sigma_{\alpha,\beta}^x = |\alpha\rangle\langle\beta| + |\beta\rangle\langle\alpha| \quad (\text{C.16})$$

$$\sigma_{\alpha,\beta}^y = -i \left(|\alpha\rangle\langle\beta| - |\beta\rangle\langle\alpha| \right) \quad (\text{C.17})$$

$$\sigma_{\alpha}^z = \sqrt{\frac{2}{\alpha(\alpha+1)}} \left(-\alpha |\alpha+1\rangle\langle\alpha+1| + \sum_{\gamma=1}^{\alpha} |\gamma\rangle\langle\gamma| \right) \quad (\text{C.18})$$

$$\sigma_0^z = \mathbb{1}_d. \quad (\text{C.19})$$

With the generalized Gell-Mann matrices as a basis, a single d -dimensional mixed state can be

expressed as

$$\rho = \sum_{\mathbf{i}} c_{\mathbf{i}} \sigma_{\mathbf{i}}, \quad (\text{C.20})$$

where \mathbf{i} is implied to run over each element in (C.16)-(C.19), and we will let Greek indices run over all except the identity. The Gell-Mann matrices are likewise orthogonal, following

$$\text{Tr}(\sigma_0^2) = d \quad (\text{C.21})$$

$$\text{Tr}(\sigma_0 \sigma_{\alpha}) = 0 \quad (\text{C.22})$$

$$\text{Tr}(\sigma_{\alpha} \sigma_{\beta}) = 2\delta_{\alpha,\beta}. \quad (\text{C.23})$$

We can likewise build an n party state in this generalized Bloch form as

$$\rho = \sum_{\mathbf{i}_1 \dots \mathbf{i}_N} c_{\mathbf{i}_1 \dots \mathbf{i}_N} \sigma_{\mathbf{i}_1 \dots \mathbf{i}_N}. \quad (\text{C.24})$$

where $c_{0\dots 0} = d^{-n}$. The same partial trace analysis allows us to find

$$\rho_1 = \sum_{\mathbf{i}} c_{\mathbf{i}} \sigma_{\mathbf{i}} \quad (\text{C.25})$$

$$\rho_2 = \sum_{\mathbf{i}, \mathbf{j}} c_{\mathbf{i}, \mathbf{j}} \sigma_{\mathbf{i}, \mathbf{j}}, \quad (\text{C.26})$$

where I am again using the shorthand, $c_{\mathbf{i}} = d^{1-n} c_{\mathbf{i}0\dots 0}$ and $c_{\mathbf{i}, \mathbf{j}} = d^{2-n} c_{\mathbf{i}, \mathbf{j}0\dots 0}$.

Up to this point, this has been a general review of the Bloch vector representation and its extension to higher dimensional particles. Let us now consider finding the Bloch vector representations of ρ_1 and ρ_2 for PSS states. This is a useful piece of analysis on its own, but it will also make determining the Hilbert-Schmidt distance and Super-Fidelity rather trivial. The goal then is to find $c_{\mathbf{i}}$ and $c_{\mathbf{i}, \mathbf{j}}$ as functions of A , B_1 - B_5 , and C . Starting with ρ_1 , it is fairly simple to recognize that

$$\rho_1 = \frac{1}{d} \mathbb{1}_d + A \sum_{i \neq j} |i\rangle\langle j| \quad (\text{C.27})$$

$$= \frac{1}{d} \mathbb{1}_d + A \sum_{\alpha < \beta} \sigma_{\alpha\beta}^x, \quad (\text{C.28})$$

meaning that $c_0 = d^{-1}$, $c_{\alpha\beta}^x = A$, and the remaining $c_{\alpha}^z = c_{\alpha\beta}^y = 0$.

The picture for ρ_2 is considerably more complex, and will be broken down into compo-

nents in the following sub-sections. The components are,

$$\begin{aligned} \rho_2 = & \underbrace{\sum_{i,j} c_{ij}^{zz} \sigma_i^z \otimes \sigma_j^z}_{\text{The Diagonal}} + \underbrace{\sum_i \sum_{\alpha < \beta} \sum_{p \in \{x,y\}} c_{i\alpha,\beta}^{zp} \left(\sigma_i^z \otimes \sigma_{\alpha,\beta}^p + \sigma_{\alpha,\beta}^p \otimes \sigma_i^z \right)}_{\text{The Semi-Off-Diagonal (Real and Imaginary)}} \\ & + \underbrace{\sum_{\alpha < \beta} \sum_{\gamma < \delta} \sum_{p,q \in \{x,y\}} c_{\alpha,\beta,\gamma,\delta}^{pq} \sigma_{\alpha,\beta}^p \otimes \sigma_{\gamma,\delta}^q}_{\text{The Fully-Off-Diagonal (Real and Imaginary)}}. \end{aligned} \quad (\text{C.29})$$

Throughout these calculations, the following identity will be often used,

$$\sum_{\alpha=i}^j \frac{1}{\alpha(\alpha+1)} = \frac{j}{j+1} - \frac{i-1}{i}. \quad (\text{C.30})$$

The Diagonal - The σ^z - σ^z Pairings

After subtracting off by $d^{-2}\sigma_{00}$, the diagonal of ρ_2 is now of the form,

$$C \left[\sum_{i \neq j=1}^d |ij\rangle\langle ij| - (d-1) \sum_{i=1}^d |ii\rangle\langle ii| \right]. \quad (\text{C.31})$$

I will now show that this can be represented in the Bloch form purely by using $c_{\alpha\beta}^{zz} = -\frac{Cd}{2}\delta_{\alpha,\beta}$.

Proof.

$$\sum_{i \neq j=1}^d |ij\rangle\langle ij| - (d-1) \sum_{i=1}^d |ii\rangle\langle ii| = -\frac{d}{2} \sum_{\alpha=1}^{d-1} \sigma_{\alpha}^z \otimes \sigma_{\alpha}^z \quad (\text{C.32})$$

$$\begin{aligned} = & -d \left[\sum_{\alpha=1}^{d-1} \frac{1}{\alpha(\alpha+1)} \left(\alpha^2 |\alpha+1 \ \alpha+1\rangle\langle \alpha+1 \ \alpha+1| \right. \right. \\ & \left. \left. + \sum_{i,j=1}^{\alpha} |ij\rangle\langle ij| - \alpha |i \ \alpha+1\rangle\langle i \ \alpha+1| - \alpha |\alpha+1 \ j\rangle\langle \alpha+1 \ j| \right) \right]. \end{aligned} \quad (\text{C.33})$$

Now consider only the terms on either side with matching indices for both parties,

$$-(d-1) \sum_{i=1}^d |ii\rangle\langle ii| = \sum_{\alpha=1}^{d-1} \frac{-d}{\alpha(\alpha+1)} \left(\alpha^2 |\alpha+1 \ \alpha+1\rangle\langle \alpha+1 \ \alpha+1| + \sum_{i=1}^{\alpha} |ii\rangle\langle ii| \right) \quad (\text{C.34})$$

$$= -d \sum_{i=1}^d \left(\frac{i-1}{i} + \sum_{\alpha=i}^{d-1} \frac{1}{\alpha(\alpha+1)} \right) |ii\rangle\langle ii| \quad (\text{C.35})$$

$$= -d \sum_{i=1}^d \left(\frac{i-1}{i} + \frac{d-1}{d} - \frac{i-1}{i} \right) |ii\rangle\langle ii| \quad (\text{C.36})$$

$$= -(d-1) \sum_{i=1}^d |ii\rangle\langle ii|. \quad (\text{C.37})$$

And now the non-matching indices for either party, starting with $i < j$,

$$\sum_{i < j} |ij\rangle\langle ij| = \sum_{\alpha=1}^{d-1} \frac{-d}{\alpha(\alpha+1)} \sum_{i < j < \alpha+2} (|ij\rangle\langle ij| - \alpha |i \alpha+1\rangle\langle i \alpha+1|) \quad (\text{C.38})$$

$$= -d \sum_{i < j} \left(-\frac{1}{j} + \sum_{\alpha=j}^{d-1} \frac{1}{\alpha(\alpha+1)} \right) |ij\rangle\langle ij| \quad (\text{C.39})$$

$$= -d \sum_{i < j} \left(-\frac{1}{j} + \frac{d-1}{d} - \frac{j-1}{j} \right) |ij\rangle\langle ij| \quad (\text{C.40})$$

$$= \sum_{i < j} |ij\rangle\langle ij|. \quad (\text{C.41})$$

And likewise for $i > j$, which completes the proof. \square

The Real Semi-Off-Diagonal - The $\sigma^z \otimes \sigma^x$ Pairings

In the computational basis, the Real Semi-Off-Diagonal is of the form,

$$B_3 \sum_{i \neq j, k} \sum_{j \neq k} (|ij\rangle\langle ik| + |ji\rangle\langle ki|) \quad (\text{C.42})$$

$$+ \Re(B_5) \sum_{j \neq k} (|jj\rangle\langle jk| + |jj\rangle\langle kj| + |jk\rangle\langle jj| + |kj\rangle\langle jj|),$$

which we will now show can be represented in the Bloch form with the following coefficients,

$$c_{0\alpha,\beta}^{zx} = \frac{d-2}{d} B_3 + \frac{2}{d} \Re(B_5), \quad (\text{C.43})$$

and

$$c_{\gamma\alpha,\beta}^{zx} = \sqrt{\frac{1}{2\gamma(\gamma+1)}} (B_3 - \Re(B_5)) \begin{cases} -2 & \beta < \gamma+1 \\ \gamma-1 & \beta = \gamma+1 \\ -1 & \alpha < \gamma+1 < \beta \\ \gamma & \alpha = \gamma+1 \\ 0 & \alpha > \gamma+1 \end{cases} \quad (\text{C.44})$$

For a fixed γ , we can visualize $c_{\gamma\alpha,\beta}^{zx}$ in an array indexed by α and β ,

$$c_{\gamma\alpha,\beta}^{zx} = \sqrt{\frac{1}{2\gamma(\gamma+1)}} (B_3 - \Re(B_5)) \begin{pmatrix} -2 & \cdots & -2 & \gamma-1 & -1 & \cdots & \cdots & -1 \\ & \ddots & \vdots & \vdots & \vdots & \ddots & & \vdots \\ & & -2 & \vdots & \vdots & & \ddots & \vdots \\ & & & \gamma-1 & -1 & \cdots & \cdots & -1 \\ & & & & \gamma & \cdots & \cdots & \gamma \\ & & & & & 0 & \cdots & 0 \\ & & & & & & \ddots & \vdots \\ & & & & & & & 0 \end{pmatrix}, \quad (\text{C.45})$$

where the $\alpha = \gamma + 1$ and $\beta = \gamma + 1$ entries have been highlighted in red and blue respectively.

What follows is a proof that these representations are equivalent.

Proof. Start by expanding the matrices of the Bloch representation and considering only the entries for which $j < k$, because the converse will follow from symmetry of $\sigma_{j,k}^x$. Likewise, we will only consider the $\sigma_{\gamma}^z \otimes \sigma_{\alpha,\beta}^x$ components, as the exchanged elements will follow from the U symmetry. In the computational basis, this leaves,

$$B_3 \sum_{i \neq j,k} \sum_{j < k} |ij\rangle \langle ik| + \Re(B_5) \sum_{j < k} (|jj\rangle \langle jk| + |kj\rangle \langle kk|), \quad (\text{C.46})$$

while in the Bloch representation we are left with,

$$\begin{aligned}
2(B_3 - \Re(B_5)) \sum_{\gamma=1}^{d-1} \frac{1}{\gamma(\gamma+1)} & \left[- \sum_{j < k < \gamma+1} \left(-\gamma |\gamma+1 \ j\rangle \langle \gamma+1 \ k| + \sum_{i=1}^{\gamma} |ij\rangle \langle ik| \right) \right. \\
& + \frac{\gamma-1}{2} \sum_{j=1}^{\gamma} \left(-\gamma |\gamma+1 \ i\rangle \langle \gamma+1 \ \gamma+1| + \sum_{i=1}^{\gamma} |ij\rangle \langle i \ \gamma+1| \right) \\
& - \frac{1}{2} \sum_{j < \gamma+1 < k} \left(-\gamma |\gamma+1 \ j\rangle \langle \gamma+1 \ k| + \sum_{i=1}^{\gamma} |ij\rangle \langle ik| \right) \\
& + \frac{\gamma}{2} \sum_{k=\gamma+2}^d \left(-\gamma |\gamma+1 \ \gamma+1\rangle \langle \gamma+1 \ k| + \sum_{i=1}^{\gamma} |i \ \gamma+1\rangle \langle ik| \right) \left. \right] \\
& + \left(\frac{d-2}{d} B_3 + \frac{2}{d} \Re(B_5) \right) \sum_{i=1}^d \sum_{j < k} |ij\rangle \langle ik|.
\end{aligned} \tag{C.47}$$

Consider first the elements of the form, $|jj\rangle \langle jk|$, which leaves, in the computational basis, only

$$\Re(B_5) \sum_{j < k} |jj\rangle \langle jk|, \tag{C.48}$$

while, in the Bloch representation, we have,

$$\begin{aligned}
2(B_3 - \Re(B_5)) \sum_{\gamma=1}^{d-1} \frac{1}{\gamma(\gamma+1)} & \left[- \sum_{j < k < \gamma+1} |jj\rangle \langle jk| + \frac{\gamma-1}{2} \sum_{j=1}^{\gamma} |jj\rangle \langle j \ \gamma+1| \right. \\
& - \frac{1}{2} \sum_{j < \gamma+1 < k} |jj\rangle \langle jk| - \frac{\gamma^2}{2} \sum_{k=\gamma+2}^d |\gamma+1 \ \gamma+1\rangle \langle \gamma+1 \ k| \left. \right] \\
& + \left(\frac{d-2}{d} B_3 + \frac{2}{d} \Re(B_5) \right) \sum_{j < k} |jj\rangle \langle jk|,
\end{aligned} \tag{C.49}$$

which can be evaluated further to,

$$\begin{aligned}
& \sum_{j < k} |jj\rangle \langle jk| \left\{ \frac{d-2}{d} B_3 + \frac{2}{d} \Re(B_5) \right. \\
& \left. + (B_3 - \Re(B_5)) \left[-2 \sum_{\gamma=k}^{d-1} \frac{1}{\gamma(\gamma+1)} + \frac{k-2}{k(k-1)} - \sum_{\gamma=j}^{k-2} \frac{1}{\gamma(\gamma+1)} - \frac{j-1}{j} \right] \right\}.
\end{aligned} \tag{C.50}$$

We can now evaluate the sums over γ in the Bloch representation using (C.30), leaving,

$$\begin{aligned}
& \sum_{j < k} |jj\rangle \langle jk| \left\{ \frac{d-2}{d} B_3 + \frac{2}{d} \Re(B_5) \right. \\
& \left. + (B_3 - \Re(B_5)) \left[-2 \frac{d-1}{d} + 2 \frac{k-1}{k} + \frac{k-2}{k(k-1)} - \frac{k-2}{k-1} + \frac{j-1}{j} - \frac{j-1}{j} \right] \right\},
\end{aligned} \tag{C.51}$$

which indeed evaluates to (C.46). Now consider elements of the form, $|kj\rangle \langle kk|$ for $j \neq k$, which,

in the computational basis, leaves,

$$\Re(B_5) \sum_{j < k} |kj\rangle \langle kk|, \quad (\text{C.52})$$

and in the Bloch representation we have,

$$\begin{aligned} & 2(B_3 - \Re(B_5)) \sum_{\gamma=1}^{d-1} \frac{1}{\gamma(\gamma+1)} \left[- \sum_{j < k < \gamma+1} |kj\rangle \langle kk| \right. \\ & \left. - \frac{\gamma(\gamma-1)}{2} \sum_{j=1}^{\gamma} |\gamma+1 \ j\rangle \langle \gamma+1 \ \gamma+1| \right] + \left(\frac{d-2}{d} B_3 + \frac{2}{d} \Re(B_5) \right) \sum_{j < k} |kj\rangle \langle kk|, \end{aligned} \quad (\text{C.53})$$

which can be expressed as

$$\sum_{j < k} |kj\rangle \langle kk| \left\{ \frac{d-2}{d} B_3 + \frac{2}{d} \Re(B_5) - (B_3 - \Re(B_5)) \left[2 \sum_{\gamma=k}^{d-1} \frac{1}{\gamma(\gamma+1)} + \frac{k-2}{k} \right] \right\} \quad (\text{C.54})$$

$$= \sum_{j < k} |kj\rangle \langle kk| \left\{ \frac{d-2}{d} B_3 + \frac{2}{d} \Re(B_5) - (B_3 - \Re(B_5)) \left[2 \frac{d-1}{d} - 2 \frac{k-1}{k} + \frac{k-2}{k} \right] \right\}, \quad (\text{C.55})$$

which evaluates to (C.52). This leaves only needing to consider terms of the form, $|ij\rangle \langle ik|$, for distinct i , j , and k , which, in the computational basis, leaves

$$B_3 \sum_{i \neq j, k} \sum_{j < k} |ij\rangle \langle ik|. \quad (\text{C.56})$$

Turning to the Bloch representation, naively we can simplify equation (C.47) by eliminating the first terms in the second and fourth lines, then changing the sums over i to skip over j and k . To evaluate further, however, we need to address how each remaining term behaves as the value of i ranges from $i < j$, to $j < i < k$, and finally to $i > k$. Starting with $i < j$, all that survives is

$$\begin{aligned} & \sum_{i \neq j, k} \sum_{j < k} |ij\rangle \langle ik| \left\{ \frac{d-2}{d} B_3 + \frac{2}{d} \Re(B_5) \right. \\ & \left. + (B_3 - \Re(B_5)) \left[-2 \sum_{\gamma=k}^{d-1} \frac{1}{\gamma(\gamma+1)} + \frac{k-2}{k(k-1)} - \sum_{\gamma=j}^{k-2} \frac{1}{\gamma(\gamma+1)} + \frac{1}{j} \right] \right\}. \end{aligned} \quad (\text{C.57})$$

For $j < i < k$, the surviving terms are

$$\begin{aligned} & \sum_{i \neq j, k} \sum_{j < k} |ij\rangle \langle ik| \left\{ \frac{d-2}{d} B_3 + \frac{2}{d} \Re(B_5) \right. \\ & \left. + (B_3 - \Re(B_5)) \left[-2 \sum_{\gamma=k}^{d-1} \frac{1}{\gamma(\gamma+1)} + \frac{k-2}{k(k-1)} - \sum_{\gamma=i}^{k-2} \frac{1}{\gamma(\gamma+1)} + \frac{1}{i} \right] \right\}, \end{aligned} \quad (\text{C.58})$$

while for $i > k$, the surviving terms are

$$\sum_{i \neq j, k} \sum_{j < k} |ij\rangle \langle ik| \left\{ \frac{d-2}{d} B_3 + \frac{2}{d} \Re(B_5) + (B_3 - \Re(B_5)) \left[-2 \sum_{\gamma=i}^{d-1} \frac{1}{\gamma(\gamma+1)} + \frac{2}{i} \right] \right\}. \quad (\text{C.59})$$

Each of these indeed evaluate to (C.56). \square

Interestingly, we also know that the $\mathbb{1}_d \otimes \sigma^x$ and $\sigma^x \otimes \mathbb{1}_d$ correspond to the single-party marginal, meaning that $c_{0,\alpha,\beta}^x = c_{\alpha,\beta,0}^x = A$, which confirms that $A = (d-2)B_3 + 2\Re(B_5)$.

The Imaginary Semi-Off-Diagonal - The $\sigma^z \otimes \sigma^y$ Pairings

In the computational basis, the Imaginary Semi-Off-Diagonal is

$$i\Im(B_5) \sum_{j \neq k} (|jj\rangle\langle jk| + |jj\rangle\langle kj| - |jk\rangle\langle jj| - |kj\rangle\langle jj|), \quad (\text{C.60})$$

which we shall now show can be represented in the Bloch representation with coefficients,

$$c_{0\alpha,\beta}^y = 0. \quad (\text{C.61})$$

and,

$$c_{\gamma\alpha,\beta}^{zy} = -\Im(B_5) \sqrt{\frac{1}{2\gamma(\gamma+1)}} \begin{cases} 0 & \beta < \gamma+1 \\ \gamma+1 & \beta = \gamma+1 \\ 1 & \alpha < \gamma+1 < \beta \\ -\gamma & \alpha = \gamma+1 \\ 0 & \alpha > \gamma+1 \end{cases}. \quad (\text{C.62})$$

The same array visualization of $c_{\gamma\alpha,\beta}^{zy}$ is,

$$c_{\gamma\alpha,\beta}^{zy} = -\Im(B_5) \sqrt{\frac{1}{2\gamma(\gamma+1)}} \begin{pmatrix} 0 & \dots & 0 & \gamma+1 & 1 & \dots & \dots & 1 \\ & \ddots & \vdots & \vdots & \vdots & \ddots & & \vdots \\ & & 0 & \vdots & \vdots & & \ddots & \vdots \\ & & & \gamma+1 & 1 & \dots & \dots & 1 \\ & & & & -\gamma & \dots & \dots & -\gamma \\ & & & & & 0 & \dots & 0 \\ & & & & & & \ddots & \vdots \\ & & & & & & & 0 \end{pmatrix}. \quad (\text{C.63})$$

What follows is a proof that these representations are equivalent.

Proof. We can again begin by exploiting the symmetries of $\sigma_{\alpha,\beta}^y$ to only examine the following computational basis elements,

$$\sum_{j < k} (|jj\rangle\langle jk| - |kj\rangle\langle kk|), \quad (\text{C.64})$$

where we have also divided out by $i\mathfrak{S}(B_5)$. The same treatment of the Bloch representation leaves,

$$\begin{aligned} & \sum_{\gamma=1}^{d-1} \left[\frac{1}{\gamma} \sum_{j=1}^{\gamma} \left(-\gamma |\gamma+1 \ j\rangle\langle \gamma+1 \ \gamma+1| + \sum_{i=1}^{\gamma} |ij\rangle\langle i\gamma+1| \right) \right. \\ & \quad + \frac{1}{\gamma(\gamma+1)} \sum_{j < \gamma+1 < k} \left(-\gamma |\gamma+1 \ j\rangle\langle \gamma+1 \ k| + \sum_{i=1}^{\gamma} |ij\rangle\langle ik| \right) \\ & \quad \left. + \frac{1}{\gamma+1} \sum_{k=\gamma+2}^d \left(-\gamma |\gamma+1 \ \gamma+1\rangle\langle \gamma+1 \ k| + \sum_{i=1}^{\gamma} |i \ \gamma+1\rangle\langle ik| \right) \right]. \end{aligned} \quad (\text{C.65})$$

Start again with the terms of the form $|jj\rangle\langle jk|$, for $j \neq k$, in the Bloch representation,

$$\begin{aligned} & \sum_{\gamma=1}^{d-1} \left[\frac{1}{\gamma} \sum_{j=1}^{\gamma} |jj\rangle\langle j \ \gamma+1| + \frac{1}{\gamma(\gamma+1)} \sum_{j < \gamma+1 < k} |jj\rangle\langle jk| \right. \\ & \quad \left. + \frac{\gamma}{\gamma+1} \sum_{k=\gamma+2}^d |\gamma+1 \ \gamma+1\rangle\langle \gamma+1 \ k| \right], \end{aligned} \quad (\text{C.66})$$

which simplifies to

$$\sum_{j < k} |jj\rangle\langle jk| \left[\frac{1}{k-1} + \sum_{\gamma=j}^{k-2} \frac{1}{\gamma(\gamma+1)} + \frac{j-1}{j} \right] \quad (\text{C.67})$$

$$= \sum_{j < k} |jj\rangle\langle jk|, \quad (\text{C.68})$$

which agrees with (C.64). The same treatment of the $|kj\rangle\langle kk|$ terms for $j \neq k$ in the Bloch representation gives,

$$\sum_{\gamma=1}^{d-1} \left[-\sum_{j=1}^{\gamma} |\gamma+1 \ j\rangle\langle \gamma+1 \ \gamma+1| \right] \quad (\text{C.69})$$

$$= -\sum_{j < k} |kj\rangle\langle kk|, \quad (\text{C.70})$$

which again agrees with (C.64). Lastly we need to show that terms where $i \neq j, k$ vanish. Begin with $i < j$, the surviving terms evaluate to

$$\sum_{i \neq j, k} \sum_{j < k} |ij\rangle\langle ik| \left[\frac{1}{k-1} + \sum_{\gamma=j}^{k-2} \frac{1}{\gamma(\gamma+1)} - \frac{1}{j} \right] = 0. \quad (\text{C.71})$$

Terms where $j < i < k$ likewise evaluate to

$$\sum_{i \neq j, k} \sum_{j < k} |ij\rangle\langle ik| \left[\frac{1}{k-1} + \sum_{\gamma=i}^{k-2} \frac{1}{\gamma(\gamma+1)} - \frac{1}{i} \right] = 0. \quad (\text{C.72})$$

And finally there are no terms in the sum for $i > k$. □

The Real Full-Off-Diagonal - The $\sigma^x \otimes \sigma^x$ and $\sigma^y \otimes \sigma^y$ Pairings

In the computational basis, the Real Full-Off-Diagonal components are

$$\sum_{i \neq j} \left\{ B_4 |ii\rangle\langle jj| + \left(\frac{1}{d^2} + C \right) |ij\rangle\langle ji| \right. \\ \left. + \sum_{k \neq i, j} \left[\Re(B_2) (|ii\rangle\langle jk| + |jk\rangle\langle ii|) + B_3 (|ij\rangle\langle ki| + |ji\rangle\langle ik|) + \sum_{l \neq i, j, k} B_1 |ij\rangle\langle kl| \right] \right\}, \quad (\text{C.73})$$

which are represented by Bloch vector components given by

$$c_{\alpha, \beta}^x \alpha, \beta = \frac{1}{2} \left(\frac{1}{d^2} + C + B_4 \right) \quad (\text{C.74})$$

$$c_{\alpha, \beta}^x \beta, \gamma = c_{\alpha, \beta}^x \gamma, \alpha = c_{\alpha, \beta}^x \alpha, \gamma = c_{\alpha, \beta}^x \gamma, \beta = \frac{1}{2} (B_3 + \Re(B_2)) \quad (\text{C.75})$$

$$c_{\alpha, \beta}^x \gamma, \delta = B_1 \quad (\text{C.76})$$

$$c_{\alpha, \beta}^y \alpha, \beta = \frac{1}{2} \left(\frac{1}{d^2} + C - B_4 \right) \quad (\text{C.77})$$

$$c_{\alpha, \beta}^y \beta, \gamma = c_{\alpha, \beta}^y \gamma, \alpha = c_{\alpha, \beta}^y \alpha, \gamma = c_{\alpha, \beta}^y \gamma, \beta = \frac{1}{2} (B_3 - \Re(B_2)) \quad (\text{C.78})$$

$$c_{\alpha, \beta}^y \gamma, \delta = 0, \quad (\text{C.79})$$

for distinct α , β , γ , and δ . For fixed α and β , we can visualize $c_{\alpha, \beta}^x \gamma, \delta$ and $c_{\alpha, \beta}^y \gamma, \delta$ in the following arrays indexed by γ and δ ,

$$c_{\alpha, \beta \gamma, \delta}^x = \left(\begin{array}{cccccccccccccccc} \mathcal{X} & \dots & \dots & \mathcal{X} & \mathcal{Y}_+ & \mathcal{X} & \dots & \dots & \dots & \mathcal{X} & \mathcal{Y}_+ & \mathcal{X} & \dots & \dots & \dots & \mathcal{X} \\ & \ddots & & \vdots & \vdots & \vdots & \ddots & & & \vdots & \vdots & \vdots & \ddots & & & \vdots \\ & & \ddots & \vdots & \vdots & \vdots & & \ddots & & \vdots & \vdots & \vdots & & \ddots & & \vdots \\ & & & \mathcal{X} & \vdots & \vdots & & \ddots & & \vdots & \vdots & \vdots & & \ddots & & \vdots \\ & & & & \mathcal{Y}_+ & \mathcal{X} & \dots & \dots & \dots & \mathcal{X} & \mathcal{Y}_+ & \mathcal{X} & \dots & \dots & \dots & \mathcal{X} \\ & & & & & \mathcal{Y}_+ & \dots & \dots & \dots & \mathcal{Y}_+ & \mathcal{Z}_+ & \mathcal{Y}_+ & \dots & \dots & \dots & \mathcal{Y}_+ \\ & & & & & & \mathcal{X} & \dots & \dots & \mathcal{X} & \mathcal{Y}_+ & \mathcal{X} & \dots & \dots & \dots & \mathcal{X} \\ & & & & & & & \ddots & & \vdots & \vdots & \vdots & \ddots & & & \vdots \\ & & & & & & & & \ddots & \vdots & \vdots & \vdots & & \ddots & & \vdots \\ & & & & & & & & & \mathcal{X} & \vdots & \vdots & & \ddots & & \vdots \\ & & & & & & & & & & \mathcal{Y}_+ & \mathcal{X} & \dots & \dots & \dots & \mathcal{X} \\ & & & & & & & & & & & \mathcal{Y}_+ & \dots & \dots & \dots & \mathcal{Y}_+ \\ & & & & & & & & & & & & \mathcal{X} & \dots & \dots & \mathcal{X} \\ & & & & & & & & & & & & & \ddots & & \vdots \\ & & & & & & & & & & & & & & \ddots & \vdots \\ & & & & & & & & & & & & & & & \mathcal{X} \end{array} \right), \tag{C.80}$$

and

$$c_{\alpha, \beta \gamma, \delta}^y = \begin{pmatrix} 0 & \dots & \dots & 0 & \mathcal{Y}_- & 0 & \dots & \dots & \dots & 0 & \mathcal{Y}_- & 0 & \dots & \dots & \dots & 0 \\ & \ddots & & \vdots & \vdots & \vdots & \ddots & & & \vdots & \vdots & \vdots & \ddots & & & \vdots \\ & & \ddots & \vdots & \vdots & \vdots & & \ddots & & \vdots & \vdots & \vdots & & \ddots & & \vdots \\ & & & 0 & \vdots & \vdots & & \ddots & & \vdots & \vdots & \vdots & & \ddots & & \vdots \\ & & & & \mathcal{Y}_- & 0 & \dots & \dots & \dots & 0 & \mathcal{Y}_- & 0 & \dots & \dots & \dots & 0 \\ & & & & & \mathcal{Y}_- & \dots & \dots & \dots & \mathcal{Y}_- & \mathcal{L}_- & \mathcal{Y}_- & \dots & \dots & \dots & \mathcal{Y}_- \\ & & & & & & 0 & \dots & \dots & 0 & \mathcal{Y}_- & 0 & \dots & \dots & \dots & 0 \\ & & & & & & & \ddots & & \vdots & \vdots & \vdots & \ddots & & & \vdots \\ & & & & & & & & \ddots & \vdots & \vdots & \vdots & & \ddots & & \vdots \\ & & & & & & & & & 0 & \vdots & \vdots & & \ddots & & \vdots \\ & & & & & & & & & & \mathcal{Y}_- & 0 & \dots & \dots & \dots & 0 \\ & & & & & & & & & & & \mathcal{Y}_- & \dots & \dots & \dots & \mathcal{Y}_- \\ & & & & & & & & & & & & 0 & \dots & \dots & 0 \\ & & & & & & & & & & & & & \ddots & & \vdots \\ & & & & & & & & & & & & & & \ddots & \vdots \\ & & & & & & & & & & & & & & & 0 \end{pmatrix}, \quad (\text{C.81})$$

where $\mathcal{X} = B_1$, $\mathcal{Y}_\pm = \frac{1}{2}(B_3 \pm \Re(B_2))$ and $\mathcal{L}_\pm = \frac{1}{2}(d^{-2} + C \pm B_4)$. Elements where only one of the conditions, $\gamma = \alpha$, or $\delta = \alpha$, or $\gamma = \beta$, or $\delta = \beta$ are met are colored in blue, while the element in red indicates when $\gamma = \alpha$ and $\delta = \beta$.

The Imaginary Full-Off-Diagonal - The $\sigma^x \otimes \sigma^y$ Pairings

Lastly, the Imaginary Full-Off-Diagonal can be represented in the Bloch representation as

$$i\Im(B_2) \sum_{i < j} \sum_{i < k \neq j} |ii\rangle\langle jk| - |jk\rangle\langle ii| = \frac{\Im(B_2)}{2} \sum_{i > j} \sum_{i > k \neq j} \sigma_{j,i}^x \otimes \sigma_{k,i}^y + \sigma_{k,i}^y \otimes \sigma_{j,i}^x - \frac{\Im(B_2)}{2} \sum_{i < j} \sum_{i < k \neq j} \sigma_{i,j}^x \otimes \sigma_{i,k}^y + \sigma_{i,k}^y \otimes \sigma_{i,j}^x, \quad (\text{C.82})$$

meaning that the only non-zero individual components are

$$c_{\beta,\alpha\gamma,\alpha}^x{}^y = c_{\gamma,\alpha\beta,\alpha}^y{}^x = -c_{\alpha,\beta\alpha,\gamma}^x{}^y = -c_{\alpha,\gamma\alpha,\beta}^y{}^x = \frac{\Im(B_2)}{2}, \quad (\text{C.83})$$

allowing us to visualize $c_{\alpha,\beta\gamma,\delta}^x{}^y$ as

$$c_{\alpha,\beta\gamma,\delta}^x{}^y = \frac{\Im(B_2)}{2} \begin{pmatrix} 0 & \dots & \dots & \dots & \dots & \dots & 0 & 1 & 0 & \dots & 0 \\ & \ddots & & & & & \vdots & \vdots & \vdots & \ddots & \vdots \\ & & 0 & \dots & \dots & \dots & 0 & 1 & 0 & \dots & 0 \\ & & & -1 & \dots & \dots & -1 & 0 & -1 & \dots & -1 \\ & & & & 0 & \dots & 0 & 1 & 0 & \dots & 0 \\ & & & & & \ddots & \vdots & \vdots & \vdots & & \vdots \\ & & & & & & 0 & \vdots & \vdots & & \vdots \\ & & & & & & & 1 & \vdots & & \vdots \\ & & & & & & & & 0 & & \vdots \\ & & & & & & & & & \ddots & \vdots \\ & & & & & & & & & & 0 \end{pmatrix}, \quad (\text{C.84})$$

where the blue elements indicate when $\alpha = \gamma$, while red indicate $\beta = \delta$.

This completes the conversion of PSS one- and two-party reductions to the generalized Bloch vector representation. We can now turn to evaluating the alternate matrix norms for the purpose of measuring the validity of the mean field approximation.

C.2 Hilbert-Schmidt Distance

As defined in [72], the Hilbert Schmidt distance between matrices, A and B , is

$$D(A, B) = \sqrt{\frac{1}{2} \text{Tr} [(A - B)^2]}. \quad (\text{C.85})$$

By the orthonormality of the Bloch vector components, this conveniently reduces to

$$D(A, B) = \sqrt{\sum_{\alpha} \left(c_{\alpha}^{(A)} - c_{\alpha}^{(B)} \right)^2}, \quad (\text{C.86})$$

assuming, of course, that $\text{Tr}(A) = \text{Tr}(B)$, which is the case for density matrices. Given the results of the previous section, where the Bloch vectors of ρ_1 and ρ_2 were determined in terms of the computational basis matrix elements, we can fully express $D = D(\rho_1 \otimes \rho_1, \rho_2)$ in terms of B_1 - B_5 and C . Splitting the sum into the different types of Bloch vector components, we are left with

$$D = \left[S_{z,z} + S_{z,x} + S_{z,y} + S_{y,y}^{(1)} + S_{y,y}^{(2)} + S_{x,y} + S_{x-x}^{(1)} + S_{x-x}^{(2)} + S_{x-x}^{(3)} \right]^{\frac{1}{2}}, \quad (\text{C.87})$$

where

$$S_{z,z} = \sum_{\alpha=1}^{d-1} (c_{\alpha}^{z,z})^2 \quad (\text{C.88})$$

$$S_{z,x} = 2 \sum_{\gamma=1}^{d-1} \sum_{\alpha < \beta} (c_{\gamma}^{z,x})^2 \quad (\text{C.89})$$

$$S_{z,y} = 2 \sum_{\gamma=1}^{d-1} \sum_{\alpha < \beta} (c_{\gamma}^{z,y})^2 \quad (\text{C.90})$$

$$S_{y,y}^{(1)} = \sum_{\alpha < \beta} (c_{\alpha,\beta}^y)^2 \quad (\text{C.91})$$

$$S_{y,y}^{(2)} = \sum_{\alpha < \beta < \gamma} (c_{\alpha,\beta,\gamma}^y)^2 + \sum_{\gamma < \alpha < \beta} (c_{\alpha,\beta,\gamma,\alpha}^y)^2 + \sum_{\alpha < \{\beta \neq \gamma\}} (c_{\alpha,\beta,\alpha,\gamma}^y)^2 + \sum_{\{\alpha \neq \gamma\} < \beta} (c_{\alpha,\beta,\gamma,\beta}^y)^2 \quad (\text{C.92})$$

$$S_{x,y} = 2 \left[\sum_{\alpha < \beta < \gamma} (c_{\alpha,\beta,\gamma}^x)^2 + \sum_{\gamma < \alpha < \beta} (c_{\alpha,\beta,\gamma,\alpha}^x)^2 + \sum_{\alpha < \{\beta \neq \gamma\}} (c_{\alpha,\beta,\alpha,\gamma}^x)^2 + \sum_{\{\alpha \neq \gamma\} < \beta} (c_{\alpha,\beta,\gamma,\beta}^x)^2 \right] \quad (\text{C.93})$$

$$S_{x-x}^{(1)} = \sum_{\alpha < \beta} \left(c_{\alpha,\beta}^x - (c_{\alpha,\beta}^x)^2 \right)^2 \quad (\text{C.94})$$

$$S_{x-x}^{(2)} = \sum_{\alpha < \beta < \gamma} \left(c_{\alpha,\beta,\gamma}^x - (c_{\alpha,\beta}^x)^2 \right)^2 + \sum_{\gamma < \alpha < \beta} \left(c_{\alpha,\beta,\gamma,\alpha}^x - (c_{\alpha,\beta}^x)^2 \right)^2 \quad (\text{C.95})$$

$$+ \sum_{\alpha < \{\beta \neq \gamma\}} \left(c_{\alpha,\beta,\alpha,\gamma}^x - (c_{\alpha,\beta}^x)^2 \right)^2 + \sum_{\{\alpha \neq \gamma\} < \beta} \left(c_{\alpha,\beta,\gamma,\beta}^x - (c_{\alpha,\beta}^x)^2 \right)^2$$

$$S_{x-x}^{(3)} = \underbrace{\sum_{\alpha < \beta} \sum_{\gamma < \delta}}_{\text{distinct } \alpha, \beta, \gamma, \delta} \left(c_{\alpha,\beta,\gamma,\delta}^x - (c_{\alpha,\beta}^x)^2 \right)^2. \quad (\text{C.96})$$

It is now just a matter of counting and summing for each of the S terms. First is $S_{z,z}$, which is straightforward as each of the $c_{\alpha}^{z,z}$ are the same,

$$S_{z,z} = (d-1) \frac{d^2 C^2}{4}. \quad (\text{C.97})$$

Next is $S_{z,x}$, which requires a more involved sum over γ ,

$$S_{z,x} = (B_3 - \Re(B_5))^2 \sum_{\alpha < \beta} \left[\frac{\alpha-1}{\alpha} + \sum_{\gamma=\alpha}^{\beta-2} \frac{1}{\gamma(\gamma+1)} + \frac{(\beta-2)^2}{\beta(\beta-1)} + 4 \sum_{\gamma=\beta}^{d-1} \frac{1}{\gamma(\gamma+1)} \right]$$

$$= (d-1)(d-2) (B_3 - \Re(B_5))^2.$$

Likewise $S_{z,y}$ requires a similar sum,

$$S_{z,y} = \mathfrak{S}(B_5)^2 \sum_{\alpha < \beta} \left[\frac{\alpha - 1}{\alpha} + \sum_{\gamma = \alpha}^{\beta - 2} \frac{1}{\gamma(\gamma + 1)} + \frac{\beta}{\beta - 1} \right] \quad (\text{C.98})$$

$$= d(d - 1) \mathfrak{S}(B_5)^2. \quad (\text{C.99})$$

We then have $S_{y,y}^{(1)}$, which is straightforward, as each of the $c_{\alpha,\beta}^y$ are the same.

$$S_{y,y}^{(1)} = \frac{d(d - 1)}{8} \left(\frac{1}{d^2} + C - B_4 \right)^2. \quad (\text{C.100})$$

Moving to $S_{y,y}^{(2)}$, the only challenge is in the counting of terms,

$$S_{y,y}^{(2)} = \frac{1}{4} (B_3 - \mathfrak{R}(B_2))^2 \left[\sum_{\alpha < \beta < \gamma} + \sum_{\gamma < \alpha < \beta} + \sum_{\alpha < \{\beta \neq \gamma\}} + \sum_{\{\alpha \neq \gamma\} < \beta} \right] \quad (\text{C.101})$$

$$= \frac{1}{4} (B_3 - \mathfrak{R}(B_2))^2 d(d - 1)(d - 2) \left[\frac{1}{6} + \frac{1}{6} + \frac{1}{3} + \frac{1}{3} \right] \quad (\text{C.102})$$

$$= \frac{1}{4} (B_3 - \mathfrak{R}(B_2))^2 d(d - 1)(d - 2). \quad (\text{C.103})$$

The same counting of terms can be applied to determine $S_{x,y}$,

$$S_{x,y} = \frac{1}{2} d(d - 1)(d - 2) \mathfrak{S}(B_2)^2. \quad (\text{C.104})$$

Then $S_{x-x}^{(1)}$ is straightforward,

$$S_{x-x}^{(1)} = \frac{1}{2} d(d - 1) \left(\frac{1}{2d^2} + \frac{C}{2} + \frac{B_4}{2} - ((d - 2)B_3 + 2\mathfrak{R}(B_5))^2 \right)^2. \quad (\text{C.105})$$

The same counting of terms used in $S_{y,y}^{(2)}$ can be applied to $S_{x-x}^{(2)}$,

$$S_{x-x}^{(2)} = d(d - 1)(d - 2) \left(\frac{B_3}{2} + \frac{\mathfrak{R}(B_2)}{2} - ((d - 2)B_3 + 2\mathfrak{R}(B_5))^2 \right)^2. \quad (\text{C.106})$$

Lastly $S_{x-x}^{(3)}$ is just a new counting of terms,

$$S_{x-x}^{(3)} = \frac{1}{4} d(d - 1)(d - 2)(d - 3) \left(B_1 - ((d - 2)B_3 + 2\mathfrak{R}(B_5))^2 \right)^2. \quad (\text{C.107})$$

C.3 Super-Fidelity

The Super-Fidelity was originally presented in [73] as a means for bounding the Fidelity.

It is defined as

$$G(A, B) = \text{Tr}(AB) + \sqrt{(1 - \text{Tr}(A^2))(1 - \text{Tr}(B^2))}, \quad (\text{C.108})$$

which conveniently can be expressed in terms of the Bloch vectors for A and B as

$$G(A, B) = \frac{1}{d^2} + 2\vec{c}_A \cdot \vec{c}_B + \sqrt{\left(1 - \frac{1}{d^2} - 2\vec{c}_A \cdot \vec{c}_A\right) \left(1 - \frac{1}{d^2} - 2\vec{c}_B \cdot \vec{c}_B\right)}. \quad (\text{C.109})$$

Applied to $G := G(\rho_1 \otimes \rho_1, \rho_2)$, we can again expand the sums by type of Bloch vector component,

$$G = \frac{1}{d^2} + 2 \left(S_{0,x} + S_{x*x}^{(1)} + S_{x*x}^{(2)} + S_{x*x}^{(3)} \right) + \left[\left(1 - \frac{1}{d^2} - 2 \left(S_{0,x} + S_x^{(1)} + S_x^{(2)} + S_x^{(3)} \right) \right) \right. \\ \left. \times \left(1 - \frac{1}{d^2} - 2 \left(S_{0,x} + S_{z,z} + S_{z,x} + S_{z,y} + S_{y,y}^{(1)} + S_{y,y}^{(2)} + S_{x,y} + S_{x,x}^{(1)} + S_{x,x}^{(2)} + S_{x,x}^{(3)} \right) \right) \right]^{\frac{1}{2}}, \quad (\text{C.110})$$

where the new terms are

$$S_{0,x} = 2 \sum_{\alpha < \beta} \left(c_{0,\alpha,\beta}^z \right)^2 \quad (\text{C.111})$$

$$S_{x^*x}^{(1)} = \sum_{\alpha < \beta} \left(c_{\alpha,\beta}^x \right)^2 c_{\alpha,\beta}^x \quad (\text{C.112})$$

$$S_{x^*x}^{(2)} = \sum_{\alpha < \beta < \gamma} \left(c_{\alpha,\beta}^x \right)^2 c_{\alpha,\beta}^x c_{\beta,\gamma}^x + \sum_{\gamma < \alpha < \beta} \left(c_{\alpha,\beta}^x \right)^2 c_{\alpha,\beta}^x c_{\gamma,\alpha}^x \quad (\text{C.113})$$

$$+ \sum_{\alpha < \{\beta \neq \gamma\}} \left(c_{\alpha,\beta}^x \right)^2 c_{\alpha,\beta}^x c_{\alpha,\gamma}^x + \sum_{\{\alpha \neq \gamma\} < \beta} \left(c_{\alpha,\beta}^x \right)^2 c_{\alpha,\beta}^x c_{\gamma,\beta}^x$$

$$S_{x^*x}^{(3)} = \underbrace{\sum_{\alpha < \beta} \sum_{\gamma < \delta}}_{\text{distinct } \alpha, \beta, \gamma, \delta} \left(c_{\alpha,\beta}^x \right)^2 c_{\alpha,\beta}^x c_{\gamma,\delta}^x \quad (\text{C.114})$$

$$S_x^{(1)} = \sum_{\alpha < \beta} \left(c_{\alpha,\beta}^x \right)^4 \quad (\text{C.115})$$

$$S_x^{(2)} = \sum_{\alpha < \beta < \gamma} \left(c_{\alpha,\beta}^x \right)^4 + \sum_{\gamma < \alpha < \beta} \left(c_{\alpha,\beta}^x \right)^4 + \sum_{\alpha < \{\beta \neq \gamma\}} \left(c_{\alpha,\beta}^x \right)^4 + \sum_{\{\alpha \neq \gamma\} < \beta} \left(c_{\alpha,\beta}^x \right)^4 \quad (\text{C.116})$$

$$S_x^{(3)} = \underbrace{\sum_{\alpha < \beta} \sum_{\gamma < \delta}}_{\text{distinct } \alpha, \beta, \gamma, \delta} \left(c_{\alpha,\beta}^x \right)^4 \quad (\text{C.117})$$

$$S_{x,x}^{(1)} = \sum_{\alpha < \beta} \left(c_{\alpha,\beta}^x c_{\alpha,\beta}^x \right)^2 \quad (\text{C.118})$$

$$S_{x,x}^{(2)} = \sum_{\alpha < \beta < \gamma} \left(c_{\alpha,\beta}^x c_{\beta,\gamma}^x \right)^2 + \sum_{\gamma < \alpha < \beta} \left(c_{\alpha,\beta}^x c_{\gamma,\alpha}^x \right)^2 + \sum_{\alpha < \{\beta \neq \gamma\}} \left(c_{\alpha,\beta}^x c_{\alpha,\gamma}^x \right)^2 + \sum_{\{\alpha \neq \gamma\} < \beta} \left(c_{\alpha,\beta}^x c_{\gamma,\beta}^x \right)^2 \quad (\text{C.119})$$

$$S_{x,x}^{(3)} = \underbrace{\sum_{\alpha < \beta} \sum_{\gamma < \delta}}_{\text{distinct } \alpha, \beta, \gamma, \delta} \left(c_{\alpha,\beta}^x c_{\gamma,\delta}^x \right)^2. \quad (\text{C.120})$$

These calculations largely repeat of those of the previous section, so their final results are compiled below,

$$S_{0,x} = d(d-1) \left(\frac{d-2}{d} B_3 + \frac{2}{d} \mathfrak{R}(B_5) \right)^2 \quad (\text{C.121})$$

$$S_{x*x}^{(1)} = \frac{1}{4} d(d-1) ((d-2)B_3 + 2\mathfrak{R}(B_5))^2 \left(\frac{1}{d^2} + C + B_4 \right) \quad (\text{C.122})$$

$$S_{x*x}^{(2)} = \frac{1}{2} d(d-1)(d-2) ((d-2)B_3 + 2\mathfrak{R}(B_5))^2 (B_3 + \mathfrak{R}(B_2)) \quad (\text{C.123})$$

$$S_{x*x}^{(3)} = \frac{1}{4} d(d-1)(d-2)(d-3) ((d-2)B_3 + 2\mathfrak{R}(B_5))^2 B_1 \quad (\text{C.124})$$

$$S_x^{(1)} = \frac{1}{2} d(d-1) ((d-2)B_3 + 2\mathfrak{R}(B_5))^4 \quad (\text{C.125})$$

$$S_x^{(2)} = d(d-1)(d-2) ((d-2)B_3 + 2\mathfrak{R}(B_5))^4 \quad (\text{C.126})$$

$$S_x^{(3)} = \frac{1}{4} d(d-1)(d-2)(d-3) ((d-2)B_3 + 2\mathfrak{R}(B_5))^4 \quad (\text{C.127})$$

$$S_{x,x}^{(1)} = \frac{1}{8} d(d-1) \left(\frac{1}{d^2} + C + B_4 \right)^2 \quad (\text{C.128})$$

$$S_{x,x}^{(2)} = \frac{1}{4} d(d-1)(d-2) (B_3 + \mathfrak{R}(B_2))^2 \quad (\text{C.129})$$

$$S_{x,x}^{(3)} = \frac{1}{4} d(d-1)(d-2)(d-3) B_1^2. \quad (\text{C.130})$$

Bibliography

- [1] A. Einstein, B. Podolsky, and N. Rosen, “Can Quantum-Mechanical Description of Physical Reality Be Considered Complete?,” *Physical Review* **47** (May, 1935) 777–780.
- [2] B. S. Cirel’son, “Quantum generalizations of bell’s inequality,” *Letters in Mathematical Physics* **4** no. 2, (Mar, 1980) 93–100.
- [3] M. Riebe, H. Häffner, C. F. Roos, W. Hänsel, J. Benhelm, G. P. T. Lancaster, T. W. Körber, C. Becher, F. Schmidt-Kaler, D. F. V. James, and R. Blatt, “Deterministic quantum teleportation with atoms,” *Nature* **429** (June, 2004) 734–737.
- [4] C. H. Bennett and G. Brassard, “Quantum cryptography: Public key distribution and coin tossing,” in *Proceedings of IEEE International Conference on Computers, Systems, and Signal Processing*, p. 175. India, 1984.
- [5] A. Galindo and M. A. Martín-Delgado, “Information and computation: Classical and quantum aspects,” *Rev. Mod. Phys.* **74** (May, 2002) 347–423.
- [6] L. K. Grover, “A Fast quantum mechanical algorithm for database search,” arXiv:quant-ph/9605043 [quant-ph].
- [7] P. W. Shor, “Algorithms for quantum computation: Discrete logarithms and factoring,” in *Proceedings of the 35th Annual Symposium on Foundations of Computer Science, SFCS ’94*, pp. 124–134. IEEE Computer Society, Washington, DC, USA, 1994.
- [8] T. J. Osborne and M. A. Nielsen, “Entanglement, quantum phase transitions, and density matrix renormalization,” *Quantum Information Processing* **1** no. 1, (Apr, 2002) 45–53.
- [9] J. Maldacena, “The large-n limit of superconformal field theories and supergravity,” *International Journal of Theoretical Physics* **38** no. 4, (Apr, 1999) 1113–1133.
- [10] C. Eltschka and J. Siewert, “Quantifying entanglement resources,” *Journal of Physics A: Mathematical and Theoretical* **47** no. 42, (2014) 424005.
- [11] M. A. Nielsen and I. L. Chuang, *Quantum Computation and Quantum Information: 10th Anniversary Edition*. Cambridge University Press, New York, NY, USA, 10th ed., 2011.

- [12] C. H. Bennett, D. P. DiVincenzo, J. A. Smolin, and W. K. Wootters, “Mixed-state entanglement and quantum error correction,” *Phys. Rev. A* **54** (Nov, 1996) 3824–3851.
- [13] K. Życzkowski, P. Horodecki, A. Sanpera, and M. Lewenstein, “Volume of the set of separable states,” *Phys. Rev. A* **58** (Aug, 1998) 883–892.
- [14] H. Barnum and N. Linden, “Monotones and invariants for multi-particle quantum states,” *Journal of Physics A: Mathematical and General* **34** no. 35, (2001) 6787.
- [15] W. K. Wootters, “Entanglement of formation of an arbitrary state of two qubits,” *Phys. Rev. Lett.* **80** (Mar, 1998) 2245–2248.
- [16] A. Uhlmann, “Optimizing entropy relative to a channel or a subalgebra,” in *Quantum group. Proceedings, Symposium at the 21st International Colloquium on Group Theoretical Methods in Physics, Group’21, ICGTMP’96, Goslar, Germany, July 15-20, 1996*. 1996. arXiv:quant-ph/9701014 [quant-ph].
- [17] S. Lee, D. P. Chi, S. D. Oh, and J. Kim, “Convex-roof extended negativity as an entanglement measure for bipartite quantum systems,” *Phys. Rev. A* **68** (Dec, 2003) 062304.
- [18] D. P. DiVincenzo, C. A. Fuchs, H. Mabuchi, J. A. Smolin, A. Thapliyal, and A. Uhlmann, “Entanglement of assistance,” in *1st NASA Conference on Quantum Computing and Quantum Communications Palm Springs, California, February 17-20, 1998*. 1998. arXiv:quant-ph/9803033 [quant-ph].
- [19] V. Coffman, J. Kundu, and W. K. Wootters, “Distributed entanglement,” *Phys. Rev. A* **61** (Apr, 2000) 052306.
- [20] V. Vedral and M. B. Plenio, “Entanglement measures and purification procedures,” *Phys. Rev. A* **57** (Mar, 1998) 1619–1633.
- [21] M. Koashi, V. Bužek, and N. Imoto, “Entangled webs: Tight bound for symmetric sharing of entanglement,” *Phys. Rev. A* **62** (Oct, 2000) 050302.
- [22] O. Bucicovschi, J. R. Grice, and D. A. Meyer, “Achievable concurrences for three qubits,” *To Appear* .
- [23] A. Coffman, A. J. Schwartz, and C. Stanton, “The algebra and geometry of steiner and other quadratically parametrizable surfaces,” *Comput. Aided Geom. Des.* **13** no. 3, (Apr., 1996) 257–286.
- [24] G. W. Allen, O. Bucicovschi, and D. A. Meyer, “Entanglement constraints on states locally connected to the greenberger-horne-zeilinger state,” 2017.
- [25] E. Ising, “Beitrag zur theorie des ferromagnetismus,” *Zeitschrift für Physik* **31** no. 1, (Feb, 1925) 253–258.

- [26] M. Van den Nest, A. Miyake, W. Dür, and H. J. Briegel, “Universal resources for measurement-based quantum computation,” *Phys. Rev. Lett.* **97** (Oct, 2006) 150504.
- [27] P. Ribeiro, J. Vidal, and R. Mosseri, “Exact spectrum of the lipkin-meshkov-glick model in the thermodynamic limit and finite-size corrections,” *Phys. Rev. E* **78** (Aug, 2008) 021106.
- [28] S. S. Ivanov, P. A. Ivanov, I. E. Linington, and N. V. Vitanov, “Scalable quantum search using trapped ions,” *Phys. Rev. A* **81** (Apr, 2010) 042328.
- [29] M. Aulbach, D. Markham, and M. Muraio, “Geometric entanglement of symmetric states and the majorana representation,” in *Theory of Quantum Computation, Communication, and Cryptography*, W. van Dam, V. M. Kendon, and S. Severini, eds., pp. 141–158. Springer Berlin Heidelberg, Berlin, Heidelberg, 2011.
- [30] D. Baguette, T. Bastin, and J. Martin, “Multiqubit symmetric states with maximally mixed one-qubit reductions,” *Phys. Rev. A* **90** (Sep, 2014) 032314.
- [31] L. Arnaud and N. J. Cerf, “Exploring pure quantum states with maximally mixed reductions,” *Phys. Rev. A* **87** (Jan, 2013) 012319.
- [32] R. H. Dicke, “Coherence in spontaneous radiation processes,” *Phys. Rev.* **93** (Jan, 1954) 99–110.
- [33] E. Majorana, “Atomi orientati in campo magnetico variabile,” *Il Nuovo Cimento (1924-1942)* **9** no. 2, (Feb, 1932) 43–50.
- [34] M. Aulbach, *Classification of Entanglement in Symmetric States*. PhD thesis, Leeds U., 2011. arXiv:1110.5200 [quant-ph].
- [35] M. Sanz, I. L. Egusquiza, R. di Candia, H. Saberi, L. Lamata, and E. Solano, “Entanglement classification with matrix product states,” *Scientific Reports* **6** (Jul, 2016) 30188, arXiv:1504.07524 [quant-ph].
- [36] A. Acín, A. Andrianov, E. Jané, and R. Tarrach, “Three-qubit pure-state canonical forms,” *Journal of Physics A: Mathematical and General* **34** no. 35, (Aug, 2001) 6725–6739.
- [37] P. Ribeiro and R. Mosseri, “Entanglement in the symmetric sector of n qubits,” *Phys. Rev. Lett.* **106** (May, 2011) 180502.
- [38] A. Mandilara, T. Coudreau, A. Keller, and P. Milman, “Entanglement classification of pure symmetric states via spin coherent states,” *Phys. Rev. A* **90** (Nov, 2014) 050302.
- [39] A. Meill and D. A. Meyer, “Symmetric three-qubit-state invariants,” *Phys. Rev. A* **96** (Dec, 2017) 062310.
- [40] A. Higuchi and A. Sudbery, “How entangled can two couples get?,” *Physics Letters A* **273** no. 4, (2000) 213 – 217.

- [41] R. Hübener, M. Kleinmann, T.-C. Wei, C. González-Guillén, and O. Gühne, “Geometric measure of entanglement for symmetric states,” *Phys. Rev. A* **80** (Sep, 2009) 032324.
- [42] M. Grassl, M. Rötteler, and T. Beth, “Computing local invariants of quantum-bit systems,” *Phys. Rev. A* **58** (Sep, 1998) 1833–1839.
- [43] H. A. Carteret, N. Linden, S. Popescu, and A. Sudbery, “Multiparticle entanglement,” *Foundations of Physics* **29** no. 4, (Apr, 1999) 527–552.
- [44] J. Kempe, “Multiparticle entanglement and its applications to cryptography,” *Phys. Rev. A* **60** (Aug, 1999) 910–916.
- [45] B. Kraus, “Local unitary equivalence of multipartite pure states,” *Phys. Rev. Lett.* **104** (Jan, 2010) 020504.
- [46] R. Laflamme, C. Miquel, J. P. Paz, and W. H. Zurek, “Perfect quantum error correction code,” arXiv:quant-ph/9602019 [quant-ph].
- [47] H.-T. Cui, J.-L. Tian, C.-M. Wang, and Y.-C. Chen, “Topology of entanglement in multipartite states with translational invariance,” *The European Physical Journal D* **67** no. 7, (Jul, 2013) 154.
- [48] J. Vidal, G. Palacios, and R. Mosseri, “Entanglement in a second-order quantum phase transition,” *Phys. Rev. A* **69** (Feb, 2004) 022107.
- [49] A. De Pasquale, G. Costantini, P. Facchi, G. Florio, S. Pascazio, and K. Yuasa, “Xx model on the circle,” *The European Physical Journal Special Topics* **160** no. 1, (Jul, 2008) 127–138.
- [50] K. M. O’Connor and W. K. Wootters, “Entangled rings,” *Phys. Rev. A* **63** (Apr, 2001) 052302.
- [51] A. Meill and D. A. Meyer, “Pairwise concurrence in cyclically symmetric quantum states,” 2018.
- [52] T. Yu and J. H. Eberly, “Evolution from entanglement to decoherence of bipartite mixed "x" states,” *Quantum Info. Comput.* **7** no. 5, (July, 2007) 459–468.
- [53] M. Koashi and A. Winter, “Monogamy of quantum entanglement and other correlations,” *Phys. Rev. A* **69** (Feb, 2004) 022309.
- [54] J. Ginibre, “Reduced density matrices of quantum gases. ii. cluster property,” *Journal of Mathematical Physics* **6** no. 2, (1965) 252–262, <https://doi.org/10.1063/1.1704276>.
- [55] W. Greenberg, “Critical temperature bounds of quantum lattice gases,” *Communications in Mathematical Physics* **13** no. 4, (Dec, 1969) 335–344.

- [56] M. Fannes, B. Nachtergaele, and R. F. Werner, “Finitely correlated states on quantum spin chains,” *Communications in Mathematical Physics* **144** no. 3, (Mar, 1992) 443–490.
- [57] M. B. Hastings, “An area law for one-dimensional quantum systems,” *Journal of Statistical Mechanics: Theory and Experiment* **2007** no. 08, (Aug, 2007) P08024–P08024.
- [58] I. Affleck, T. Kennedy, E. H. Lieb, and H. Tasaki, “Valence bond ground states in isotropic quantum antiferromagnets,” *Communications in Mathematical Physics* **115** no. 3, (Sep, 1988) 477–528.
- [59] G. Evenbly and G. Vidal, “Tensor network states and geometry,” *Journal of Statistical Physics* **145** no. 4, (Nov, 2011) 891–918.
- [60] A. Almheiri, X. Dong, and D. Harlow, “Bulk locality and quantum error correction in ads/cft,” *Journal of High Energy Physics* **2015** no. 4, (Apr, 2015) 163.
- [61] G. Vidal, “Efficient classical simulation of slightly entangled quantum computations,” *Phys. Rev. Lett.* **91** (Oct, 2003) 147902.
- [62] D. Perez-Garcia, F. Verstraete, M. M. Wolf, and J. I. Cirac, “Matrix product state representations,” arXiv:quant-ph/0608197.
- [63] C. Hubig, “Abelian and non-abelian symmetries in infinite projected entangled pair states,” *SciPost Phys.* **5** (2018) 47.
- [64] N. Shenvi, J. Kempe, and K. B. Whaley, “Quantum random-walk search algorithm,” *Phys. Rev. A* **67** (May, 2003) 052307.
- [65] B. Allés, S. Gündüç, and Y. Gündüç, “Maximal entanglement from quantum random walks,” *Quantum Information Processing* **11** no. 1, (Feb, 2012) 211–227.
- [66] D. A. Meyer and T. G. Wong, “Nonlinear quantum search using the gross–pitaevskii equation,” *New Journal of Physics* **15** no. 6, (Jun, 2013) 063014.
- [67] E. P. Gross, “Structure of a quantized vortex in boson systems,” *Il Nuovo Cimento (1955-1965)* **20** no. 3, (May, 1961) 454–477.
- [68] J. Rogel-Salazar, “The gross–pitaevskii equation and bose–einstein condensates,” *European Journal of Physics* **34** no. 2, (Jan, 2013) 247–257.
- [69] C. Bennett, E. Bernstein, G. Brassard, and U. Vazirani, “Strengths and weaknesses of quantum computing,” *SIAM Journal on Computing* **26** no. 5, (1997) 1510–1523, <https://doi.org/10.1137/S0097539796300933>.
- [70] R. Jozsa, “Fidelity for mixed quantum states,” *Journal of Modern Optics* **41** no. 12, (1994) 2315–2323, <https://doi.org/10.1080/09500349414552171>.

- [71] C. A. Fuchs and C. M. Caves, “Ensemble-dependent bounds for accessible information in quantum mechanics,” *Phys. Rev. Lett.* **73** (Dec, 1994) 3047–3050.
- [72] I. Bengtsson and K. Życzkowski, *The space of density matrices*, p. 219–248. Cambridge University Press, 2 ed., 2017.
- [73] Z.-H. Ma, F.-L. Zhang, Z.-H. Chen, and J.-L. Chen, “Super fidelity and related metric,” 2008.
- [74] R. A. Bertlmann and P. Krammer, “Bloch vectors for qudits,” *Journal of Physics A: Mathematical and Theoretical* **41** no. 23, (May, 2008) 235303.
- [75] F. Bloch, “Nuclear induction,” *Phys. Rev.* **70** (Oct, 1946) 460–474.